UNIVERSITY OF CALIFORNIA

Los Angeles

Cavitation: Testing the Eulerian and Lagrangian Descriptions of the Dynamics of Soft Materials

A dissertation submitted in partial satisfaction of the requirements for the degree Doctor of Philosophy in Physics

by

Justin Gabriel Little

2024

ABSTRACT OF THE DISSERTATION

Cavitation: Testing the Eulerian and Lagrangian Descriptions of the Dynamics of Soft Materials

by

Justin Gabriel Little
Doctor of Philosophy in Physics
University of California, Los Angeles, 2024
Professor Robijn F. Bruinsma, Chair

The systems encountered in biophysics typically straddle the line between solid and fluid, and are thus subject to large deformations even at modest stress values. This, along with the presence of material properties such as visco-elasticity and strain hardening, necessitate the use of non-linear elasticity when describing the physics of these systems. In this dissertation, we explore the use of non-linear elasticity theory in describing soft matter physics, with a focus on the specific example of cavitation in polymer gels and similar systems.

We first look at cavitation in the context of equilibrium mechanics. In simple materials that obey neo-Hookean elasticity, we show that compressibility effects strongly enhance cavitation. On the other hand, cavitation phenomena in gels of flexible polymers in a binary solvent that phase separates are surprisingly similar to those of incompressible materials. We find that, as a function of the interfacial energy between the two solvent components, there is a sharp transition between cavitation and classical nucleation-and-growth. Finally, biopolymer gels are characterized by strain hardening, and even very low levels of strain hardening are shown to suppress cavitation in polymer gel that obey Flory-Huggins theory in the absence of strain hardening.

Next, we explore the dynamics of cavitation in non-linear incompressible materials. We find that, while purely elastic systems can be described entirely within either a Lagrangian or Eulerian frame of reference, and viscous fluids with no elasticity can be described entirely within an Eulerian frame, visco-elastic materials such a Maxwell materials cannot be fully described without making use both frames, translating between the two using a known deformation mapping.

The dissertation of Justin Gabriel Little is approved.

Joseph A. Rudnick

Dolores Bozovic

Mayank R. Mehta

Robijn F. Bruinsma, Committee Chair

University of California, Los Angeles

2024

Contents

List of Figures

Acknowledgments

I would like to acknowledge my advisor Robijn Bruinsma for his support, without which I would not have been able to complete this dissertation. I also acknowledge the other members of my committee: Joe Rudnick, Dolores Bozovic, and Mayank Mehta. I in particular would like to thank Professors Bozovic and Mehta for agreeing to join the committee at relatively short notice. I also acknowledge my former committee member, the late Alex Levine, as well as Amit R. Singh, both of whom co-authored the paper Finite-Strain Elasticity Theory and Liquid-Liquid Phase Separation in Compressible Gels, published in Phys. Rev. E Volume 107 in 2023 [13], alongside Professor Bruinsma and myself. Professor Bruinsma was the PI, Professor Levine contributed to the development of the theoretical work, and Professor Singh helped perform a finite element analysis using the FEBIO STUDIO [14] software package. Much of chapter four is an adaptation of this paper.

I also want to thank Brenda Buenrostro for her help with reforming my committee after my leave of absence, as well as helping with filing the dissertation. Finally, I want to acknowledge my mother for providing immense support, and my grandmother for graciously providing me housing while I finished the dissertation.

Vita

2011-2015: B.S. in Physics, University of California Santa Barbara, Santa Barbara, CA

2015-2016: M.S. in Physics, University of California Los Angeles, Los Angeles, CA

Publications

Justin Little, Alex J Levine, Amit R Singh, and Robijn Bruinsma. Finite-strain elasticity theory and liquid-liquid phase separation in compressible gels. *Phys. Rev. E,* 107:024418, 2023.

1 Introduction

1.1 Non-Linear Elasticity

The theory of linear elasticity is highly familiar to most physicists. It is typically written in the form of a Landau theory, with the free energy of the system written as a function of invariants of the strain tensor [10]. While linear elasticity is applicable to many systems, the kind of systems found in biophysics often see the linear theory become inadequate. This is because materials such as polymer networks or biogels are soft, having strains on the order of unity even when under modest stress. Such large deformations leads not only to the strain tensor becoming inherently non-linear, but more importantly introduces a fundamental distinction between the initial and final states of the system. Specifically, quantities evaluated in the initial state can no longer be directly compared to those evaluated in the deformed state - each state now is a completely distinct vector space. In addition to these geometric non-linearities, the systems found in biophysics also typically have additional non-linearities resulting form their material properties. They are inherently visco-elastic, and often feature strain-hardening [9, 17, 22].

There are two potential approaches to handling the distinction between the initial and deformed vector spaces introduced by large deformations, known as the Lagrangian and Eulerian formulations of non-linear elasticity. The Lagrangian picture follows individual material elements, labelling them by their initial positions. All quantities are then written as functions of these initial, "reference space" positions. This allows for a very natural way of defining the non-linear version of the strain tensor, and acts as a direct generalization of the traditional theory of linear elasticity as a result. It does, however, introduce some complications when it comes to defining physical quantities that are measured in the current, deformed state of the system, such as the stress tensor. The Lagrangian

picture is primarily used for the study of non-linear elasticity in solid materials, and has an extensive history of use in the engineering literature.

The Eulerian picture, meanwhile, takes its approach from fluid mechanics. Rather than following material elements, the Eulerian picture measures quantities at fixed physical positions, keeping track of how they change over time. In this picture, the strain tensor becomes a very unnatural object, as there is no natural "reference space" to measure particle displacements from. Instead, quantities such as stress and velocity become much simpler to define, written now as simply functions of space and time. In particular, the Eulerian picture is an inherently dynamic one, and allows for the introduction of dissipative forces far more readily than the Lagrangian picture would.

Both formulations of non-linear elasticity have advantages and disadvantages. The systems of interest in biophysics straddle the line between solid and fluid, and we will see that, depending on the question being asked, one formulation may become advantageous to use over the other. In particular, the Lagrangian formulation becomes advantageous when discussing equilibrium mechanics, allowing for a more direct generalization of the language of linear elasticity familiar to most physicists. However, when discussing the dynamics of these systems, particular those for which dissipative forces are important, the Eulerian picture becomes far more natural.

1.2 Cavitation

Cavitation refers to the problem of the expansion of a pressurized cavity in either a solid or liquid material. In the liquid case, such a cavity will grow in an unlimited way when the pressure exceeds the Laplace capillary pressure. The same is true for a cavity in a solid material, although the pressure must typically

exceed a larger value given by $\frac{5}{2}\mu$, where μ is the shear modulus of the material. This instability is not predicted by linear continuum mechanics, and is in fact the result of the inherently non-linear nature of large deformations.

The dynamics of cavitation in a viscous fluid was first derived by W. H. Besant in 1859, although a simpler derivation was found by Lord Rayleigh in 1917 [1, 18]. As for cavitation in an elastic solid, the problem has been well explored in the engineering literature, specifically in the context of elastic rubbers [6]. In the Physics literature, however, this problem has been explored very little. Not only that, but rubber materials have a number of key differences when compared to the biogels we are mostly interested in. Unlike biogels, rubbers are incompressible, single-component materials, and can typically be treated as purely elastic, with no energy dissipation, even for fairly large deformations. Biogels, meanwhile, are two-component systems, consisting of a visco-elastic polymer network and a viscous solvent. The polymer network, being able to absorb and expel solvent, is now compressible. Biogels also typically feature material non-linearities in addition to the geometric ones inherent to large deformations, such as strain-hardening.

Cavitation is a particularly attractive example problem in which to explore the use of non-linear elasticity. It features spherical symmetry, which greatly simplifies the mathematics involved. Not only this, but it is an inherently non-linear effect, necessitating the use of non-linear theory. It is also directly relevant to the problem of liquid-liquid phase separation in biogels. We will see that the spherical symmetry of the problem allows one to know an exact form for the deformation mapping in the incompressible case, and to reasonably approximate one in the compressible case. This in turn will allow us to translate between the Lagrangian and Eulerian formalisms, enabling both direct comparison of the two, as well as the derivation of new results.

1.3 Liquid-Liquid Phase Separation and Cavitation in Biogels

While liquid-liquid phase separation is well studied in the context of simple binary liquids, similar phenomena in biogels are quite different and less understood. For example, liquid-liquid phase separation in cells produces a distribution of droplets with constant radii, with a complete absence of Oswald ripening [25, 27]. This difference is attributed to the presence of actin biopolymer networks in the cytoplasm of cells, as well as the interior of the cell nucleus. Growth of minority-phase droplets can be stopped by the elastic deformation of the surrounding polymer network [28].

The cytoplasm can be modelled by systems of permanently cross-linked synthetic gels with a simple binary liquid acting as a solvent [23]. In such a system, it has been found that at lower levels of supersaturation droplet growth is arrested by the polymer network, but that droplets begin to grow in an unlimited fashion when the osmotic pressure of the minority phase exceeds a critical value on the order of the network's elastic modulus. This is qualitatively similar to cavitation, and thus understanding the physics of cavitation in a biogel setting is of high interest.

1.4 Overview

The aim of this dissertation is to explore the use of non-linear elasticity theory in describing soft matter physics, with a focus on the specific example of cavitation. As discussed in the previous sections, cavitation was chosen as a focus due to the simplicity introduced by spherical symmetry, as well as its relevance

to liquid-liquid phase separation in biogels. Chapters two and three are dedicated to developing the formalism we are to use, with chapter two acting as an overview of linear elasticity and chapter three developing the formalism for non-linear elasticity. Both a Lagrangian and Eulerian picture is developed, with key differences and advantages discussed. Chapter four applies the formalism developed in chapters two and three to address the equilibrium mechanics of cavitation. A Lagrangian formalism is used, with which the case of an incompressible system is solved exactly, and the case of a compressible system solved approximately using a variational ansatz. The effects of adding a material non-linearity in the form of shear hardening is also explored. Chapter five explores the dynamics of cavitation. We first include a brief discussion of the formalism, showing how the Eulerian picture becomes more natural in a dynamical setting. We then apply this Eulerian formalism to solve the case of both a purely elastic solid and a visco-elastic Maxwell material, assuming incompressibility for both. Finally, chapter six summarized the results discussed in chapters four and five, and provides concluding thoughts on the subject of non-linear elasticity in biogels.

2 Linear Elasticity

This section contains a brief review of the theory of linear elasticity, primarily following Landau and Lifshitz book on the subject [10].

2.1 The Displacement Vector Field and the Linearized Strain Tensor

The version of elasticity theory most familiar to the majority of physicists is that of linear elasticity, which is concerned only with small deformations. We describe the internal configuration of the body by the positions of material elements that form a coarse-grained description of the underlying molecular structure of the material. If a material element is located at position $\vec{x}$ prior to the deformation, and at position $\vec{X}$ after the deformation, then we define the displacement vector of this material element as the vector $\vec{u}(\vec{x}) = \vec{X} - \vec{x}$. It is standard in linear elasticity theory to write the displacement vector field as a function of the initial coordinates of the material elements, i.e. to use a "Lagrangian" frame of reference. The deformation of the body is then entirely determined by this displacement field. For the rest of this section, we will use a curvilinear coordinate system with metric tensor g_{ij}. Covariant derivatives will be denoted as $\frac{D}{Dx^i}$, with associated Christoffel symbols Γ^i_{jk}.

As the body deforms, the distance between material elements changes. Consider two infinitesimally close material elements, $\vec{x}$ and $\vec{x}+d\vec{x}$, with $d\vec{x}$ the differential line element pointing from one to the other. After the deformation, these same two elements will now be located at new positions $\vec{X} = \vec{x} + \vec{u}(\vec{x})$ and $\vec{X} + d\vec{X} = \vec{x} + d\vec{x} + \vec{u}(\vec{x} + d\vec{x})$. Here, we may write the components of $d\vec{X}$ as

$$dX^i = dx^i + dx^j \frac{\partial u^i}{\partial x^j} = \left(\frac{\partial u^i}{\partial x^j} + \delta^i_j \right) dx^i \tag{1}$$

The norm squared of the line element thus transforms under deformation as

$$\left| d\vec{X} \right|^2 = \left(\delta^i_j + \frac{\partial u^i}{\partial x^j} + \frac{\partial u_j}{\partial x_i} + \frac{\partial u_k}{\partial x_i} \frac{\partial u^k}{\partial x^j} \right) dx_i dx^j \tag{2}$$

In linear elasticity we assume the displacement $\vec{u}(\vec{x})$ is small compared to $\vec{x}$, and as such we may drop the second order term for now. We thus write

$$\left|d\vec{X}\right|^2 - |d\vec{x}|^2 = \left(\frac{\partial u_i}{\partial x^j} + \frac{\partial u_j}{\partial x^i}\right) dx^i dx^j = 2u_{ij} dx^i dx^j \tag{3}$$

where $u_{ij} = \frac{1}{2}\left(\frac{\partial u_i}{\partial x^j} + \frac{\partial u_j}{\partial x^i}\right)$ is known as the (linearized) strain tensor.
Now consider an infinitesimal volume element $dv = dx^1 dx^2 dx^3$ which, under deformation, transforms into a new volume element $dV = dX^1 dX^2 dX^3$, given by

$$dV = \left(1 + \frac{\partial u^1}{\partial x^1}\right)\left(1 + \frac{\partial u^2}{\partial x^2}\right)\left(1 + \frac{\partial u^3}{\partial x^3}\right) dv = \left(1 + \text{tr } u + O\left(u^2\right)\right) dv \tag{4}$$

where $\text{tr } u = u^i_i = \frac{\partial u^i}{\partial x^i}$ is the trace of the strain tensor. Clearly, in linear theory, local changes in volume are described entirely by the trace of the strain tensor. This leads us to a natural way of splitting the strain into two parts, one piece proportional to the trace that is associated with changes in volume, and a traceless piece associated with volume-preserving shear, denoted $\bar{u}$:

$$u^i_j = \frac{1}{3}\delta^i_j \text{tr } u + \bar{u}^i_j \tag{5}$$

2.2 The Elastic Free Energy and the Stress Tensor

The free-energy density of a material is, for an isotropic body, written as a function of invariants of the strain tensor. In linear elasticity, we only include invariants up to second order, of which there are two:

$$f_{\text{LE}} = \frac{1}{2}\lambda\left(\text{tr } u\right)^2 + \mu \text{tr}\left(u^2\right) \tag{6}$$

where λ and μ are known as the Lame coefficients. It is also common to re-write the free energy in terms of the trace and traceless pieces of the strain discussed above:

$$f_{\mathrm{LE}} = \frac{1}{2}\kappa \left(\mathrm{tr}\ u\right)^2 + \mu \mathrm{tr}\left(\bar{u}^2\right) \tag{7}$$

where $\kappa = \lambda + \frac{2}{3}\mu$ is the compressional modulus. In this context, μ is typically referred to as the shear modulus. It should be noted that the condition that the strain-free state must be a free-energy minimum implies that both κ and μ are strictly positive.

Given a body $\mathcal{B}$, the momentum of this body may be written as

$$\int_{\mathcal{B}} dV\ \rho \vec{v} \tag{8}$$

where ρ is the local density of the material element dV, and $\vec{v}$ is its velocity vector. Suppose this body is placed under an external force per unit volume $\vec{b}$, and its surface is placed under an external contact force per unit area $\vec{t}$. Newton's second law then gives us that

$$\int_{\mathcal{B}} dV\ \vec{b} + \oint_{\partial\mathcal{B}} dS\ \vec{t} = \frac{d}{dt}\int_{\mathcal{B}} dV\ \rho\vec{v} \tag{9}$$

In mechanical equilibrium, the body is at rest, and the right-hand side of the above equation can be set to zero. To derive a local form for this equation of mechanical equilibrium, we make the assumption that we may write the local force (or traction) $\vec{T}$ acting on a surface element $d\vec{S} = dS\ \hat{N}$ of the body, with unit normal vector $\hat{N}$, may be written as $T^i = \sigma^i_j N^j$, where σ is a rank-two tensor known as the Cauchy stress tensor. In the context of linear elasticity, this is often abbreviated as simply the stress tensor. This will always be possible assuming that the internal force $\vec{T}$ depends linearly on $\hat{N}$, an assumption known as Cauchy's fundamental postulate. Substituting this

expression into the integral equation of mechanical equilibrium, we obtain

$$\int_{\mathcal{B}} dV\ b^i + \oint_{\partial\mathcal{B}} dS\ \sigma^{ij} N_j = 0 \tag{10}$$

Using the divergence theorem, this may now be written as

$$\frac{D\sigma^{ij}}{Dx^j} + b^i = 0 \tag{11}$$

We may similarly derive an equation for the conservation of angular momentum, which in local form reduces to the condition that σ is symmetric, i.e. $\sigma^{ij} = \sigma^{ji}$. The stress tensor may be related to the strain tensor via the elastic free-energy. Suppose the displacement vector of a material element $\vec{u}$ is changed by a small amount $\delta\vec{u}$. The total work done by internal stresses on the body as a result of this change may be written as

$$\delta F = \int_{\mathcal{B}} dV\ \frac{D\sigma^{ij}}{Dx^j}\delta u_i \tag{12}$$

Integrating by parts and making the assumption that the stress goes to zero at infinity, as well as taking advantage of the symmetry of the stress tensor, we may write

$$\delta F = -\int_{\mathcal{B}} dV\ \sigma^{ij}\delta u_{ij} \tag{13}$$

where δu_{ij} is the change in the strain tensor. This implies that the stress tensor may be written as $\sigma^{ij} = \frac{\partial f}{\partial u_{ij}}$, where f is the free-energy density. Substituting in equation 7, we obtain

$$\sigma^i_j = \kappa\delta^i_j \mathrm{tr}\ u + 2\mu\bar{u}^i_j \tag{14}$$

If we insert this expression into the equation of mechanical equilibrium, we may write it in terms of the displacement field, here written in vector notation:

$$\mu\nabla^2\vec{u} + \left(\kappa + \frac{1}{3}\mu\right)\vec{\nabla}\left(\vec{\nabla}\cdot\vec{u}\right) + \vec{b} = 0 \tag{15}$$

3 Finite-Strain Elasticity

3.1 Non-linearities in Elasticity

While linear elasticity is only valid for small deformations, finite-strain elasticity allows for large deformations. This introduces several major differences, primarily stemming from the fact that the configuration prior to deformation and the configuration after the deformation can no longer be treated as the same space. This introduces what I will refer to as "geometric" non-linearities, which are inherent to finite-strain elasticity - they are always present regardless of material properties. The most immediate example is the second-order term in the strain tensor that we already encountered in linear elasticity.

In addition to these geometric non-linearities, additional non-linear effects may be introduced as a result of specific material properties. A particularly important example for biogels is that of strain hardening. This refers to an increase of the differential shear modulus under increasing level of strain. Material non-linearities such as this have an entirely different origin than geometric non-linearities. Interestingly, some phenomena that result from the introduction of geometric non-linearities may actually be suppressed by material non-linearities, as we will see for the example of cavitation.

3.2 The Lagrangian versus Eulerian Formalisms

Finite-strain elasticity is typically formulated in one of two different, but ultimately equivalent, ways: the Lagrangian formalism and the Eulerian formalism. The language and notation used to describe these formalisms differs from source to source [7, 15, 16]

The Lagrangian formalism has its origins in traditional linear elasticity, and is well suited to describing elastostatics. As before, the internal configuration of the body is described by the positions of material elements that form a coarse-grained description of the underlying molecular structure, and physical quantities are expressed as functions of these "reference" positions. The Eulerian formalism, meanwhile, has its origins in fluid mechanics. Rather than follow material elements around, we instead keep track of how much material is present, and how fast it is moving, at every location in physical space at any given time. This makes the Eulerian formalism a naturally dynamic formalism.

3.3 The Reference and Deformed Spaces

Regardless of which formalism one uses, it is useful to keep track of the material elements, where they started, and where they are currently. We define the reference configuration of the material to be a state with neither internal nor external stresses, which we treat as the initial configuration of the system. By assumption, the material elements are uniformly distributed in this state. We denote the set of positions of each material element in the reference state by $\mathcal{B}_0$. When the material is exposed to external stress, it deforms into a new configuration $\mathcal{B}$. This deformation is described by a continuous, bijective mapping of each position $\vec{x} \in \mathcal{B}_0$ in the reference configuration to a new position $\vec{X} \in \mathcal{B}$ in the deformed configuration,

$$\varphi : \vec{x} \mapsto \vec{X} \tag{16}$$

referred to as the deformation mapping or deformation map form here on. While

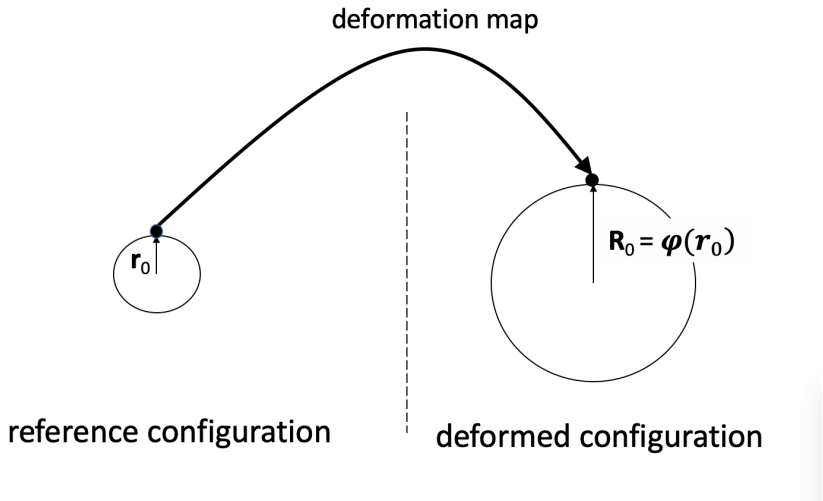

Figure 1: Schematic deformation map of a spherical cavity that has a radius r_0 in a strain-free reference configuration. When pressurized, the radius of the cavity increases to R_0. The deformation map $\varphi(r)$ relates points in the reference configuration to points in the deformed configuration. The figure shows the mapping for the case of a point on the cavity surface

I have used vector notation for $\vec{x}$ and $\vec{X}$ here, there is some controversy in the finite-strain elasticity literature as to whether they should be treated as actual vectors. This comes from a difference in what physicists usually mean when they say vector, versus what a mathematician, particularly a differential geometer, means.

In the language of differential geometry, we refer to $\mathcal{B}_0$ and $\mathcal{B}$ as Riemannian manifolds. To give a concrete definition of this, we first need to give a few definitions of some simpler structures [12]. A topological space is a set S, together with a collection of subsets of S, $\mathcal{T}$, called a topology on S. The members of $\mathcal{T}$ are called open subsets of S. Elements of a topological space are typically referred to as "points."

A topological manifold, or simply manifold, M is a special kind of topological

space that has three additional properties:

(1) M is a Hausdorff space: for every pair of points $x, y \in M$, there exist disjoint open subsets $U, V \subseteq M$ such that $p \in U$ and $q \in V$.

(2) M is second-countable: there exists a countable basis for the topology of M.

(3) M is locally Euclidean: each point of M has a neighborhood (an open subset that contains it) that is homeomorphic to an open subset of Euclidean space $\mathbb{R}^n$, i.e. there exists a homeomorphism mapping the neighborhood to some open subset of $\mathbb{R}^n$.

The manifold being locally Euclidean allows us to describe points in the manifold via coordinates in $\mathbb{R}^n$ using the homeomorphisms mentioned above, which are known as coordinate charts, or simply charts. Charts generally only have subsets of M as their domains - multiple charts are typically needed to cover the entirety of the manifold. A collection of charts whose domains cover M is known as an atlas of M. Given two charts φ and ψ with domains U and V that are not disjoint, $U \cap V \neq \emptyset$, the composite map $\psi \circ \varphi^{-1}$ is called a transition map from φ to ψ. If the transition map is a diffeomorphism, then the two charts are said to be smoothly compatible. An atlas $\mathcal{A}$ is called a smooth atlas if any two charts in $\mathcal{A}$ are smoothly compatible.

A differentiable, or smooth, structure on M is a smooth atlas that is not contained within any larger smooth atlas. A differentiable, or smooth manifold, is then a manifold paired with a differentiable structure. One can think of a differentiable structure as a prescription for how to differentiate functions defined on the manifold. A Riemannian manifold is a differentiable manifold with one additional piece of information, namely a metric. A metric allows one to define the concept of distance between any two points in the manifold, and is defined either globally in terms of a distance function, or locally in terms of a metric tensor.

Given a finite-dimensional vector space V, any norm on V determines a topology with a natural differentiable structure associated with it. This turns V into a differentiable manifold. However, given a differentiable manifold M, there is no similarly natural way to define vector space operations on it. Of course, in most physical applications, manifolds like the reference or deformed spaces can be thought of as subspaces of $\mathbb{R}^3$, and thus may be interpreted as vector spaces. Even so, it is important to distinguish between the vectors that describe points on the manifold, and vectors that live in tangent and cotangent spaces on the manifold, as these are fundamentally different kinds of objects.

As mentioned at the start of this section, the reference space $\mathcal{B}_0$ and the deformed space $\mathcal{B}$ are two distinct differentiable manifolds. This has an immediate, and very important, consequence: we can no longer properly define the displacement vector of a material element. After all, $\vec{x}$ and $\vec{X}$ now live in two entirely different vector spaces. Not only this, but tensors defined on the reference space and those defined on the deformed space must now also be considered as living in distinct spaces, and cannot be directly compared. In all that follows, vectors and tensors defined in or on the reference space will carry Greek indices, while vectors and tensors defined in or on the deformed space will carry Latin indices. We will also be using a curvilinear coordinate sytem for both spaces, with $g_{\alpha\beta}$ the metric tensor of the reference space and G_{ij} that of the deformed space. Covariant derivatives in the reference space will be denoted as $\frac{D}{Dx^\alpha}$, while those in the deformed space will be denoted as $\frac{D}{DX^i}$. The associated Christoffel symbols are $\Gamma^\alpha_{\beta\gamma}$ and $\bar{\Gamma}^i_{jk}$, respectively. When working with tensorial quantites, indices will be raised or lowered using the two metric tensors.

3.4 The Lagrangian Formalism

3.4.1 The Deformation Mapping and the Deformation Gradient Matrix

In the Lagrangian formalism, we follow the motion of material elements, each labelled by their position in the reference configuration $\vec{x} \in \mathcal{B}_0$. The deformation is described by the deformation mapping, defined in the previous section. Physical quantities will always be written as functions of $\vec{x}$, and will ultimately be constructed from the deformation map and its derivatives.

Consider a line element in the reference space dx^α. This is transformed into a new line element dX^i in the deformed space by the local deformation gradient matrix:

$$dX^i = A^i{}_\alpha dx^\alpha \tag{17}$$

with

$$A^i{}_\alpha \equiv \frac{\partial \varphi^i}{\partial x^\alpha} \tag{18}$$

Note the mixed indices of the deformation gradient matrix - it has both a Greek, reference space index, and a Latin, deformed space index. As such, it is not a proper tensor in either space. The engineering literature refers to this kind of object as a "two-point tensor."

It is often useful to, using the polar decomposition theorem, write the deformation gradient matrix as the product of a rotation matrix R and symmetric, positive-definite matrices U and V, referred to as the left and right stretch tensors respectively:

$$A^i{}_\alpha = R^i{}_\beta U^\alpha_\beta = V^i_j R^j{}_\alpha \tag{19}$$

Note that U is defined on the reference space, while V is defined on the deformed space. These two matrices have identical eigenvalues, denoted $\lambda_{i=1,2,3}$, which

correspond to the principal stretch ratios in the sense that a spherical volume in the reference space is transformed into an ellipsoid in the deformed space whose principal axes are along the direction of the eigenvectors, while the stretching ratios along the principal axes are λ_i. The scalar invariants that enter the free-energy are often written in terms of the principal stretches in the engineering literature.

3.4.2 The Green-Lagrange Strain Tensor

The norm-squared of the line element $d\vec{x}$ transforms as

$$\left|d\vec{X}\right|^2 = A^{i\alpha}A_{i\beta}dx_\alpha dx^\beta = \left(2\mathcal{U}^\alpha_\beta + \delta^\alpha_\beta\right)dx_\alpha dx^\beta \tag{20}$$

Here

$$\mathcal{U}^\alpha_\beta \equiv \frac{1}{2}\left(A^{i\alpha}A_{i\beta} - \delta^\alpha_\beta\right) \tag{21}$$

is the Green-Lagrange strain tensor defined on the reference space. It is the non-linear equivalent of the strain tensor of linear elasticity. In the limit of small deformations, we no longer make a distinction between the reference and deformed spaces, allowing us to use Latin indices for both. We may thus write

$$A^i{}_j = \frac{\partial\varphi^i}{\partial x^j} = \frac{\partial u^i}{\partial x^j} + \delta^i_j \tag{22}$$

where $\vec{u}$ is the displacement vector of linear elasticity. This allows us to re-write the Green-Lagrange strain tensor in terms of $\vec{u}$, revealing it to be identical to the original definition of the strain tensor

$$\mathcal{U}^\alpha_\beta = \frac{1}{2}\left(\frac{\partial u^i}{\partial x^j} + \frac{\partial u_j}{\partial x_i} + \frac{\partial u^k}{\partial x^j}\frac{\partial u_k}{\partial x_i}\right) = u^i_j + O\left(u^2\right) \tag{23}$$

where u^i_j is the linearized strain tensor of linear elasticity [10].

3.4.3 Volume and Area Elements

Consider a volume element in the reference space dv. This will transform under the deformation into a new volume element dV in the deformed space by $dV = Jdv$, where $J = \det A$ is the Jacobian of the deformation map. Conservation of mass allows us to write J in terms of the local densities of the material before and after the deformation,

$$\rho dV = \rho_0 dv \Rightarrow J = \frac{\rho_0}{\rho} \tag{24}$$

so $J = 1$ for incompressible systems. For convenience, the ratio $\rho_r = \frac{\rho}{\rho_0} = \frac{1}{J}$ will be referred to as the relative density. The Jacobian can be expressed as $J = \det A = \det U = \det V = \lambda_1\lambda_2\lambda_3$. In the limit of small deformations, we may approximate this as

$$\begin{aligned} J = \det A = \sqrt{\det\left(A^{\mathrm{T}}A\right)} = \sqrt{\det\left(2\mathcal{U} + I\right)} \\ = 1 + \operatorname{tr} u + O\left(u^2\right) \end{aligned} \tag{25}$$

recovering the result from linear elasticity that a volume-preserving deformation would correspond to a traceless linearized strain tensor. Note, however, that this will no longer be true outside of the small deformation limit - $\operatorname{tr} \mathcal{U}$ will be non-zero even for a volume-preserving shear.

Now consider a surface element in the reference space $d\vec{s} = ds\ \hat{n}$ with unit normal vector $\hat{n}$, as well as a line element $d\vec{x}$. Together, we can build a volume element $dx^\alpha ds_\alpha$, which will transform under deformation as

$$dX^i dS_i = J dx^\alpha ds_\alpha \tag{26}$$

where $dX^i = A^i{}_\alpha dx^\alpha$. This gives for the transformed area element

$$dS^i = J\left(A^{-1}\right)^i_\alpha ds^\alpha \tag{27}$$

where A^{-1} is the inverse deformation gradient matrix:

$$\left(A^{-1}\right)^\alpha_i \equiv \frac{\partial\left(\varphi^{-1}\right)^\alpha}{\partial X^i} \tag{28}$$

3.4.4 The Nonlinear Shear Strain Tensor

For large deformations, the Jacobian will no longer be well approximated by one plus the trace of the Green-Lagrange strain tensor. As such, the shear strain tensor must be constructed differently. To do this, let's first write a general deformation mapping φ as the product of two successive mappings:

$$\varphi\left(\vec{x}\right) = \varphi_{\text{shr}}\left(\varphi_{\text{cmp}}\left(\vec{x}\right)\right) \tag{29}$$

The first map φ_{cmp} is here a pure dilation given by

$$\varphi_{\text{cmp}}\left(\vec{x}\right) = J^{1/3}\vec{x} \tag{30}$$

with J the Jacobian of the full deformation φ. The second map φ_{shr} is a volume-preserving shear. Using the chain rule, the deformation gradient matrix of the full map φ is

$$A^i{}_\alpha = \frac{\partial\varphi^i_{\text{shr}}}{\partial\varphi^j_{\text{cmp}}}\frac{\partial\varphi^j_{\text{cmp}}}{\partial x^\alpha} = J^{1/3}\bar{A}^i{}_\alpha \tag{31}$$

The new deformation gradient matrix $\bar{A}$ is volume-preserving since

$$\det\bar{A} = \det\left(J^{-1/3}A\right) = \frac{1}{J}\det A = 1 \tag{32}$$

The associated Green-Lagrange shear strain tensor is then given by

$$\begin{aligned}\bar{\mathcal{U}}^{\alpha}_{\beta} = \frac{1}{2}\left(\bar{A}^{i\alpha}\bar{A}_{i\beta} - \delta^{\alpha}_{\beta}\right) = \frac{1}{2}\left(J^{-2/3}A^{i\alpha}A_{i\beta} - \delta^{\alpha}_{\beta}\right) \\ = J^{-2/3}\mathcal{U}^{\alpha}_{\beta} + \frac{1}{2}\left(J^{-2/3} - 1\right)\delta^{\alpha}_{\beta}\end{aligned} \tag{33}$$

While this non-linear shear strain tensor is volume-preserving, it is - unlike its linearized counterpart - not traceless. For completeness, we confirm that this non-linear shear strain tensor correctly simplifies to its traceless linear counterpart in the limit of small deformations as follows:

$$\begin{aligned}\bar{\mathcal{U}}^{\alpha}_{\beta} = (1 + \text{tr } u)^{-2/3}\, u^{\alpha}_{\beta} + \frac{1}{2}\left[(1 + \text{tr } u)^{-2/3} - 1\right]\delta^{\alpha}_{\beta} + O\left(u^2\right) \\ = u^{\alpha}_{\beta} - \frac{1}{3}\delta^{\alpha}_{\beta}\text{tr } u + O\left(u^2\right) = \bar{u}^{\alpha}_{\beta} + O\left(u^2\right)\end{aligned} \tag{34}$$

3.4.5 Stress Tensors

An important part of finite-strain elasticity theory are the definitions of the different stress tensors that can enter the equation for mechanical equilibrium. The variational method we use for the static case does not involve the stress tensor, but it will be useful for potential extensions to dynamics. The basic definition of the stress tensor is identical to that used in linear elasticity - if a force $\vec{T}$ is acting on a surface element $d\vec{S} = dS\ \hat{N}$, then the Cauchy stress tensor at the location of the surface element is defined such that $T^i = \sigma^{ij}dS_j$. The Cauchy stress tensor is defined in the deformed space, the physical space in which external and internal forces are being applied. When external stresses or pressures are applied to the surface of the material then the Cauchy stress tensor provides a direct approach to implement boundary conditions. However, within the Lagrangian formalism, it is useful to also construct a stress tensor in terms of the coordinates of the undeformed reference space.

We start from the integral equation of mechanical equilibrium, given in equation

10. We would like to change variables in this equation to those of the undeformed space. Recall that volume and area elements transform under the deformation as $dV = Jdv$ and $dS_i = J\left(A^{-1}\right)^{\alpha}_{\ i} ds_\alpha$. We thus may write, now integrating over the reference space,

$$\int_{\mathcal{B}_0} dv\, JB^i + \oint_{\partial\mathcal{B}_0} ds\, J\left(A^{-1}\right)^{\alpha}_{\ j} n_\alpha \sigma^{ij} = 0 \tag{35}$$

where $B^i(\vec{x}) = b^i\left(\varphi^{-1}\left(\vec{X}\right)\right)$ is the body force per unit volume written as a function of the reference space coordinates. Define the first Piola-Kirchoff stress tensor $S^{i\alpha} \equiv J\left(A^{-1}\right)^{\alpha}_{\ i}\sigma^{ij}$. Note that, due to its mixed indices, this is not a standard tensor in either space, but rather a "two-point tensor," similar to the deformation gradient matrix. Using the divergence theorem, this can be expressed as a local equation for mechanical equilibrium:

$$\frac{DS^{i\alpha}}{Dx^\alpha} + JB^i = 0 \tag{36}$$

The engineering literature typically refers to the first Piola-Kirchoff stress tensor as the "Piola transform" of the Cauchy stress tensor, and the change of variables we performed in the integral equation as a "Piola transformation."

While the first Piola-Kirchoff stress tensor suffices for most circumstances, it is also useful to define another stress tensor, one that lives entirely within the reference space - i.e., one that is not a two-point tensor with mixed indices, but rather a standard rank-two tensor on the reference space. Using the language of differential geometry, we can "pull back" the first Piola-Kirchoff stress tensor to the reference space:

$$s^{\alpha\beta} \equiv \left(A^{-1}\right)^{\alpha}_{\ i} S^{i\beta} = J\left(A^{-1}\right)^{\alpha}_{\ i}\sigma^{ij}\left(A^{-1}\right)^{\beta}_{\ j} \tag{37}$$

The tensor s is known as the second Piola-Kirchoff stress tensor. This tensor is particularly useful for relating the equation of mechanical equilibrium to the free-energy. In linear elasticity, equation 13 showed that the stress and strain tensors are thermodynamically conjugate, and as such the stress tensor could be written as a derivative of the free-energy density. In finite-strain elasticity, however, this is no longer the case. This is because the Cauchy stress and the Green-Lagrange strain tensors no longer live in the same vector space - in fact, one can show that the Cauchy stress does not, in fact, have a thermodynamically conjugate tensor. We can, however, still construct a tensor that is thermodynamically conjugate to the Green-Lagrange strain. This tensor, it turns out, is the second Piola-Kirchoff stress tensor. Suppose we make a small change to the deformation map, $\varphi \to \varphi + \delta\varphi$. This will result in changes to the deformation gradiant matrix and Green-Lagrange strain tensors:

$$\delta A^i{}_\alpha = \frac{\partial \delta\varphi^i}{\partial x^\alpha} \tag{38}$$

$$\delta \mathcal{U}_{\alpha\beta} = \frac{\partial \mathcal{U}_{\alpha\beta}}{\partial A^j{}_\gamma} \delta A^j{}_\gamma = A^i{}_\alpha \delta A_{i\beta} \tag{39}$$

The contribution to the free-energy from internal stresses will thus change as

$$\delta F = \int_{\mathcal{B}_0} dv \; \frac{DS^{i\alpha}}{Dx^\alpha} \delta\varphi_i \tag{40}$$

Integrating by parts and assuming the first Piola-Kirchoff stress goes to zero at infinity, we obtain

$$\delta F = -\int_{\mathcal{B}_0} dv \; S^{i\alpha} \delta A_{i\alpha} \tag{41}$$

which shows that the first Piola-Kirchoff stress is thermodynamically conjugate to the deformation gradient matrix. Using equation 39, we can also re-write

this as

$$\delta F = -\int_{\mathcal{B}_0} dv\ s^{\alpha\beta}\delta\mathcal{U}_{\alpha\beta} \tag{42}$$

thus showing that the second Piola-Kirchoff stress is thermodynamically conjugate to the Green-Lagrange strain.

3.4.6 Elastic Free-Energy Densities and the Neo-Hookean Model

In finite-strain elasticity theory, the free-energy density of a material is, in general, expressed as a combination of scalar invariants obtained from the Green-Lagrange strain tensor $\mathcal{U}$. A major difference from linear elasticity, however, is that many models make use of the lowest-order invariant, tr $\mathcal{U}$. The equivalent invariant in linear elasticity, tr u, is linear in the displacement gradient and, as such, is excluded from the free-energy to ensure the stability of the strain-free state. In finite-strain elasticity, however, it is important to remember that the Green-Lagrange strain is an inherently non-linear object and, for specific kinds of materials, tr $\mathcal{U}$ may be minimized in the strain-free state.

There are many different model for the free-energy density that are used in the engineering literature, each specialized for different kinds of materials. The most common model is the Neo-Hookean model, which was originally designed to describe rubber elasticity. In the traditional Neo-Hookean model, the free-energy density is given by

$$f_{\mathrm{NH}} = \mu \mathrm{tr}\ \mathcal{U} = \frac{1}{2}\mu\left(\sum_{i=1}^{3}\lambda_i^2 - 3\right) \tag{43}$$

Here, the invariant $\sum_{i=1}^{3}\lambda_i^2$ is usually referred to as I_1 in the literature. While this model is attractive for is mathematical simplicity, it is no longer appropriate for highly compressible materials.

Another common model is the St. Venant-Kirchhoff model, which uses a direct

extension of the free-energy of linear elasticity:

$$f_{\mathrm{VK}} = \frac{1}{2}\lambda \left(\mathrm{tr}\ \mathcal{U}\right)^2 + \mu \mathrm{tr}\left(\mathcal{U}^2\right) \tag{44}$$

While more general than the traditional Neo-Hookean model, the St. Venant-Kirchhoff model is unable to be cleanly split into independent shear and compression terms - in finite-strain elasticity, the Jacobian J is no longer well approximated by $1 + \mathrm{tr}\ \mathcal{U}$.

For our work, we first made use of a model that generalized the Neo-Hookean model so as to be appropriate for highly compressible materials, which we call the modified Neo-Hookean model. Our goal was to write a free-energy density that was a sum of two terms - a term dependent only on the relative density ρ_r associated purely with compression, and a term associated purely with shear. Contributions to the free-energy that only depend on the relative density can be expressed in terms of $J = 1/\rho_r$. Meanwhile, free-energy densities associated purely with shear strain can be constructed from invariants of the shear strain tensor $\bar{\mathcal{U}}$ defined in equation 33. The lowest order invariant of $\bar{\mathcal{U}}$ is again its trace:

$$\mathrm{tr}\ \bar{\mathcal{U}} = \frac{1}{2}\left(J^{-2/3}\sum_{i=1}^{3}\lambda_i^2 - 3\right) \tag{45}$$

Thus, we take as our free-energy density

$$f_{\mathrm{MNH}} = \mu' \mathrm{tr}\ \bar{\mathcal{U}} + \frac{1}{2}\kappa' \frac{1}{J}\left(1 - J\right)^2 \tag{46}$$

where μ' and κ' are constants. Our choice for the compression term comes from the typical equation of state for compressible materials - it can be expressed in the deformed space as $\frac{\kappa'}{2}\left(\frac{\rho}{\rho_0} - 1\right)^2$. The factor $\frac{1}{J}$ is normally not included in the engineering literature when a term of this type is used, but that is not appropriate for highly compressible materials - it must be included to allow for

the transformation of volume elements when going from the deformed to the reference space.

The constants μ' and κ' may be identified by going to the limit of infinitesimal deformation. To second order, first note that

$$J = 1 + \text{tr } u + \frac{1}{2}\left[(\text{tr } u)^2 - \text{tr}\left(u^2\right)\right] + O\left(u^3\right) \tag{47}$$

The compression term may then be expanded to second order, obtaining

$$\frac{1}{2}\kappa'\frac{1}{J}(1-J)^2 = \frac{1}{2}\kappa'(\text{tr } u)^2 + O\left(u^3\right) \tag{48}$$

Clearly, κ' may be identified with the bulk modulus of linear elasticity, κ. As for the shear term, first note that

$$J^{-2/3} = 1 - \frac{2}{3}\text{tr } u + \frac{1}{3}\left[\frac{2}{3}(\text{tr } u)^2 + \text{tr}\left(u^2\right)\right] + O\left(u^3\right) \tag{49}$$

Plugging this into equation 33 and expanding, we find

$$\mu'\text{tr } \bar{\mathcal{U}} = \mu'\text{tr}\left(\bar{u}^2\right) + O\left(u^3\right) \tag{50}$$

where $\bar{u}^\alpha_\beta = u^\alpha_\beta - \frac{1}{3}\delta^\alpha_\beta \text{tr } u$ is the traceless part of the linearized strain tensor. It follows that one can equate μ' with the shear modulus of linear elasticity, μ.

3.4.7 Strain Hardening

Thus far, we have only discussed those non-linearities that are inherent to elasticity, introduced due to the distinction between the reference and deformed spaces. These "geometric" non-linearities are not, however, the only non-linearities we could introduce. Many materials have additional non-linearities that result from their material properties. One such example of particular im-

portance in biogels is that of shear strain hardening. Following Shokef and Safran [21], one can extend the expression for the shear strain free-energy to include shear hardening by imposing a maximum shear strain $1/\eta$ through

$$\begin{aligned} f_s &= \mu \text{tr}\, \bar{\mathcal{U}} \frac{1}{1 - \eta \text{tr}\, \bar{\mathcal{U}}} \\ &\simeq \mu \text{tr}\, \bar{\mathcal{U}} \left(1 + \eta \text{tr}\, \bar{\mathcal{U}} + \eta^2 \left(\text{tr}\, \bar{\mathcal{U}}\right)^2 + \dots\right) \end{aligned} \tag{51}$$

It should be noted that, in a more general approach, the coefficients in the geometric series above may be different for each term. For the work discussed here, we will not be doing this, and instead simply use equation 37 unmodified.

3.4.8 The Flory-Huggins Model

While the modified neo-Hookean model is useful in providing insight into how compressiblity affects the kind of systems that are well studied in the engineering literature, such as rubber elasticity, the area of actual interest to us is that of polymer gels. Of particular interest is the cytoskeleton, which consists of a network of actin filaments. From the viewpoint of finite-strain elasticity, there is an important new ingredient when it comes to polymer gels. A cross-linked polymer gel placed in a one-component solvent can swell or shrink by absorbing or releasing solvent. On the one hand, in good solvent the free energy associated with volume interactions between the monomers and the solvent molecules decreases under swelling. On the other hand, swelling stretches the polymer chains, which reduces the entropic configurational entropy. In the state of swelling equilibrium, the swelling pressure is balanced by the elastic stress of the stretched polymers [3, 20]. It should be noted that the state of swelling equilibrium is not stress-free. As a result, it cannot be used as the reference frame. In the theory of gel elasticity, the stress-free reference state is actually the dry, solvent-free gel. With no solvent, there is no stretching of the polymer

chains [4] and no surface energy.

To compute the elastic deformation free-energy $F[\varphi]$ of a polymer gel, we will use the Flory-Huggins mean-field theory of gels in which polymer chains are treated as ideal Gaussian chains composed of N_x identical segments [4]. It has been established that the physical properties of gels composed of flexible polymers are well described by Flory-Huggins theory, which can also be extended to include liquid-liquid phase separation [27].

In Flory-Huggins theory, the free-energy density is the sum of the entropic elasticity free-energy of the Gaussian chains and the mixing free-energy of the monomers [3, 20]:

$$f_{\mathrm{FH}} = C_1(\phi)\,\mathrm{tr}\,\mathcal{U} + \frac{k_B T}{w}\left[(1-\phi)\log(1-\phi) + \chi\phi(1-\phi)\right] \tag{52}$$

where we have followed the notation of references [3, 4]. Here, ϕ is the volume fraction of monomers, where $\phi = 1$ in the state of the dry, solvent-free gel. If we take the dry, solvent-free state as the reference state, then $\phi = \frac{1}{J}$ - it is equivalent to the relative density ρ_r. Next, $C_1(\phi) = \frac{k_B T \phi}{w N_x}$, where w is the volume per Kuhn segment of the polymer chains. $\mathcal{U}$ is, as before, the Green-Lagrange strain tensor of finite-strain elasticity theory, which will be equal to zero in the dry state. It will be useful to write $\mathrm{tr}\,\mathcal{U}$ in terms of the principal stretch ratios λ_i, as in equation 45. For a uniformly swollen gel, the stretch ratios are equal to each other and to $\phi^{-1/3}$ because of mass conservation. Hence $\mathrm{tr}\,\mathcal{U} = \frac{3}{2}\left(\phi^{-2/3} - 1\right)$ for a uniformly swollen gel. Finally, χ is the Flory χ parameter. For good solvents, the Flory parameter is less than 1/2. Note that equation 52 gives the free-energy in the *deformed* space, rather than the reference space. Note also that, unlike the modified neo-Hookean elastic free-energy, the Flory-Huggins free-energy density is *not* the sum of separate shear and compression term, since the first term of f_{FH} describes simultaneously the energy cost of stretching the

polymers both under shear strain and under isotropic swelling.

The state of swelling equilibrium is found by minimizing the free-energy density in the reference space, $f_{\rm FH}/\phi$, with respect to ϕ. The appearance of the factor $1/\phi$ is understood here by noting that the volume element dV in the physical space of the swollen gel transforms to the volume element $dv = \phi dV$ in the dry gel. Minimizing $f_{\rm FH}/\phi$ with respect to ϕ gives, for $N_x \gg 1$, the result that

$$\phi_{\rm eq} \simeq \left[\left(\frac{1}{2} - \chi\right) N_x\right]^{-3/5} \tag{53}$$

This same result is obtained if one sets the osmotic pressure $\Pi(\phi)$ of the gel to zero, where

$$\Pi(\phi) = \phi^2 \frac{d\left(f_{\rm FH}/\phi\right)}{d\phi} = -\frac{k_B T}{w}\left[\left(\chi\phi + 1\right)\phi + \log\left(1-\phi\right) + \frac{\phi^{1/3}}{N_x}\right] \tag{54}$$

It the deformation away from the state of swelling equilibrium is infinitesimal, then the free-energy density associated with the deformation has the same form as the elastic free-energy density of uniform materials that obey linear elasticity (Eq. 7). The shear modulus is given by

$$\mu = \frac{k_B T}{w N_x}\phi^{1/3} \tag{55}$$

and the osmotic modulus $\kappa = \phi\frac{d\Pi}{d\phi}$ by

$$\kappa = \frac{k_B T}{w}\left(\left(\frac{1}{1-\phi} - 2\chi\right)\phi^2 - \frac{\phi^{1/3}}{3N_x}\right) \tag{56}$$

[4]. For a Flory-Huggins gel, shear and bulk moduli are thus replaced as control parameters by the number of polymer segments N_x per link and the Flory χ parameter, the latter being a measure of the solubility of the polymers in terms of the majority component liquid.

We will also want to make use of a version of the Flory-Huggins model that includes shear strain hardening. Because in the Flory-Huggins free-energy density, shear strain, and expansion or compresion strain both contribute to the first term, we cannot include strain hardening only in the shear strain. We will include strain hardening by replacing the first term of f_{FH} by

$$C_1(\phi)\,\mathrm{tr}\,\mathcal{U}\left[1+\eta\mathrm{tr}\,\mathcal{U}+\eta^2\left(\mathrm{tr}\,\mathcal{U}\right)^2+\ldots\right] \tag{57}$$

3.5 The Eulerian Formalism

While the Lagrangian formalism is very well suited to systems in mechanical equilibrium, we will eventually want to apply finite-strain elasticity to solve problems for dynamical systems, particular visco-elastic ones. We will find that the Eulerian formalism is very well suited to these sorts of applications when we eventually discuss them in section 5. As such, this subsection contains a basic overview of the Eulerian formalism, as well as the machinery for translating between the Lagrangian and Eulerian formalisms [7, 11, 15, 16].

3.5.1 Fluid Mechanics

While the Lagrangian formalism is built off of the formalism of linear elasticity, the Eulerian formalism has its origins in fluid mechanics. As such, it is helpful to first review the basic formalism of fluid mechanics, before adapting it to finite-strain elasticity [11].

As in elasticity, a fluid is typically treated as a collection of material elements, forming a coarse-grained description of the underlying molecular structure. However, rather than labelling these fluid elements by their positions in a reference frame, we instead use the coordinates of the ambient physical space in which the fluid exists. The motion of the fluid itself is described in terms of

multiple fields. The first is the velocity field $\vec{V}\left(\vec{X},t\right)$, which tells us the velocity of the fluid element located at spatial position $\vec{X}$ at time t. In addition to this, the density $\rho\left(\vec{X},t\right)$ is typically given. Again, these fields are all written as functions of spatial position, rather than in terms of a reference space. It should also be noted that we have included explicit time dependence - the use of the velocity field necessitates this. The Eulerian formalism is thus a naturally dynamic formalsim.

From here, equations of state relating the $\vec{V}$, ρ, and various thermodynamic quantities may be derived. First, consider a given region of space $\mathcal{B}$ occupied by a portion of the fluid. The total mass contained in this region is $\int_{\mathcal{B}} dV\ \rho$. There are two ways to express the rate of change of this quantity - we may directly take its time derivative, or we may calculate the amount of mass flowing into or out of this region per unit time using the velocity field:

$$\frac{\partial}{\partial t}\int_{\mathcal{B}} dV\ \rho = -\oint_{\partial\mathcal{B}} dS_i\ \rho V^i \tag{58}$$

where $d\vec{S} = dS\hat{n}$ is a surface area element, with $\hat{n}$ the unit normal to the surface. Using the divergence theorem, we obtain a local form of this equation, known as the equation of continuity:

$$\frac{\partial\rho}{\partial t} + \frac{D}{Dx^i}\left(\rho V^i\right) = \frac{\partial\rho}{\partial t} + \rho\frac{DV^i}{Dx^i} + V^i\frac{\partial\rho}{\partial x^i} = 0 \tag{59}$$

Now, before continuing, it will be important to briefly discuss a subtlety regarding time differentiation in the Eulerian formalism. This topic will be discussed in more detail in section 5, but for now, consider the rate of change of a *particular* fluid element's velocity. This quantity is known in the Eulerian formalism as a material derivative, and is naturally defined in a Lagrangian frame of reference as simply $\frac{\partial}{\partial t}\vec{v}(\vec{x},t)$, where $\vec{x}$ is now the position of the material element in the

reference frame. Here $\vec{v}\,(\vec{x},t)$ is referred to as the material velocity. Changing variables to the spatial frame, we find that this becomes

$$\frac{DV^i}{Dt} = \frac{\partial V^i}{\partial t} + V^j \frac{DV^i}{DX^j} \tag{60}$$

When working in the Eulerian formalism, we will denote material time derivatives by $\frac{D}{Dt}$. Notice that the equation of continuity may also be written in terms of a material derivative:

$$\frac{D\rho}{Dt} + \rho \frac{DV^i}{DX^i} = 0 \tag{61}$$

Here $\frac{D\rho}{Dt}$ represents the rate of change of the density of a particular fluid volume element.

Next, consider a specific collection of fluid elements, which occupy a space $\mathcal{B}_t \subset \mathbb{R}^3$ at time t. Note that this is not a fixed region of space - $\mathcal{B}_t$ will change over time as the fluid flows. For a compressible fluid, its volume may not even stay fixed. Assume the fluid experiences a body force per unit volume $\vec{b}\,(\vec{x},t)$ and a contact force per unit area $\vec{t}\,(\vec{x},t)$. As in elasticity, we make the assumption that we can write $\vec{t}$ in terms of a stress tensor, $t^i = \sigma^i_j \hat{N}^j$, analogous to the Cauchy stress. Momentum conservation gives us that

$$\frac{d}{dt}\int_{\mathcal{B}_t} dV\ \rho V^i = \int_{\mathcal{B}_t} dV\ b^i + \oint_{\partial\mathcal{B}_t} dS\ \sigma^{ij}\hat{N}_j \tag{62}$$

Unlike in section 3.4.5, we are not in mechanical equilibrium, and thus cannot set the right-hand side of equation 62 to zero. If we wish to derive a local form of this equation, we will need to evaluate this time derivative. To do so, it is actually convenient to temporarily go back to a Lagrangian frame of reference. Let $\mathcal{B}_0$ be the configuration of the system at time $t = 0$, which we will treat as the Lagrangian reference state, and let $\varphi\,(\vec{x},t) : \mathcal{B}_0 \times \mathbb{R} \to \mathbb{R}^3$ be the deformation map that takes positions in $\mathcal{B}_0$ to their new positions at time t. We will assume

that, at a fixed time t, the map $\varphi_t(\vec{x}) = \varphi(\vec{x}, t)$ is smooth and bijective, and thus has a smooth inverse map $\varphi_t^{-1}\left(\vec{X}\right)$. Consider an integral of the form

$$\int_{\mathcal{B}_t} dV\ f\left(\vec{X}, t\right) \tag{63}$$

Changing variables, we obtain

$$\int_{\mathcal{B}_0} dv\ J(\vec{x}, t)\, f(\varphi(\vec{x}, t), t) \tag{64}$$

where J is the Jacobian as defined in section 3.4.3. We thus have

$$\begin{aligned}\frac{d}{dt}\int_{\mathcal{B}_t} dV\ f\left(\vec{X}, t\right) = \int_{\mathcal{B}_0} dv \Bigg[& \frac{\partial J}{\partial t} f(\varphi(\vec{x}, t)) + J\ \frac{\partial f}{\partial t}\bigg|_{\vec{X}=\varphi(\vec{x},t)} \\ & + J\ \frac{\partial f}{\partial X^i}\bigg|_{\vec{X}=\varphi(\vec{x},t)} \frac{\partial \varphi^i}{\partial t}\Bigg]\end{aligned} \tag{65}$$

Here $\frac{\partial \varphi^i}{\partial t}$ is simply the velocity of the material element, $v^i(\vec{x}, t) = V^i\left(\varphi_t^{-1}\left(\vec{X}\right), t\right)$. As for the time derivative of the Jacobian, we have

$$\begin{aligned}\frac{\partial}{\partial t} J(\vec{x}, t) &= J\left(A_t^{-1}\right)^{\alpha}_{\ i} \frac{\partial}{\partial t} A^i_{\ \alpha}(\vec{x}, t) = J\left(A_t^{-1}\right)^{\alpha}_{\ i} \frac{\partial^2 \varphi^i}{\partial t \partial x^\alpha} \\ &= J \frac{\partial\left(\varphi_t^{-1}\right)^{\alpha}}{\partial X^i} \frac{\partial v^i}{\partial x^\alpha} = J\ \frac{DV^i}{DX^i}\bigg|_{\vec{X}=\varphi(\vec{x},t)}\end{aligned} \tag{66}$$

Therefore,

$$\begin{aligned}\frac{d}{dt}\int_{\mathcal{B}_t} dV\ f &= \int_{\mathcal{B}_0} dv\ J\left[\frac{\partial f}{\partial t} + V^i \frac{\partial f}{\partial X^i} + f \frac{DV^i}{DX^i}\right]_{\vec{X}=\varphi(\vec{x},t)} \\ &= \int_{\mathcal{B}_t} dV \left[\frac{\partial f}{\partial t} + V^i \frac{\partial f}{\partial X^i} + f \frac{DV^i}{DX^i}\right]\end{aligned} \tag{67}$$

This is known as the transport theorem. We will derive a more general form of this equation in section 3.5.7. Applying equation 67 to the momentum density

ρV^i, we obtain

$$\frac{d}{dt}\int_{\mathcal{B}_t} dV\ \rho V^i = \int_{\mathcal{B}_t} dV\left[\frac{\partial}{\partial t}\left(\rho V^i\right) + V^j\frac{\partial}{\partial X^j}\left(\rho V^i\right) + \rho V^i\frac{DV^j}{DX^j}\right] \tag{68}$$

Hence

$$\frac{D}{Dt}\left(\rho V^i\right) + \rho V^i\frac{DV^j}{DX^j} = b^i + \frac{D\sigma^{ij}}{DX^j} \tag{69}$$

Note that, using the equation of continuity,

$$\frac{D}{Dt}\left(\rho V^i\right) = \frac{D\rho}{Dt}V^i + \rho\frac{DV^i}{Dt} = \rho\left(\frac{DV^i}{Dt} - V^i\frac{DV^j}{DX^j}\right) \tag{70}$$

This allows us to simplify equation 69, obtaining

$$\rho\frac{DV^i}{Dt} = b^i + \frac{D\sigma^{ij}}{DX^j} \tag{71}$$

This equation is known as the Navier-Stokes equation, and is the equation of motion for a fluid.

For an isotropic fluid, the stress tensor σ^i_j is typically split into two pieces: the hydrostatic pressure $-p\delta^i_j$, and the "viscous" stress σ'^i_j, which results from internal friction between fluid elements. To lowest order in the velocity field, this viscous piece may be written as

$$\sigma'^i_j = \eta\left(\frac{DV^i}{DX^j} + \frac{DV_j}{DX_i} - \frac{2}{3}\delta^i_j\frac{DV^k}{DX^k}\right) + \zeta\delta^i_j\frac{DV^k}{DX^k} \tag{72}$$

where η and ζ are scalar coefficients independent of the velocity, referred to as the first and second viscosity coefficients, or just viscosities. For future convenience, we will define the spatial velocity gradient $K^i_{\ j} = \frac{DV^i}{DX^j}$, so that $\sigma'^i_j = \eta\left(K^i_{\ j} + K_j^{\ i} - \frac{2}{3}\delta^i_j\mathrm{tr}\ K\right) + \zeta\delta^i_j\mathrm{tr}\ K$. The symmetric part of K, $\Sigma = \frac{1}{2}\left(K + K^{\mathrm{T}}\right)$, is often referred to as the Eulerian strain rate in the engineering literature,

though it should be noted that it cannot be written as the time derivative of a strain tensor and, as such, is not really a strain rate itself. We will see, however, that it is the push-forward of the rate of change of the Green-Lagrange strain tensor onto the deformed space.

Assume that the viscosity coefficients are uniform throughout the fluid. Plugging equation 72 into the Navier-Stokes equation, we obtain the more familiar form of the equation for an isotropic, viscous fluid:

$$\rho \frac{DV^i}{Dt} = b^i - \frac{\partial p}{\partial X_i} + \eta \nabla^2 V^i + \left(\zeta - \frac{1}{3}\eta\right) \frac{D}{DX_i} \frac{DV^j}{DX^j} \tag{73}$$

where $\nabla^2 = \frac{D}{DX^i} \frac{D}{DX_i}$ is the Laplacian operator.

3.5.2 Lagrangian versus Eulerian Frame of Reference

As we dicussed in the previous ection, the Eulerian formalism has its origins in fluid dynamics, though many concepts from the Lagrangian formalism do still carry over. In particular, we still describe the configuration of a material at time t by Riemannian manifold $\mathcal{B}_t$, though now this manifold is interpreted as a subset of real space $\mathbb{R}^3$. Just as in the Lagrangian formalism, it is conventional to choose $t = 0$ to correspond to a stress and strain-free configuration, i.e. the reference configuration $\mathcal{B}_0$. However, it should be noted that, aside from the strain-free assumption, there is nothing special about $\mathcal{B}_0$, and it is to be treated on equal footing as any other configuration $\mathcal{B}_t$. In statics, this difference between the Lagrangian and Eulerian formalisms ultimately amounts to a difference in coordinates. In the case of dynamics, though, the difference becomes much more fundamental. We are no longer concerned with individual material elements, but rather with locations in real space.

3.5.3 The Time-Dependent Deformation Map

The deformation mapping of the Lagrangian formalism, $\varphi(\vec{x})$, maps the positions of material elements at $t = 0$ to their final positions. We can easily generalize this concept by introducing a time-dependent mapping $\varphi(\vec{x}, t) : \mathcal{B}_0 \times \mathbb{R} \to \mathbb{R}^3$. There are some subtleties introduced by making such a generalization, however. In the Lagrangian formalism, we made the assumption that the deformation map $\varphi(\vec{x}) : \mathcal{B}_0 \to \mathcal{B} \subset \mathbb{R}^3$ was smooth and bijective, allowing us to define a smooth inverse map $\varphi^{-1}\left(\vec{X}\right) : \mathcal{B} \to \mathcal{B}_0$. For a body that does not occupy all of real space, however, the range of the deformation map, i.e. the configuration $\mathcal{B}_t$, will now be time-dependent. this is why the time-dependent map is written as having a co-domain of $\mathbb{R}^3$ rather than $\mathcal{B}_t$ - at time t, the body may occupy positions it does not occupy at time t'. Mathematically, this means that the time-dependent deformation mapping will no longer be surjective in general. To facilitate the definition of the inverse map, we define the deformation map at fixed time t, $\varphi_t(\vec{x}) : \mathcal{B}_0 \to \mathcal{B}_t \subset \mathbb{R}^3$, which we may safely treat as bijective. Note this means that we cannot, in general, write a time-dependent inverse mapping $\varphi^{-1}\left(\vec{X}, t\right)$, only inverse mappings at fixed times, $\varphi_t^{-1}\left(\vec{X}\right)$.

The issue of the inverse mapping leads directly to a question regarding whether we may take its time derivative. While not important in the case of statics, this will be a very important question in the case of dynamics. We argue that, assuming the deformation map is smooth in both space and time, this derivative can still be well defined, though some care has to be taken. We define the time derivative of the inverse mapping φ_t^{-1} at the real space position $\vec{X}$ as:

$$\frac{\partial}{\partial t}\varphi_t^{-1}\left(\vec{X}\right) = \lim_{\delta t \to 0^+} \frac{\varphi_{t+\delta t}^{-1}\left(\vec{X}\right) - \varphi_t^{-1}\left(\vec{X}\right)}{\delta t} \tag{74}$$

Note that the material element present at this location is different at the times t and $t + \delta t$ - it is the physical location that is being held fixed.

3.5.4 Elasticity in the Eulerian Formalism

Adapting the formalism of fluid mechanics to elasticity is fairly straightforward - we simply interpret the stress tensor as the Cauchy stress defined in section 3.4.5. It should be noted that, for a purely elastic system, viscous stress does not typically play a role - the Cauchy stress is assumed to be independent of velocity. Including viscous stress along with the original elastic Cauchy stress will be necessary for visco-elastic systems, but we will save that discussion until section 5.

As before, there are many potential forms the Cauchy stress may take. For a purely elastic system (no energy dissipation), we will typically assume that the Cauchy stress has no explicit time dependence, and may be written as a function of the deformation gradient matrix alone: $\sigma = G(A)$. A material that has a constitutive law of this form is known as a Cauchy elastic material, and the function $G(A)$ is called the response function. Note that, because A is defined relative to a reference configuration, the exact form of the response function $G(A)$ will depend on our choice of reference state. Ultimately, the Cauchy stress should be independent of this choice - if we change our choice of reference state from $\mathcal{B}_0$ to a new state $\mathcal{B}'_0$, resulting in a new deformation gradient matrix A' and new response function G', we must have that $G(A) = G'(A')$.

For many materials, there is a well defined free-energy density function, related to the Cauchy stress by

$$\sigma^{ij} = \frac{1}{J} A^i{}_\alpha \frac{\partial f}{\partial \mathcal{U}_{\alpha\beta}} A^j{}_\beta \tag{75}$$

Materials for which this holds true are known as either Green elastic or hyper-elastic materials.

3.5.5 Vector, Covector, and Tensor Fields

As we will see when generalizing to dynamics in section 5, it is important to be able to translate between the Lagrangian and Eulerian formalisms. To facilitate this, the next three subsections will review some additional concepts and tools from differential geometry [12]. For the basic definition of a differential manifold, see section 3.3.

We have been working with vectors, such as the velocity $\vec{V}$, throughout this section, but we have not provided a rigorous mathematical definition of them. The most common definition of a tangent vector in differential geometry is as a kind of linear map called a derivation. Let $\mathcal{M}$ be a differential manifold, and $x \in \mathcal{M}$ be a point on that manifold. A derivation at x is a linear map $v : \mathcal{C}^\infty(\mathcal{M}) \to \mathbb{R}$ from the space of smooth functions on $\mathcal{M}$ to the real numbers that satisfies the product (also sometimes called the Leibniz) rule: for all $f, g \in \mathcal{C}^\infty(\mathcal{M})$,

$$v(fg) = f(x)\, v(g) + v(f)\, g(x) \tag{76}$$

The set of all derivations at x is called the tangent space at x, denoted $T_x\mathcal{M}$, and an element of $T_x\mathcal{M}$ is referred to as a tangent vector based at x. The disjoint union of all of $\mathcal{M}$'s tangent spaces, $\coprod_{x\in\mathcal{M}} T_x\mathcal{M}$, is known as the tangent bundle of $\mathcal{M}$, and is denoted as $T\mathcal{M}$.

Suppose we have two differential manifolds $\mathcal{M}$ and $\mathcal{N}$, and a smooth mapping $\varphi : \mathcal{M} \to \mathcal{N}$ between them. We define the differential (also sometimes called the tangent map or push-forward) of φ at $x \in \mathcal{M}$ to be the mapping $d_x\varphi : T_x\mathcal{M} \to T_{\varphi(x)}\mathcal{N}$ such that, for all $\vec{v} \in T_x\mathcal{M}$ and $f \in \mathcal{C}^\infty(\mathcal{N})$,

$$d_x\varphi(\vec{v})(f) = \vec{v}(f \circ \varphi) \tag{77}$$

This definition is also easily generalized to a global differential $d\varphi : T\mathcal{M} \to T\mathcal{N}$ that restricts to the local differential $d_x\varphi$ when the domain is restricted to $T_x\mathcal{M}$. To relate these concepts to the more intuitive concept of vectors from physics, let's consider taking $\mathbb{R}^3$ as our manifold. In this case, our definition tells us that a tangent vector $\vec{v} \in T_x\mathbb{R}^3$ (where $\vec{x} \in \mathbb{R}^3$) is really just a directional derivative:

$$\vec{v}\,(f) = \left.\frac{d}{ds} f\left(\vec{x} + s\vec{v}\right)\right|_{s=0} = v^i \frac{\partial f}{\partial x^i} \tag{78}$$

Here the (scalar) quantities $v^{i=1,2,3}$ are referred to as the components of $\vec{v}$ in the coordinates $\left\{x^i\right\}$. When interpreting $\vec{v}$ as a directional derivative in this manner, the set of operators $\left\{ \frac{\partial}{\partial x^i}\big|_x \right\}$ is a basis for $T_x\mathbb{R}^3$. Note this is not the only basis we could choose, though it is the most common choice.

Using the concepts of a coordinate chart (see section 3.3) and the differential map defined in equation 77, we may similarly interpret tangent vectors on a general manifold as directional derivatives. Let $\mathcal{M}$ be an n-dimensional smooth manifold and $\chi : \mathcal{M} \supseteq U \to \mathbb{R}^n$ be a coordinate chart on some open subset of $\mathcal{M}$. The differential $d_x\chi$ will then take a tangent vector $\vec{v} \in T_x\mathcal{M}$ based at a point $x \in U \subset \mathcal{M}$ to a directional derivative $v^i \frac{\partial}{\partial x^i} \in T_{\chi(x)}\mathbb{R}^n$:

$$d_x\chi\left(\vec{v}\right) = v^i \left.\frac{\partial}{\partial x^i}\right|_{\chi(x)} \tag{79}$$

Clearly, we can take $\left\{ \frac{\partial}{\partial x^i}\big|_{\chi(x)} \right\}$ as a basis for $T_x\mathcal{M}$, and $\left\{v^i\right\}$ as the components of $\vec{v}$ in this basis.

When dealing with smooth maps between manifolds $\mathcal{M}$ and $\mathcal{N}$, to connect back to our notation developed for the Lagrangian formalism, we will denote vector (or tensor) components in the domain manifold $\mathcal{M}$ using Greek indices, and vector (or tensor) components in the co-domain manifold $\mathcal{N}$ using Latin indices. The differential of a smooth map $\varphi : \mathcal{M} \to \mathcal{N}$, when expressed in coordinates,

can be shown to be analogous to the deformation gradient matrix: using coordinate charts $x^\alpha = x^\alpha(\vec{x})$ and $X^i = X^i\left(\vec{X}\right)$ for $\mathcal{M}$ and $\mathcal{N}$ respectively,

$$\left(d_x\varphi\right)^i_{\ \alpha} = \frac{\partial\varphi^i}{\partial x^\alpha} \tag{80}$$

where $\varphi^i = X^i \circ \varphi$.

A vector field on a manifold $\mathcal{M}$ is defined as a smooth map $\vec{v} : \mathcal{M} \to T\mathcal{M}$ such that, for any point $x \in \mathcal{M}$, $\vec{v}(x) \in T_x\mathcal{M}$, i.e. points are mapped to tangent vectors within their own tangent space. In the language of differential geometry, vector fields are often referred to as "sections" of the projection map $\pi : T\mathcal{M} \to \mathcal{M}$, which maps tangent vectors to their base points. Suppose $\vec{v}$ is a vector field on a differential manifold $\mathcal{M}$, and that $\varphi : \mathcal{M} \to \mathcal{N}$ is a smooth map between differential manifolds. Then φ will induce a vector field on $\mathcal{N}$, called the push-forward of $\vec{v}$ by φ, denoted $\varphi_*\vec{v}$, defined such that, for all $X \in \mathcal{N}$,

$$\left(\varphi_*\vec{v}\right)(X) = \left(d_{\varphi^{-1}(X)}\varphi\right)\left(\vec{v}\left(\varphi^{-1}(X)\right)\right) \tag{81}$$

We may also define a mapping in the opposite direction by making use of the inverse mapping $\varphi^{-1} : \mathcal{N} \to \mathcal{M}$. Define the pull-back of a vector field $\vec{V}$ on $\mathcal{N}$ by φ to be its push-forward by φ^{-1}: for all $x \in \mathcal{M}$,

$$\left(\varphi^*\vec{V}\right)(x) = \left(d_{\varphi(x)}\varphi^{-1}\right)\left(\vec{V}\left(\varphi(x)\right)\right) \tag{82}$$

The push-forward and pull-back provide us with a means of "translating" vector fields on one manifold into vector fields on the other.

The tangent space $T_x\mathcal{M}$ is a vector space and, as such, has a dual space $T_x^*\mathcal{M}$, referred to as the cotangent space. Rigorously, it is defined as the space of linear operators $\underline{\omega} : T_x\mathcal{M} \to \mathbb{R}$. Elements of the cotangent space are referred

to as cotangent vectors (or sometimes co-vectors), and the disjoint union of all of $\mathcal{M}$'s cotangent spaces is referred to as the cotangent bundle, $T^*\mathcal{M}$. The basis cotangent vectors dual to $\left\{ \frac{\partial}{\partial x^i}\big|_x \right\}$ are typically denoted as $\left\{dx^i\right\}$ - the reasoning for this notation will be apparent soon.

Covector fields are defined analogously to vector fields: they are smooth maps $\underline{\omega} : \mathcal{M} \to T^*\mathcal{M}$ such that points $x \in \mathcal{M}$ are mapped to cotangent vectors within their own cotangent space $T_x^*\mathcal{M}$. An important example of a cotangent field is the differential of a smooth function $f \in C^\infty(\mathcal{M})$, defined as the map $df : \mathcal{M} \to T^*\mathcal{M}$ such that, for all $x \in \mathcal{M}$ and $\vec{v} \in T_x\mathcal{M}$,

$$(df(x))(\vec{v}) = \vec{v}(f) = v^i \frac{\partial f}{\partial x^i} \tag{83}$$

It is the fact that the differential of a function is a cotangent field that leads to the notational choice of writing the natural basis vectors of $T_x^*\mathcal{M}$ as dx^i - they can be interpreted as the differentials of the coordinate chart. In these coordinates, $df = \frac{\partial f}{\partial x^i} dx^i$.

Given a smooth map $\varphi : \mathcal{M} \to \mathcal{N}$, the differential $d_x\varphi : T_x\mathcal{M} \to T_{\varphi(x)}\mathcal{N}$ has associated with it a dual map $d_x^*\varphi : T_{\varphi(x)}^*\mathcal{N} \to T_x^*\mathcal{M}$, called either the cotangent or pull-back map of φ. It is defined such that, for all $\vec{v} \in T_x\mathcal{M}$ and $\underline{\Omega} \in T_{\varphi(x)}^*\mathcal{N}$,

$$(d_x^*\varphi(\underline{\Omega}))(\vec{v}) = \underline{\Omega}(d_x\varphi(\vec{v})) \tag{84}$$

Just as, given a vector field $\vec{v}$ on $\mathcal{M}$, φ induced a vector field on $\mathcal{N}$, the dual to the differential map allows φ to, given a covector field $\underline{\Omega}$ on $\mathcal{N}$, induce a covector field on $\mathcal{M}$:

$$(\varphi^*\underline{\Omega})(x) = (d_x^*\varphi)(\underline{\Omega}(\varphi(x))) \tag{85}$$

This covector field is referred to as the pull-back of $\underline{\Omega}$ by φ. Similarly to before, we also define the push-forward of a covector field $\underline{\omega}$ on $\mathcal{M}$ by φ to be its pull-back by φ^{-1}:

$$\left(\varphi_* \underline{\omega}\right)(X) = \left(d^*_X \varphi^{-1}\right)\left(\underline{\omega}\left(\varphi^{-1}(X)\right)\right) \tag{86}$$

In coordinates, the push-forward and pull-back of vector and covector fields are given as follows. Let $\vec{v}$ be a vector field on $\mathcal{M}$, $\vec{V}$ a vector field on $\mathcal{N}$, $\underline{\omega}$ a covector field on $\mathcal{M}$, and $\underline{\Omega}$ a covector field on $\mathcal{N}$. Then, given and smooth mapping $\varphi : \mathcal{M} \to \mathcal{N}$ with smooth inverse φ^{-1}, we have

$$\left(\varphi_* \vec{v}\right)^i (X) = \left.\frac{\partial \varphi^i}{\partial x^\alpha}\right|_{x=\varphi^{-1}(X)} v^\alpha\left(\varphi^{-1}(X)\right) \tag{87}$$

$$\left(\varphi^* \vec{V}\right)^\alpha (x) = \left.\frac{\partial\left(\varphi^{-1}\right)^\alpha}{\partial X^i}\right|_{X=\varphi(x)} V^i(\varphi(x)) \tag{88}$$

$$\left(\varphi_* \underline{\omega}\right)_i (X) = \left.\frac{\partial\left(\varphi^{-1}\right)^\alpha}{\partial X^i}\right|_{X} \omega_\alpha\left(\varphi^{-1}(X)\right) \tag{89}$$

$$\left(\varphi^* \underline{\Omega}\right)_\alpha (x) = \left.\frac{\partial \varphi^i}{\partial x^\alpha}\right|_{x} \Omega_i(\varphi(x)) \tag{90}$$

All of the definitions and results discussed in this subsection may be readily generalized to the case of tensors and tensor fields. When performing a push-forward or pull-back on a tensor field, each index is pushed or pulled back individually. In the case of tensors on a Riemannian manifold, where raising and lowering indices is well defined, it should be noted that the act of raising/lowering an index *does not* commute taking a push-forward or pull-back. In coordinates, the push-forward of a type (m, n) reference space tensor $\mathbf{t}$ and the

pull-back of a type (m,n) deformed space tensor $\mathbf{T}$ are given by

$$(\varphi_*\mathbf{t})^{i_1\ldots i_m}_{\quad j_1\ldots j_n} = A^{i_1}_{\alpha_1}\ldots A^{i_m}_{\alpha_m} t^{\alpha_1\ldots\alpha_m}_{\quad\beta_1\ldots\beta_n} \left(A^{-1}\right)^{\beta_1}_{j_1}\ldots\left(A^{-1}\right)^{\beta_n}_{j_n} \tag{91}$$

$$(\varphi^*\mathbf{T})^{\alpha_1\ldots\alpha_m}_{\quad\beta_1\ldots\beta_n} = \left(A^{-1}\right)^{\alpha_1}_{i_1}\ldots\left(A^{-1}\right)^{\alpha_m}_{i_m} T^{i_1\ldots i_m}_{\quad j_1\ldots j_n} A^{j_1}_{\beta_1}\ldots A^{j_n}_{\beta_n} \tag{92}$$

3.5.6 Flows and the Convective Derivative

In fluid mechanics, an important concept is that of the flow-line (or streamline), which refers to the path a fluid elements takes as it flows through space. In differential geometry, this concept is formalized through integral curves and flow operators, which we define as follows. First, suppose $\mathcal{M}$ is a differential manifold and $\vec{v}$ is a potentially time-dependent vector field on $\mathcal{M}$. An integral curve of $\vec{v}$ is a curve $\gamma : \mathbb{R} \supseteq \mathcal{I} \to \mathcal{M}$ (here $\mathcal{I}$ is an open interval in the reals) to which $\vec{v}$ is tangent at every point: for all $t \in \mathcal{I}$,

$$\frac{d\gamma}{dt} = \vec{v}\left(\gamma\left(t\right), t\right) \tag{93}$$

An integral curve is called maximal if it domain $\mathcal{I}$ cannot be extended to any larger open interval. We will typically only consider maximal integral curves. Given a vector field, we can define the flow-lines generated by it as the totatility of all of its integral curves. Rigorously, we say that the (time-dependent) flow of $\vec{v}$ is a smooth map $\psi : \mathcal{I}\times\mathcal{I}\times\mathcal{M} \supseteq \mathcal{E} \to \mathcal{M}$ with the following properties:
(1) For all $t_0 \in \mathcal{I}$ and $x \in \mathcal{M}$, the set $\mathcal{E}^{(t_0,x)} = \{t \in \mathcal{I} \mid (t, t_0, x) \in \mathcal{E}\}$ is an open interval of the reals with $t_0 \in \mathcal{E}^{(t_0,x)}$, and $\psi^{(t_0,x)} : t \mapsto \psi\left(t, t_0, x\right)$ is the unique maximal integral curve of $\vec{v}$ with $\psi^{(t_0,x)} = x$
(2) If $t \in \mathcal{E}^{(t_0,x)}$ and $y = \psi^{(t_0,x)}\left(t\right)$, then $\mathcal{E}^{(t,y)} = \mathcal{E}^{(t_0,x)}$ and $\psi^{(t,y)} = \psi^{(t_0,x)}$
(3) For all $t, t_0 \in \mathcal{I}$, the set $U_{t,t_0} = \{x \in \mathcal{M} \mid (t, t_0, x) \in \mathcal{E}\}$ is an open subset of $\mathcal{M}$, and the map $\psi_{t,t_0} : x \mapsto \psi\left(t, t_0, x\right)$ is a diffeomorphism from U_{t,t_0} onto

$U_{t_0,t}$ (i.e. it is smooth and bijective, with smooth inverse), with inverse map $\psi_{t,t_0}^{-1} = \psi_{t_0,t}$

and finally, (4) if $x \in U_{t,t_0}$ and $\psi_{t,t_0}(x) \in U_{t',t}$, then $x \in U_{t',t_0}$ and $\psi_{t',t}(\psi_{t,t_0}(x)) = \psi_{t',t_0}(x)$.

All vector fields will generate a flow. For specifically the velocity field $\vec{V}(X,t)$ of a moving body, the map $\psi(t,t_0,X)$ tells us where a material element that was located at position X at time t_0 will be at time t. The curves $\psi^{(t_0,X)}$ are the flow-lines of the material elements, and the maps $\psi_{t,t_0}(X)$ may be expressed in terms of the time-dependent deformation map and its inverse as

$$\psi_{t,t_0}(x) = \varphi_t\left(\varphi_{t_0}^{-1}(X)\right) \tag{94}$$

As physicists, we are familiar with the concept of covariant differentiation. It is a way of defining the directional derivative of a vector (or more generally, a tensor) field on a manifold. To properly define covariant differentiation, an additional piece of information called the connection (or equivalently, the Christoffel symbols) needs to be provided. For a Riemannian manifold, a unique torsion-free connection is automatically provided by the metric, but for a general manifold a connection needs to be introduced separately. However, the concept of a flow now provides us with another, alternative method of generalizing directional derivatives to act on vectors, one that does not rely on any additional information.

Suppose $\mathcal{M}$ is a differentiable manifold, $\vec{v}$ a smooth vector field on $\mathcal{M}$, and $\mathbf{T}$ a smooth tensor field on $\mathcal{M}$. Let ψ be the flow generated by $\vec{v}$. The map ψ_{t,t_0} is a smooth map from $\mathcal{M}$ to itself, and as such will induce push-forwards and pull-backs of tensor fields. In particular, we can imagine pulling back the tensor $\mathbf{T}(X,t)$ to the position $x = \psi_{t_0,t}(X)$. This pull-back action thus provides us with an alternative means of comparing tensors at two positions besides parallel

transport. With this in mind, we define the convective derivative of a tensor field $\vec{T}$ with respect to a vector field $\vec{v}$ (both of which may be time-dependent) as

$$\frac{\mathcal{D}_{\vec{v}}\mathbf{T}}{\mathcal{D}t}(X,t) = \lim_{\delta t \to 0^+} \frac{\left(\psi^*_{t+\delta t,t}\mathbf{T}\right)(X,t+\delta t) - \mathbf{T}(X,t)}{\delta t} = \frac{d}{dt'}\left(\psi^*_{t',t}\mathbf{T}(t')\right)\Big|_{t'=t} \tag{95}$$

where ψ is the flow generated by $\vec{v}$. The above derivative is often split into two pieces using the chain rule - one piece that differentiates the explicit time dependence of $\mathbf{T}$, and one that does not:

$$\frac{\mathcal{D}_{\vec{v}}\mathbf{T}}{\mathcal{D}t}(X,t) = \frac{\partial \mathbf{T}}{\partial t} + \frac{d}{dt'}\left(\psi^*_{t',t}\mathbf{T}(t)\right)\Big|_{t'=t} = \frac{\partial \mathbf{T}}{\partial t} + \mathcal{L}_{\vec{v}}\mathbf{T} \tag{96}$$

where the second term is known as the Lie derivative (the convective derivative is referred to as the Lie derivative in some texts, in which case the fixed-time part is referred to as the autonomous Lie derivative). When the field we are differentiating with respect to is clear from context, we will usually drop the subscript $\vec{v}$ in the notation, denoting the convective derivative as $\frac{\mathcal{D}}{\mathcal{D}t}$ and the Lie derivative as $\mathcal{L}$.

Let $\mathcal{A}^i{}_j(t',t) = \frac{\partial \psi^i_{t',t}}{\partial X^j} = A^i{}_\alpha(t')\left(A^{-1}\right)^\alpha{}_j(t)$. We may then write the convective derivative in coordinate form as

$$\begin{aligned}\left(\frac{\mathcal{D}\mathbf{T}}{\mathcal{D}t}\right)^{i_1\ldots i_m}{}_{j_1\ldots j_n} &= \frac{d}{dt'}\left[T^{i'_1\ldots i'_m}{}_{j'_1\ldots j'_n}\left(\psi_{t',t}(x),t'\right)(t)\prod_{p=1}^{m}\mathcal{A}^{i_p}{}_{i'_p}(t,t')\right.\\ &\qquad\left.\cdot\prod_{q=1}^{n}\mathcal{A}^{j_q}{}_{j'_q}(t',t)\right]\Bigg|_{t'=t}\\ &= \frac{\partial T^{i_1\ldots i_m}{}_{j_1\ldots j_n}}{\partial t} + V^k\frac{\partial T^{i_1\ldots i_m}{}_{j_1\ldots j_n}}{\partial X^k} - \sum_{p=1}^{m} T^{i_1\ldots i_{p-1}ki_{p+1}\ldots i_m}{}_{j_1\ldots j_n}\frac{\partial V^{i_p}}{\partial X^k}\\ &\qquad + \sum_{q=1}^{n} T^{i_1\ldots i_m}{}_{j_1\ldots j_{q-1}kj_{q+1}\ldots j_n}\frac{\partial V^k}{\partial X^{j_q}}\end{aligned} \tag{97}$$

For a torsion-free connection, such as that provided by a metric, we may replace the spatial partial derivatives in the above equation with covariant derivatives if we so choose. If we do, then the first two terms above become the material time derivative $\frac{D\mathbf{T}}{Dt}$. Notice that, unlike the material derivative, the convective derivative depends on not just the velocity field, but also its gradient. The two derivatives will be equivalent only when we are differentiating a scalar field, or when the velocity field is uniform.

3.5.7 Differential Forms and Integration on Manifolds

In physics, we describe integration over volumes and surfaces is described in terms of infinitesimal volume or area elements. In differential geometry, integrals over manifolds are defined using different, but ultimately equivalent language. First, let's consider the simple case of a line integral. As we discussed in section 3.5.5, the differential of a function is in fact a covector field. As such, it makes sense that covector fields are the natural kind of object that we can perform line integrals on. To actually evaluate such an integral, we need to pull-back the covector field onto the real line. If $\gamma : [a, b] \to \mathcal{M}$ is a smooth curve on a manifold $\mathcal{M}$, and $\underline{\omega}$ is a covector field on $\mathcal{M}$, we define the line integral of $\underline{\omega}$ along γ as

$$\int_\gamma \underline{\omega} = \int_a^b \gamma^* \underline{\omega} = \int_a^b dt \, \frac{d\gamma^i}{dt} \omega_i \left(\gamma\left(t\right)\right) \tag{98}$$

where $\gamma^*\underline{\omega}$ is the pull-back of $\underline{\omega}$ onto $\mathbb{R}$ by γ.

It can be shown that the appropriate object to represent k-dimensional volume elements by is an anti-symmetric, fully covariant rank k tensor, typically referred to as a differential k-form, or simply k-forms. Before discussing integration of k-forms, let's first briefly cover some basic properties of k-forms.

Let $T^{*k}\mathcal{M}$ be the bundle of rank k covariant tensors on $\mathcal{M}$ (i.e. tensors of the form $\mathbf{T} = T_{i_1 \ldots i_k} dx^{i_1} \ldots dx^{i_k}$). The vector space consisting of those tensor fields

that are anti-symmetric in all of their indices, i.e. k-forms, is denoted $\Omega^k\mathcal{M}$. Given a k-form $\underline{\alpha} \in \Omega^k\mathcal{M}$ and an l-form $\underline{\beta} \in \Omega^l\mathcal{M}$, we define their wedge product to be the $(k+l)$-form given by

$$\left(\underline{\alpha} \wedge \underline{\beta}\right)_{i_1 \ldots i_{k+l}} = \frac{1}{k!l!} \sum_{\sigma \in S_{k+l}} (\text{sgn } \sigma)\, \alpha_{\sigma(i_1)\ldots\sigma(i_k)} \beta_{\sigma(i_{k+1})\ldots\sigma(i_{k+l})} \tag{99}$$

where S_{k+l} is the set of all permutations of $k+l$ elements. The wedge product is, like a typical tensor product, bilinear and associative. However, unlike a typical tensor product, the wedge product is anti-commutative: $\underline{\alpha} \wedge \underline{\beta} = (-1)^{kl}\, \underline{\beta} \wedge \underline{\alpha}$. Note this implies that the wedge product of a k-form with itself is zero. A very useful formula involving the wedge product is as follows. Let $\underline{\omega}_1, \ldots, \underline{\omega}_k$ be covectors, and $\vec{v}_1, \ldots, \vec{v}_k$ be vectors. Then

$$(\underline{\omega}_1 \wedge \cdots \wedge \underline{\omega}_k)_{i_1 \ldots i_k}\, v_1^{i_1} \cdots v_k^{i_k} = \det\left(\underline{\omega}_j\left(\vec{v}_i\right)\right) \tag{100}$$

Given a coordiate chart $\left\{x^i\right\}$, any k-form $\underline{\omega}$ may be written in the form

$$\underline{\omega} = \sum_{i_1 < \cdots < i_k} \omega_{i_1 \ldots i_k} dx^{i_1} \wedge \cdots \wedge dx^{i_k} \tag{101}$$

Another important operation involving k-forms is that of interior multiplication. Let $\underline{\omega}$ be a k-form and $\vec{v}$ be a vector. Then interior product of $\underline{\omega}$ by $\vec{v}$ is defined as the $(k-1)$-form obtained by contracting $\vec{v}$ with the first index of $\underline{\omega}$:

$$\left(i_{\vec{v}}\underline{\omega}\right)_{i_1 \ldots i_{k-1}} = v^j \omega_{j i_1 \ldots i_{k-1}} \tag{102}$$

Interior multiplication is nilpotent, so $i_{\vec{v}} \circ i_{\vec{v}} = 0$. The interior product of a wedge product is given, for k-form $\underline{\alpha}$ and l-form $\underline{\beta}$, by a graded product rule:

$$i_{\vec{v}}\left(\underline{\alpha} \wedge \underline{\beta}\right) = \left(i_{\vec{v}}\underline{\alpha}\right) \wedge \underline{\beta} + (-1)^k\, \underline{\alpha} \wedge \left(i_{\vec{v}}\underline{\beta}\right) \tag{103}$$

An operator that satisfies a graded product rule is known as an antiderivation. Another important antiderivation is exterior differentiation. Given an n-dimensional manifold $\mathcal{M}$, $k = 0, 1, \ldots$, there exists a unique linear operator $d : \Omega^k\mathcal{M} \to \Omega^{k+1}\mathcal{M}$ that is an antiderivation, nilpotent, and for $k = 0$ is equivalent to the differential. In coordinates $\left\{x^i\right\}$, we have

$$d\underline{\omega} = \sum_{i_1<\cdots<i_k} \sum_{j=1}^{n} \frac{\partial \omega_{i_1 \ldots i_k}}{\partial x^j} dx^j \wedge dx^{i_1} \wedge \cdots \wedge dx^{i_k} \tag{104}$$

An additional important property of the exterior derivative is that it commutes with pull-backs and push-forwards. Also, an very useful relationship between the exterior derivative, interior multiplication, and the Lie derivative exists called Cartan's magic formula. If $\underline{\omega} \in \Omega^k\mathcal{M}$ and $\vec{v}$ be a vector field on $\mathcal{M}$, then

$$\mathcal{L}_{\vec{v}}\, \underline{\omega} = d\left(i_{\vec{v}}\, \underline{\omega}\right) + i_{\vec{v}}\left(d\underline{\omega}\right) \tag{105}$$

As mentioned earlier, k-forms are the natural object to represent k-dimensional volume forms by. Let $\mathcal{M}$ be a differentiable manifold, $\underline{\omega}$ be a compactly supported k-form on $\mathcal{M}$. In a coordinate chart $\left\{x^i\right\}$, we can write $\underline{\omega}$ in the form $\underline{\omega} = \omega dx^1 \wedge \cdots \wedge dx^k$, where $\omega\left(x^1, \ldots, x^k\right)$ is a scalar field. We then define the integral of $\underline{\omega}$ over $\mathcal{M}$ analogously to how we defined line integrals in equation 98:

$$\int_{\mathcal{M}} \underline{\omega} = \int_{\chi(\mathcal{M})} dx^1 \cdots dx^n\, \omega\left(x^1, \ldots, x^n\right) \tag{106}$$

Suppose we have two differentiable manifolds $\mathcal{M}$ and $\mathcal{N}$, and a smooth, orientation preserving map $\varphi : \mathcal{M} \to \mathcal{N}$ between them. We may express an integral over $\mathcal{M}$ as an integral over $\mathcal{N}$ or vice versa as:

$$\int_{\mathcal{M}} \underline{\omega} = \int_{\mathcal{N}} \varphi_* \underline{\omega}, \quad \int_{\mathcal{N}} \underline{\Omega} = \int_{\mathcal{M}} \varphi^* \underline{\Omega} \tag{107}$$

Using the formalism of differential forms, we can derive the general forms of both Stoke's law, as well as the transport theorem. For Stoke's theorem, we have

$$\int_{\mathcal{M}} \underline{\omega} = \oint_{\partial \mathcal{M}} d\underline{\omega} \tag{108}$$

As for the transport theorem, we have

$$\frac{d}{dt} \int_{\mathcal{B}_t} \underline{\Omega}\,(X,t) = \int_{\mathcal{B}_t} \frac{\mathcal{D}}{\mathcal{D}t} \underline{\Omega}\,(X,t) \tag{109}$$

3.5.8 Translating Between the Lagrangian and Eulerian Formalisms

The primary tool for translating between the Lagrangian and Eulerian formalisms is push-forwards and pull-backs. Every reference space tensor can be pushed forward to the deformed space, and vice versa. We have already seen this with the stress tensors, albeit with a small caveat: stress tensors represent forces per unit area, and as such how area elements transform under deformation must be included. Consider a deformed space tensor quantity $\mathbf{T}$. The Piola transform of $\mathbf{T}$ is defined as the reference space tensor

$$\mathbf{t} = J\varphi^* \mathbf{T} \tag{110}$$

where J is the Jacobian of the deformation, $J = \det A$. In the special case of a vector field $\vec{V}$, this is equivalent to defining the Piola transform $\vec{v}$ as the reference space vector field satisfying

$$i_{\vec{v}}\, dv = \varphi^* \left(i_{\vec{V}}\, dV \right) \tag{111}$$

With this definition, it can be shown that

$$\operatorname{div}(\mathbf{t}) = J\, (\operatorname{Div}\, \mathbf{T})|_{X=\varphi(x)} \tag{112}$$

where div represents taking a divergence in the reference space, and Div represents taking a divergence in the deformed space. The Piola transformation is the appropriate way of "pulling back" tensor densities such as the stress onto the reference state. In this language, the second Piola-Kirchhoff stress is the Piola transformation of the Cauchy stress. The first Piola-Kirchhoff stress can also be thought of as a Piola transformation, albeit only acting on one index.

There are additional important examples of quantities normally defined on one space that can be pushed forward or pulled back onto the other. One is the Green-Lagrange strain tenor $\mathcal{U}_{\alpha\beta}$. Its push-forward onto the deformed space is referred to in the engineering literature as the Euler-Almansi, or the Eulerian, stain tensor,

$$\mathcal{E}_{ij} = \left(A^{-1}\right)^{\alpha}_{\ i} \mathcal{U}_{\alpha\beta} \left(A^{-1}\right)^{\beta}_{\ j} = \frac{1}{2}\left(G_{ij} - \left(A^{-1}\right)^{\alpha}_{\ i} \left(A^{-1}\right)_{\alpha j}\right) \tag{113}$$

In the case of dynamics, the various transformations of the spatial velocity $\vec{V}(X,t)$ will be incredibly important. First, we define the material velocity $\vec{v} : \mathcal{B}_0 \times \mathbb{R} \to T\mathcal{B}_t$ as

$$\vec{v}(x,t) = \vec{V}(\varphi(x,t),t) \tag{114}$$

The material velocity gives the velocity (in real space) of the material element x at time t. It should be noted that the material velocity maps reference space positions to deformed space tangent vectors and, as such, is not a proper tensor field. It is, however, related to the deformation map in a simple way - it is just its partial time derivative:

$$v^i(x,t) = \frac{\partial \varphi^i}{\partial t} \tag{115}$$

To obtain a proper vector field on the reference space, we need to pull-back the spatial velocity. Define the convective velocity as

$$\vec{u}\,(x,t) = \varphi^* \vec{V}, \;\; u^\alpha\,(x,t) = \left(A^{-1}\right)^\alpha_{\ i}\, v^i \tag{116}$$

These different velocities are useful when discussing the rate of change of the deformation map, as well as the strain tensors.

4 Cavitation

4.1 Introduction

Now that we have developed the formalism of finite-strain elasticity theory, we may begin to apply it to actual problems. Here, we will focus on the problem of cavitation in compressible systems, with the eventual goal of exploring the specific example of biogels.

It is well known in the context of rubber elasticity that a cavity, when pressurized beyond a finite critical pressure $P_c = \frac{5}{2}\mu$, will begin to expand without limit. Realistically, of course, the expansion continues only until the elastic nature of the material breaks down, causing it to fracture, but in a hypothetical material that never breaks down the expansion would continue uninterrupted. This phenomenon is an inherently non-linear effect, and does not exist in linear elasticity.

Cavitation is not often discussed in the physics literature, though there is a significant amount of discussion about it in the engineering literature. This discussion, however, is almost exclusively done in the context of rubbers, which are treated as incompressible or nearly incompressible [6]. As such, it is not well known what effects compressibility would have on cavitation. The effects of additional, material dependent non-linearities on cavitation is also largely

unexplored.

Both compressibility and material non-linearities are present in biogels, with the latter being caused by strain-hardening. Of particular interest is the cytoskeleton if the cell, where it is known that liquid-liquid phase separation produces droplets that do not undergo Oswald ripening, or coarsening, which refers to the growth of larger droplets of the minority phase and a corresponding shrinkage of smaller droplets. In contrast, liquid-liquid phase separation in cell produces a distribution of droplets with constant radii. This is attributed to the fact that the cell is permeated by networks of biopolymers - growth of minority-phase droplets can be stopped by elastic deformation of the surrounding polymer network. However, when the osmotic pressure of the minority phase exceeds a critical value on the order of the polymer network's elastic modulus, droplets begin to grow in an unlimited fashion. This appears very similar to cavitation, and motivates exploring how cavitation is altered in a biogel setting.

4.2 The Cavitation Problem in Linear Elasticity

Let us first discuss cavitation in the setting of linear elasticity, where we will see that it actually does not exist. In the cavitation problem, a spherical cavity of initial radius r_0 is pressurized, causing it to expand to a new radius R_0. Due to the spherical symmetry of the system, the displacement field will be entirely radial, and will only depend on the distance from the center of the cavity:

$$\vec{u}\left(\vec{x}\right) = u\left(r\right)\hat{r} \tag{117}$$

For such a function, it can be easily shown that $\nabla^2\vec{u} = \vec{\nabla}\left(\vec{\nabla}\cdot\vec{u}\right)$. This leads to a simplified equation of mechanical equilibrium,

$$\nabla^2\vec{u} = 0 \tag{118}$$

Considering that the displacement field must go to zero at infinity, this has solution

$$u(r) = (R_0 - r_0)\left(\frac{r_0}{r}\right)^2 \tag{119}$$

This leads to a (linearized) strain tensor given (in spherical coordinates) by

$$\mathbf{u}(r) = \begin{pmatrix} u'(r) & 0 & 0 \\ 0 & \frac{u(r)}{r} & 0 \\ 0 & 0 & \frac{u(r)}{r} \end{pmatrix} = \frac{u(r)}{r}\begin{pmatrix} -2 & 0 & 0 \\ 0 & 1 & 0 \\ 0 & 0 & 1 \end{pmatrix} \tag{120}$$

Note that the strain tensor is traceless:

$$\text{tr } u = \vec{\nabla} \cdot \vec{u} = 0 \tag{121}$$

and thus this deformation is volume-preserving. This will no longer be true in finite-strain elasticity.

There are two methods by which we could calculate the relationship between the cavity pressure and its final radius R_0 - free-energy minimization, or making use of the boundary condition at the cavity surface. We will first show the latter. At the cavity surface, we must have

$$\sigma_r^r(r_0) = \frac{2\gamma}{R_0} - P \tag{122}$$

where P is the pressure inside the cavity, and γ represents a surface tension of the cavity, which is treated as an external force per unit area. It should be noted that, in linear elasticity, we assume that $\delta r_0 \equiv R_0 - r_0 \ll r_0$, and can thus make the approximation

$$\sigma_r^r(r_0) = \frac{2\gamma}{r_0}\left(1 - \frac{R_0 - r_0}{r_0}\right) - P + O\left(\delta r_0^2\right) \tag{123}$$

Recall that the stress is related to the (linearized) strain by equation 14. We thus have

$$\sigma_r^r\left(r_0\right) = \kappa \mathrm{tr}\ u + 2\mu\bar{u}_r^r = 2\mu u_r^r = -4\mu\frac{R_0 - r_0}{r_0} \tag{124}$$

where we have made use of the fact that, to first-order, the strain tensor is traceless. Inserting this into equation 123 and solving for the pressure, we obtain that

$$P = \frac{2\gamma}{R_0} + 4\mu\frac{R_0 - r_0}{r_0} = \frac{2\gamma}{r_0} + \left(4\mu - \frac{2\gamma}{r_0}\right)\frac{R_0 - r_0}{r_0} + O\left(\delta r_0^2\right) \tag{125}$$

Alternatively, we could minimize the free-energy, which is given by

$$F_{\mathrm{LE}} = \gamma\left(4\pi R_0^2\right) - P\left(\frac{4\pi}{3}R_0^3\right) + 4\pi\int_{r_0}^{\infty} dr\ r^2 f_{\mathrm{LE}}\left(r\right) \tag{126}$$

where f_{LE} is the free-energy density given in equation 6:

$$f_{\mathrm{LE}} = \frac{1}{2}\kappa\left(\mathrm{tr}\ u\right)^2 + \mu\mathrm{tr}\left(u^2\right) = 6\left(R_0 - r_0\right)^2\frac{r_0^4}{r^6} \tag{127}$$

Integrating, we obtain

$$F_{\mathrm{LE}} = \gamma\left(4\pi R_0^2\right) - P\left(\frac{4\pi}{3}R_0^3\right) + 8\pi\mu\left(R_0 - r_0\right)^2 r_0 \tag{128}$$

We now minimize with respect to R_0:

$$2\gamma R_0 - PR_0^2 + 4\mu\left(R_0 - r_0\right)r_0 = 0 \tag{129}$$

Solving for P and taking the limit $R_0 - r_0 \ll r_0$, we find

$$\begin{aligned} P = \frac{2\gamma}{R_0} + 4\mu r_0 \frac{R_0 - r_0}{R_0^2} &= \frac{2\gamma}{R_0} + 4\mu \frac{R_0 - r_0}{r_0 + 2\left(R_0 - r_0\right) + O\left(\delta r_0^2\right)} \\ &= \frac{2\gamma}{r_0} + \left(4\mu - \frac{2\gamma}{r_0}\right) \frac{R_0 - r_0}{r_0} + O\left(\delta r_0^2\right) \end{aligned} \tag{130}$$

When it comes to cavitation, taking the limit of $R_0 \to \infty$ is not well defined, since the theory of linear elasticity should only be valid for $R_0 - r_0 \ll r_0$. It is insightful, however, to see what occurs when P is at the cavitation critical pressure, $P_c = \frac{5}{2}\mu$:

$$\begin{aligned} \frac{5}{2}\mu = \frac{2\gamma}{R_0} + 4\mu \frac{R_0 - r_0}{r_0} \Rightarrow \frac{5}{2}\mu R_0 &= 2\gamma + 4\mu\left(R_0 - r_0\right) + O\left(\delta r_0^2\right) \\ \Rightarrow R_0 &= \frac{1}{8}\left(13 r_0 - \frac{4\gamma}{\mu}\right) \end{aligned} \tag{131}$$

Hence R_0 is finite at the cavitation critical pressure, and it would appear cavitation does not occur. It should, of course, be noted that, for this solution to be stable, we must have $R_0 > r_0$. This will be the case as long as $\gamma < \frac{5}{4}\mu r_0$ - above this threshold value, the surface tension will overcome the pressure and cause the cavity to shrink.

4.3 Spherical Symmetry

For the cavitation problem, one assumes spherical symmetry. The reference configuration $\mathcal{B}_0$ will be defined to be a strain-free state that has a spherical cavity of radius r_0 at the origin. The cavity is then pressurized with a pressure P, causing it to expand. The new, deformed configuration $\mathcal{B}$ is described by a mapping from a material point at $(r, \theta, \phi) \in \mathcal{B}_0$ to a new location $(\varphi(r), \theta, \phi) \in \mathcal{B}$. The radius of the swollen cavity in $\mathcal{B}$ is then $R_0 = \varphi(r_0)$ (See figure 1). The introduction of spherical symmetry simplifies our expressions for the deformation

gradient matrix, strain tensor, and Jacobian:

$$A^i{}_\alpha = \frac{\partial \varphi^i}{\partial x^\alpha} = \begin{pmatrix} \varphi' & 0 & 0 \\ 0 & 1 & 0 \\ 0 & 0 & 1 \end{pmatrix} \tag{132}$$

$$J = \sqrt{\frac{\det G}{\det g}} \det A = \frac{\varphi^2}{r^2}\varphi' \tag{133}$$

$$\mathcal{U}^\alpha_\beta = \frac{1}{2} \begin{pmatrix} \varphi'^2 - 1 & 0 & 0 \\ 0 & \frac{\varphi^2}{r^2} - 1 & 0 \\ 0 & 0 & \frac{\varphi^2}{r^2} - 1 \end{pmatrix} \tag{134}$$

$$\operatorname{tr} \mathcal{U} = \frac{1}{2}\varphi'^2 + \frac{\varphi^2}{r^2} - \frac{3}{2} \tag{135}$$

$$\operatorname{tr} \bar{\mathcal{U}} = J^{-2/3} \left(\frac{1}{2}\varphi'^2 + \frac{\varphi^2}{r^2} \right) - \frac{3}{2} \tag{136}$$

4.4 Cavitation in the Incompressible Case

4.4.1 The Deformation Map

Recall that the density $\rho(R)$ of the deformed material is related to that of the undeformed material by the Jacobian $J(R) = \frac{\rho_0}{\rho(R)} = 1/\rho_r$. It follows from the conservation of mass that $\rho(R) R^2 dR = \rho_0 r^2 dr$, which gives $\rho_r = \frac{1}{J} = \frac{r^2}{\varphi(r)^2 \varphi'(r)}$, where $\varphi'(r)$ is the derivative of the deformation map. For an incompressible system with fixed Jacobian $J = 1$, this reduces to the differential equation $\varphi'(r) = \frac{r^2}{\varphi(r)^2}$, with exact solution

$$\varphi(r) = \left(R_0^3 + r^3 - r_0^3 \right)^{1/3} \tag{137}$$

4.4.2 Minimization of the Free Energy

There are two approaches to deriving cavitation for an incompressible material. The first is to minimize the free energy. Because the material is incompressible, the Jacobian will not enter its free-energy density, which can be written simply as

$$f_{\text{inc}} = \mu \text{tr}\, \mathcal{U} = \mu \left(\frac{\varphi^2}{r^2} + \frac{1}{2}\varphi'^2 - \frac{3}{2} \right) \tag{138}$$

The stretch ratio along the radial direction is

$$\lambda(r) \equiv \frac{\varphi(r)}{r} = \frac{1}{r}\left(r^3 + R_0^3 - r_0^3\right)^{1/3} \tag{139}$$

The stretch ratio at the surface of the cavity is then $\lambda(r_0) = R_0/r_0$, which we will denote by λ_0. Since $\varphi' = 1/\lambda^2$, one can write the elastic free-energy density as

$$f_{\text{inc}}(r) = \mu \left(\lambda(r)^2 + \frac{1}{2\lambda(r)^4} - \frac{3}{2} \right) \tag{140}$$

The total free-energy F is written as

$$F = \gamma\left(4\pi R_0^2\right) - P\left(\frac{4\pi}{3}R_0^3\right) + 4\pi \int_{r_0}^{\infty} dr\; r^2 f_{\text{inc}} \tag{141}$$

Here, P is the pressure inside the cavity and γ represents a surface tension of the cavity, which is treated as an external force per unit area. The last term is the contribution to the free-energy from elastic forces, which for our incompressible system is given by

$$F_{\text{el}} = 4\pi\mu \int_{r_0}^{\infty} dr\; r^2 \left(\lambda^2 + \frac{1}{2\lambda^4} - \frac{3}{2} \right) \tag{142}$$

Change the integration variable from r to λ using

$$\lambda(r) = \frac{1}{r}\left(r^3 + R_0^3 - r_0^3\right)^{1/3} \Rightarrow r(\lambda)^3 = \frac{R_0^3 - r_0^3}{\lambda^3 - 1} \tag{143}$$

and

$$d\lambda = \frac{1}{r}\left(\varphi' - \frac{\varphi}{r}\right)dr = -\frac{\lambda - \lambda^{-2}}{r}dr \Rightarrow \frac{dr}{r} = -\frac{\lambda^2}{\lambda^3 - 1}d\lambda \tag{144}$$

This gives

$$\begin{aligned} F_{\text{el}} &= 4\pi\mu\left(R_0^3 - r_0^3\right)\int_1^{\lambda_0} d\lambda\left(\frac{\lambda}{\lambda^3 - 1}\right)^2\left(\lambda^2 + \frac{1}{2\lambda^4} - \frac{3}{2}\right) \\ &= 2\pi\mu\left(R_0^3 - r_0^3\right)\int_1^{\lambda_0} d\lambda\frac{2\lambda^6 - 3\lambda^4 + 1}{\lambda^2\left(\lambda^3 - 1\right)^2} \end{aligned} \tag{145}$$

This integral can be evaluated using partial fraction decomposition as follows. Our goal is to rewrite the integrand as a sum of partial fractions:

$$\begin{aligned} \frac{2\lambda^6 - 3\lambda^4 + 1}{\lambda^2\left(\lambda^3 - 1\right)^2} &= \frac{A_1}{\lambda} + \frac{A_2}{\lambda^2} + \frac{B_1}{\lambda - 1} + \frac{B_2}{(\lambda - 1)^2} \\ &\quad + \frac{C_1\lambda + D_1}{\lambda^2 + \lambda + 1} + \frac{C_2\lambda + D_2}{\left(\lambda^2 + \lambda + 1\right)^2} \end{aligned} \tag{146}$$

Re-writing this, we have

$$\begin{aligned} 2\lambda^6 - 3\lambda^4 + 1 &= A_1\lambda\left(\lambda^3 - 1\right)^2 = A_1\lambda\left(\lambda^3 - 1\right)^2 + A_2\left(\lambda^3 - 1\right)^2 \\ &\quad + B_1\lambda^2\left(\lambda^3 - 1\right)\left(\lambda^2 + \lambda + 1\right) + B_2\lambda^2\left(\lambda^2 + \lambda + 1\right)^2 \\ &\quad + \left(C_1\lambda + D_1\right)\lambda^2\left(\lambda^3 - 1\right)(\lambda - 1) + \left(C_2\lambda + D_2\right)\lambda^2(\lambda - 1)^2 \end{aligned} \tag{147}$$

$$\begin{aligned} &= \left(A_1 + B_1 + C_1\right)\lambda^7 + \left(A_2 + B_1 - C_1 + D_1\right)\lambda^6 + \left(B_1 + C_2 - D_1\right)\lambda^5 \\ &\quad + \left(-2A_1 - B_1 + B_2 - C_1 - 2C_2 + D_2\right)\lambda^4 \\ &\quad + \left(-2A_2 - B_1 + B_2 + C_1 + C_2 - D_1 - 2D_2\right)\lambda^3 \\ &\quad + \left(-B_1 + B_2 + D_1 + D_2\right)\lambda^2 + A_1\lambda + A_2 \end{aligned} \tag{148}$$

Solving term-by-term, we find:

Zeroth-order:

$$A_2 = 1 \tag{149}$$

First-order:

$$A_1 = 0 \tag{150}$$

Second-order:

$$-B_1 + B_2 + D_1 + D_2 = 0 \Rightarrow B_1 = B_2 + D_1 + D_2 \tag{151}$$

Third-order:

$$\begin{aligned} -2A_2 - B_1 + B_2 + C_1 + C_2 - D_1 - 2D_2 = 0 \\ \Rightarrow C_1 = 2 - C_2 + 2D_1 + 3D_2 \end{aligned} \tag{152}$$

Fourth-order:

$$\begin{aligned} -2A_1 - B_1 + B_2 - C_1 - 2C_2 + D_2 = -3 \\ \Rightarrow C_2 = 1 - 3D_1 - 3D_2 \Rightarrow C_1 = 1 + 5D_1 + 6D_2 \end{aligned} \tag{153}$$

Fifth-order:

$$\begin{aligned} B_1 + D_2 - D_1 = 0 \Rightarrow D_1 = \frac{1}{3}\left(1 + B_2 - 2D_2\right) \\ \Rightarrow B_1 = \frac{1}{3}\left(1 + 4B_2 + D_2\right), \;\; C_1 = \frac{1}{3}\left(8 + 5B_2 - 2D_2\right), \;\; C_2 = -B_2 - D_2 \end{aligned} \tag{154}$$

Sixth-order:

$$\begin{aligned} A_2 + B_1 - C_1 + D_1 = 2 \Rightarrow D_2 = -1 \\ \Rightarrow B_1 = \frac{4}{3}B_2, \;\; C_1 = \frac{5}{3}B_2, \;\; C_2 = 1 - B_2, \;\; D_1 = 1 + \frac{1}{3}B_2 \end{aligned} \tag{155}$$

Seventh-order:

$$A_1 + B_1 + C_1 = 0 \Rightarrow B_1 = B_2 = C_1 = 0, \;\; C_2 = D_1 = 1, \;\; D_2 = -1 \tag{156}$$

Therefore we may write the integrand as

$$\frac{2\lambda^6 - 3\lambda^4 + 1}{\lambda^2 \left(\lambda^3 - 1\right)^2} = \frac{1}{\lambda^2} + \frac{1}{\lambda^2 + \lambda + 1} + \frac{\lambda - 1}{\left(\lambda^2 + \lambda + 1\right)} \tag{157}$$

We may now directly perform the integral as follows:

$$\begin{aligned} F_{\text{el}} = 2\pi\mu \left(R_0^3 - r_0^3\right) \int_1^{\lambda_0} d\lambda \Bigg[& \frac{1}{\lambda^2} + \frac{1}{\lambda^2 + \lambda + 1} \\ & + \frac{\lambda - 1}{\left(\lambda^2 + \lambda + 1\right)^2} \Bigg] \end{aligned} \tag{158}$$

The first term gives

$$\int_1^{\lambda_0} \frac{d\lambda}{\lambda^2} = 1 - \frac{1}{\lambda_0} \tag{159}$$

The second term gives

$$\int_1^{\lambda_0} \frac{d\lambda}{\lambda^2 + \lambda + 1} = \frac{2}{\sqrt{3}} \left[\arctan\left(\frac{2\lambda_0 + 1}{\sqrt{3}} \right) - \frac{\pi}{3} \right] \tag{160}$$

Finally, the third term gives

$$\begin{aligned} \int_1^{\lambda_0} d\lambda \frac{\lambda - 1}{\left(\lambda^2 + \lambda + 1\right)^2} = & \frac{2}{3} - \frac{\lambda_0 + 1}{\lambda_0^2 + \lambda_0 + 1} \\ & - \frac{2}{\sqrt{3}} \left[\arctan\left(\frac{2\lambda_0 + 1}{\sqrt{3}} \right) - \frac{\pi}{3} \right] \end{aligned} \tag{161}$$

Hence

$$\begin{aligned} F_{\text{el}} &= 2\pi\mu r_0^3 \left(\lambda_0^3 - 1\right) \left(\frac{5}{3} - \frac{1}{\lambda_0} - \frac{\lambda_0 + 1}{\lambda_0^2 + \lambda_0 + 1} \right) \\ &= 4\pi\mu r_0^3 \left(\frac{5}{6}\lambda_0^3 - \lambda_0^2 + \frac{1}{2\lambda_0} - \frac{1}{3} \right) \end{aligned} \tag{162}$$

Minimization of the full free-energy F with respect to λ_0 gives

$$\left(\frac{5}{2}-\frac{P}{\mu}\right)\lambda_0^2+2\left(\frac{\gamma}{\mu r_0}-1\right)\lambda_0-\frac{1}{2\lambda_0^2}=0 \tag{163}$$

so

$$P/\mu=\left(\frac{2\gamma}{\mu r_0}\right)\frac{1}{\lambda}+\left(\frac{5}{2}-\frac{2}{\lambda}-\frac{1}{2\lambda^4}\right) \tag{164}$$

where we have dropped the subscript of λ_0. The first term above is the Laplace capillary pressure. In the following, surface tension will be expressed in dimensionless form as $\bar{\gamma}=\frac{\gamma}{\mu r_0}$. The second term reproduces the known relation between pressure and radial extension for cavitation in incompressible materials [6].

4.4.3 Solving the Equation of Motion

An alternative derivation for the result in equation 164 involves solving the equation of motion, which in the Lagrangian formalism is given by equation 36. Here, the first Piola-Kirchoff stress tensor is given by

$$S^{i\alpha}=\frac{\partial}{\partial A_{i\alpha}}\left(f_{\text{inc}}-\pi\left(J-1\right)\right)=\mu A^{i\alpha}-J\pi\left(A^{-1}\right)^{\alpha i} \tag{165}$$

where $\pi\left(r,t\right)$ is a Lagrange multiplier that enforces the incompressibility condition. To ensure that the stress properly goes to zero infinitely far from the cavity, we must have $\lim_{r\to\infty}\pi=\mu$. In spherical coordinates, the divergence of the first Piola-Kirchhoff stress tensor is given by

$$\begin{aligned}\frac{\partial S_r^R}{\partial r}+\frac{2}{r}\left(S_r^R-\lambda S_\theta^\Theta\right)&=\frac{\partial}{\partial r}\left(\mu\lambda^{-2}-J\pi\lambda^2\right)\\&+\frac{2}{r}\left(\mu\lambda^{-2}-J\pi\lambda^2-\lambda\left(\mu-J\pi\lambda^{-2}\right)\right)\\&=-J\lambda^2\frac{d\pi}{dr}+2\mu\frac{\lambda^3-1}{\lambda^3}\frac{d\lambda}{dr}\end{aligned} \tag{166}$$

Setting this divergence to zero, setting $J = 1$, and integrating over r, we obtain

$$\begin{aligned} \int_{\pi(r_0)}^{\mu} d\pi &= 2\mu \int_{\lambda_0 = R_0/r_0}^{1} d\lambda \frac{\lambda^3 - 1}{\lambda^5} \\ \Rightarrow \pi(r_0) &= \mu \left(\frac{5}{2} - \frac{2}{\lambda_0} + \frac{1}{2\lambda_0^4} \right) \end{aligned} \tag{167}$$

Let P be the pressure inside the cavity, and γ be the surface tension of the cavity surface. Because the stress tensor must be continuous, we have

$$\pi(r_0) = P - \frac{2\gamma}{R_0} - \mu\lambda_0^{-4} = P - \frac{2\gamma}{r_0\lambda_0} - \mu\lambda_0^{-4} \tag{168}$$

Here we have used the fact that $\sigma_R^R = \left(\frac{1}{J}\lambda^{-2} S_r^R\right) \circ \varphi^{-1} = \mu \left(\lambda \circ \varphi^{-1}\right)^{-4} - p$, where $p = \pi \circ \varphi^{-1}$ is the hydrostatic pressure. Plugging this into equation 167, we recover the result from the previous section:

$$P/\mu = \frac{2\bar{\gamma}}{\lambda_0} + \left(\frac{5}{2} - \frac{2}{\lambda_0} - \frac{1}{2\lambda_0^4} \right) \tag{169}$$

It should be noted that it was only possible to directly solve the equation of motion because of the fact that the system is incompressible, and thus the deformation map must have a known, simple form. For a compressible system, this is no longer possible, as the full differential equation for $\varphi(r)$ is significantly more complicated.

4.4.4 The Critical Pressure and the Cavitation-Nucleation Transition

The physical meaning of equation 164 can be illustrated by expanding it to second order in the dimensionless radial extension $\epsilon = \lambda - 1 = R_0/r_0 - 1$. This gives

$$P/\mu = 2\bar{\gamma} + (4 - 2\bar{\gamma})\,\epsilon + (-7 + 2\bar{\gamma})\,\epsilon^2 + O\left(\epsilon^3\right) \tag{170}$$

The zeroth-order term $2\bar{\gamma}$ is the Laplace capillary pressure of the original cavity. The first-order term $(4-2\bar{\gamma})\,\epsilon$ is the result that would have been obtained if one had used linear elasticity and expanded the Laplace Law pressure to first order in ϵ. If one keeps only the zeroth-order and first-order terms for a cavity that is not under pressure (so, for $P=0$), then the radial strain is $\epsilon = -2\bar{\gamma}/\left(4-2\bar{\gamma}\right)$. This is a negative quantity, which is reasonable since the capillary pressure exerted by surface tension should cause the radius of an unpressurized cavity to shrink. The second-order term $(2\bar{\gamma}-7)\,\epsilon^2$ is the lowest-order nonlinear correction term. It states that, for $\bar{\gamma}$ less than $7/2$, the actual cavity radius will be larger than the radius obtained from linear elasticity. The effect of finite-strain elasticity is thus to soften the material.

(The paper has a brief discussion of the expanding balloon toy model, potentially add it here).

Equation 164 has a finite pressure solution when we set λ to infinity, namely, $P_\infty = \frac{5}{2}\mu$, independent of surface tension. This is the known critical cavitation pressure of the rubber elasticity literature.

Figure 2 shows that the radial extension $\left(R_0 - r_0\right)/r_0$ diverges continuously as the pressure approaches P_∞, provided $\bar{\gamma}$ is less than one. There are no other solution for $\bar{\gamma}$ less than one. These plots are, in fact, fully stable solutions.

If $\bar{\gamma}$ is larger than one, then the cavity radius does not diverge at $P = P_\infty$. For $P > P_\infty$, there are two solution branches. One of these - the bottom one in Figure 2 - is stable since the radius increases with pressure, while the top branch is unstable as the radius decreases with increasing pressure. This absence of a divergence at P_∞ seems mathematically puzzling, since $\lambda = \infty$ is a solution of equation 164 at P_∞. However, if $\bar{\gamma} > 1$, then equation 164 acquires additional solutions at $P = P_\infty$. One of these, $\lambda = \frac{1}{4(\bar{\gamma}-1)^{1/3}}$, is real and it is this solution that corresponds to the lower branch for $P > P_\infty$. The lower branch

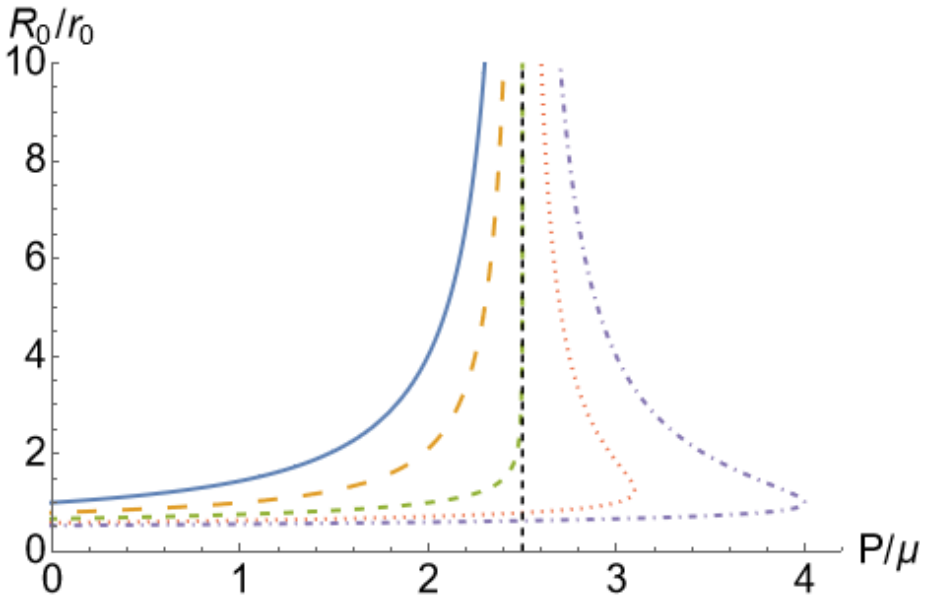

Figure 2: Dimensionless cavity pressure P/μ versus radial extension ratio for an incompressible system for different values of the dimensionless surface tension $\bar{\gamma} = \gamma/\mu r_0$. The surface tension values are $\bar{\gamma} = 0$ (solid, blue), $\bar{\gamma} = 0.5$ (dashed, yellow), $\bar{\gamma} = 1$ (dashed, green), $\bar{\gamma} = 1.5$ (dotted,red), and $\bar{\gamma} = 2$ (dash-dotted, purple). The dashed black line shows the critical pressure $P_\infty = \frac{5}{2}\mu$.

is metastable, with the upper branch corresponding to a transition-state energy maximum that separates the metastable state from the actual minimum energy state with infinite radius. The metastable solution survives under increasing pressure up to a maximum radius $r_0/\left(\bar{\gamma}-1\right)^{1/3}$, when the two branches fuse. Droplet growth for $\bar{\gamma} > 1$ is consistent with the nucleation-and-growth scenario of conventional phase separation. There is thus a well-defined transition between cavitation for $\bar{\gamma} < 1$ and nucleation for $\bar{\gamma} > 1$.

4.4.5 Effects of Shear Hardening

Shear strain hardening is included by extending the free-energy density through the use of equation 51. There are two limiting cases. If $\eta^{1/2}\lambda_0$ is small compared

to one, then one can use the perturbation series in powers of the inverse maximum shear strain η. To first order in η, the correction to the elastic free-energy is

$$\begin{aligned} F_{\mathrm{el}} &= 4\pi\mu\eta \int_{r_0}^{\infty} dr\; r^2 \left(\lambda^2 + \frac{1}{2\lambda^4} - \frac{3}{2}\right)^2 \\ &= 4\pi\mu\eta \left(R_0^3 - r_0^3\right) \int_1^{\lambda_0} d\lambda \left(\frac{\lambda}{\lambda^3 - 1}\right)^2 \left(\lambda^2 + \frac{1}{2\lambda^4} - \frac{3}{2}\right)^2 + O\left(\eta^2\right) \end{aligned} \tag{171}$$

Using a similar method as before, we can evaluate this integral and minimize the total free-energy, obtaining

$$\begin{aligned} P\left(\lambda\right)/\mu &\simeq \frac{2\bar{\gamma}}{\lambda} + \left(\frac{5}{2} - \frac{2}{\lambda} - \frac{1}{2\lambda^4}\right) \\ &+\eta\left(4\lambda - \frac{177}{20} + \frac{6}{\lambda} - \frac{2}{\lambda^2} + \frac{3}{2\lambda^4} - \frac{2}{5\lambda^5} - \frac{1}{4\lambda^8}\right) + O\left(\eta^2\lambda^3\right) \end{aligned} \tag{172}$$

The zeroth-order term in η reproduces equation 164 for $\eta = 0$. The first-order term (second line) has a term that diverges linearly in the limit of large λ. The second-order term (not shown explicitly) diverges even faster, as λ^3. Higher powers in λ appear as one includes higher order terms in the perturbation expansion in η.

Next, in the limit that $\eta^{1/2}\lambda$ approaches one, the integral in the elastic energy is determined by the singularity at $\eta^{1/2}\lambda = 1$, with the result that the pressure diverges in this limit as

$$P\left(\lambda\right)/\mu \simeq \frac{\eta^{1/2}}{2\left(1 - \eta^{1/2}\lambda\right)} \tag{173}$$

Figure 3 shows the relation between cavity radius and pressure for a strain hardening parameter $\eta = 0.01$ up to and including the second-order term in the expansion in η. The figure is restricted to λ values for which the third-order term in η can be neglected. The divergence of the radius at $P = \frac{5}{2}\mu$ has

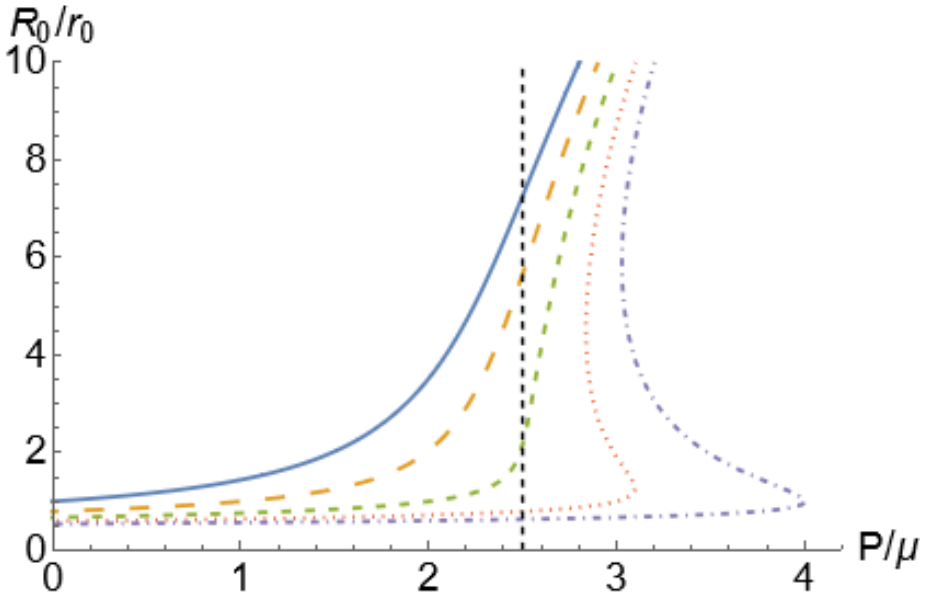

Figure 3: Dimensionless cavity pressure P/μ versus radial extension ratio for an incompressible system for various values of the dimensionless surface tension $\bar{\gamma} = \gamma/\mu r_0$ and strain hardening parameter $\eta = 0.01$. The dimensionless surface tensions are $\bar{\gamma} = 0$ (solid, blue), $\bar{\gamma} = 0.5$ (dashed, yellow), $\bar{\gamma} = 1$ (dashed, green), $\bar{\gamma} = 1.5$ (dotted, red), and $\bar{\gamma} = 2$ (dash-dotted, purple). The dashed black line shows the critical pressure $P_\infty = \frac{5}{2}\mu$.

disappeared. For increasing γ, the elastic energy again develops a maximum. Beyond a threshold pressure, the radius again increases discontinuously, but the radius now does not diverge. Instead, it saturates at a finite value. There is thus still a transition to nucleation-type behavior for larger $\bar{\gamma}$ and for dimensionless pressures larger than $\frac{5}{2}$, but droplets no longer expand without limit. For large values of the pressure, $\lambda = R_0/r_0$ increases less rapidly and eventually levels off as it approaches the maximum strain $1/\eta$, according to equation 172.

4.5 Cavitation in the Compressible Case

4.5.1 Variational Ansatz for the Deformation Map

For compressible systems, the deformation map $\varphi(r)$ is not known ahead of time. We used the following variational form:

$$\varphi(r) = r + (R_0 - r_0)\frac{1+b+c}{\left(\frac{r}{r_0}\right)^2 + b\frac{r}{r_0} + c} \tag{174}$$

with b and c variational parameters.

To see why this form is reasonable, note first that it obeys the required condition that $\varphi(r_0) = R_0$. Next, the elastic strain must go to zero in the limit of large r, so the theory of linearized elasticity must become valid in this limit. As shown in equation 119, the displacement field $u(r)$ surrounding a pressurized spherical cavity embedded in an infinite volume has the form $u(r) = (R_0 - r_0)\left(\frac{r_0}{r}\right)^2$ [10]. For the present nonlinear case, the asymptotic amplitude $R_0 - r_0$ is expected to have a different, renormalized value. For $r \gg r_0$, the displacement field $u(r) = \varphi(r) - r$ of the variational deformation map goes to zero as $1/r^2$, with amplitude $A = (R_0 - r_0)(1 + b + c)$. If $b + c$ is positive, then the amplitude of the asymptotic strain field exceeds that of linear elasticity theory, while for negative $b + c$ it is reduced. Note that, because the cavity must expand under increasing pressure, we must have $A > 0$, which forces us to have $1 + b + c > 0 \Rightarrow b + c > -1$.

Next, mass conservation requires that, as the cavity expands, material is pushed radially outward, which could potentially produce an excess density at the cavity surface (the snowplow effect). On the other hand, lateral stretching could produce a density deficit (the balloon effect). The relative density at $r = r_0$ is

given by

$$\rho_r\left(r_0\right)=\frac{\left(r_0/R_0\right)^2}{\varphi'\left(r_0\right)}=\frac{\left(r_0/R_0\right)^2}{1-\frac{R_0-r_0}{r_0}\frac{2+b}{1+b+c}} \tag{175}$$

If $2+b$ is positive, then the surface density is increased with respect to ρ_0, while it is decreased if $2+b$ is negative. The variational ansatz thus allows the density at the cavity surface and the asymptotic amplitude far from the surface to act as separate parameters in the variation. Also, it should be noted that, because the density can never become negative, we must have that $\frac{R_0-r_0}{r_0}\frac{2+b}{1+b+c}<1$, which places further restrictions on the physically allowed values of b and c.

4.5.2 Variational Results for The Modified Neo-Hookean Model

Before examining cavitation in gels, it is useful to first examine the case of cavitation in materials that obey modified neo-Hookean elasticity. The elastic free-energy density of the modified neo-Hookean model directly generalizes that which is used for incompressible materials such a rubber, as discussed in section 3.4.6.

The variational parameters b and c were obtained by numerical minimization of the functional

$$F\left[\varphi\right]=\gamma\left(4\pi R_0^2\right)-P\left(\frac{4\pi}{3}R_0^3\right)+4\pi\int_{r_0}^{\infty}dr\;r^2 f_{\mathrm{NH}} \tag{176}$$

Figure 4 shows the results. The dimensionless displacement $u\left(r\right)/r_0=\left(\varphi\left(r\right)-r\right)/r_0$ is shown as a function of r/r_0 on a linear-linear scale (top, black line) and on a log-log scale (bottom, black line) for the case of $\lambda=6$. These variational results are compared with the outcomes of a numerical solution of the equation for mechanical equilibrium using the finite-element method (FEM). This was done for cavity radial extensions of 5.52 (blue) and 6.16 (gold) that straddled $\lambda=6$. The linear-linear plot shows that the agreement is reasonable for r/r_0

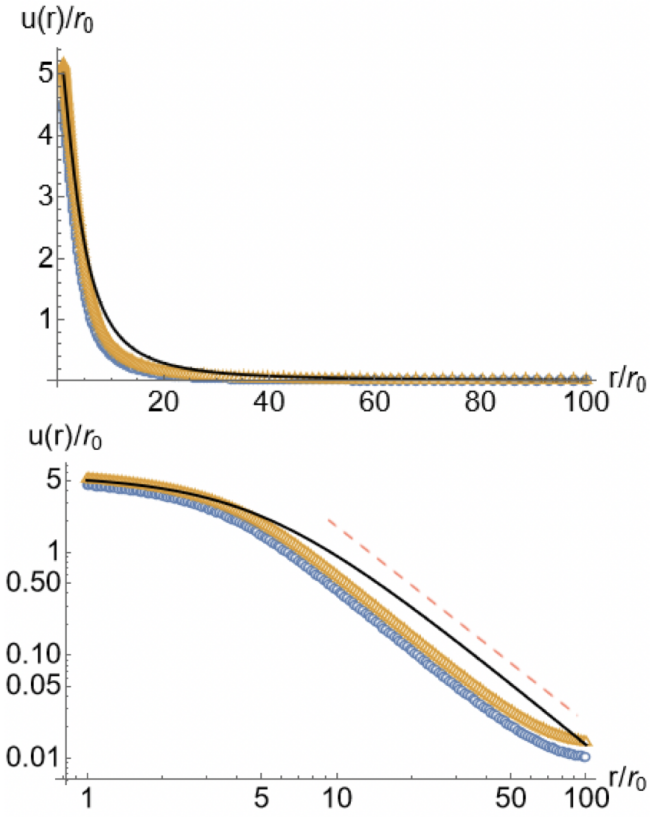

Figure 4: Top: (black line) $u(r)/r_0 = (\varphi(r) - r)/r_0$ for a cavity radial extension of 6 as obtained by the variational method. The result is compared with $u(r)/r_0$ obtained by the Finite Element Method (FEM) for cavity radial extensions of 5.52 (blue), respectively, 6.16 (gold), as carried out on a spherical sample with outer radius of $100r_0$. Bottom: same data but plotted on a log-log scale. The red dashed line has the slope of a $1/r^2$ power law.

less than about five. The log-log plot shows that for $5 \lesssim r/r_0 \lesssim 50$ the FEM radial extension is also consistent with a $1/r^2$ power law. However, the FEM results have a negative offset with respect to the variational results, which means the values of the asymptotic amplitudes $A = (R_0 - r_0)(1 + b + c)$ do not agree. Finally, the FEM result has an upturn for the largest values of r.

Starting with the last issue, the FEM analysis necessarily has to be done for a finite system. Stress-free boundary conditions were imposed at an outer ra-

dius R_2, which was set to $100r_0$. To obey this outer boundary condition, the large r displacement field must - according to linear elasticity - have the form $u(r) = ar + b/r^2$, where $a = b/R_2^3$ [10]. The linear term ar becomes comparable with the b/r^2 term when r is on the order of the outer radius R_2, which explains the upturn in the deformation map for $r \simeq R_2$. The reason for the negative offset of the FEM has to be different, because introducing a stress-free boundary condition should produce a larger, not a smaller, radial extension. It is discussed in section 4.5.5 that the FEM software package appears to be less reliable for large values of κ/μ.

Using the variational deformation map, one can construct other physical quantities. The density profile, obtained through the relation $\rho_r = \frac{r^2}{\varphi(r)^2\varphi'(r)}$, is shown in figure 5. In all cases, there is a density deficit, indicating taht the balloon

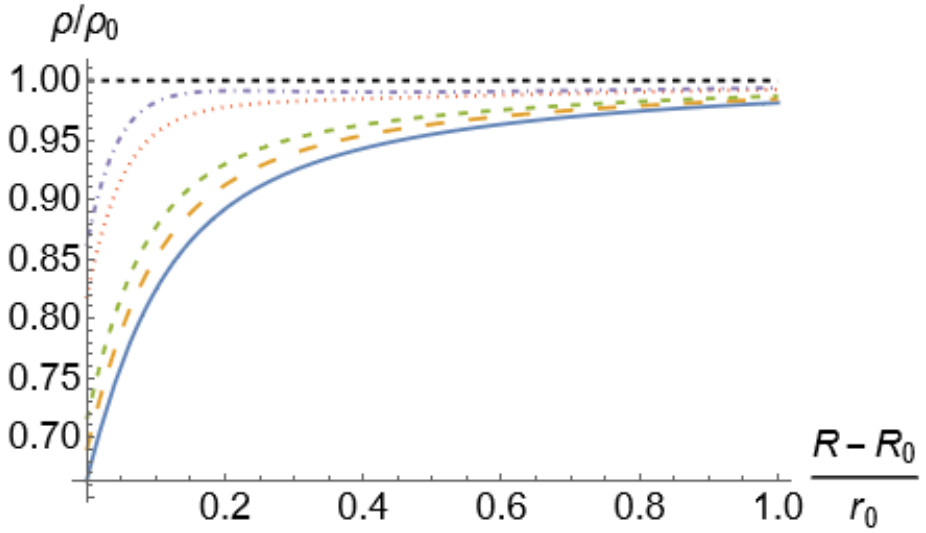

Figure 5: Relative density ρ/ρ_0 versus distance from cavity surface for the neo-Hookean model for various values of the ratio κ/μ: $\kappa/\mu = 0.1$ (blue, solid), $\kappa/\mu = 0.5$ (yellow, dashed), $\kappa/\mu = 1$ (green, dashed), $\kappa/\mu = 5$ (red, dotted), and $\kappa/\mu = 10$ (purple, dash-dotted). The final cavity radius was twice that of the initial radius.

effect overcomes the snowplow effect. For increasing values of κ/μ, the density

deficit decreases, and the density profiles approach the limit $\rho_r = 1$ of incompressible materials (the FEM method produces a denity excess at the cavity surface, see section 4.5.5).

Next, the relation between pressure P and radial extension is obtained by inserting the variational deformation map into the elastic free-energy density of equation 46. After integration over the volume to obtain $F_{\text{el}}[\varphi]$, the total free-

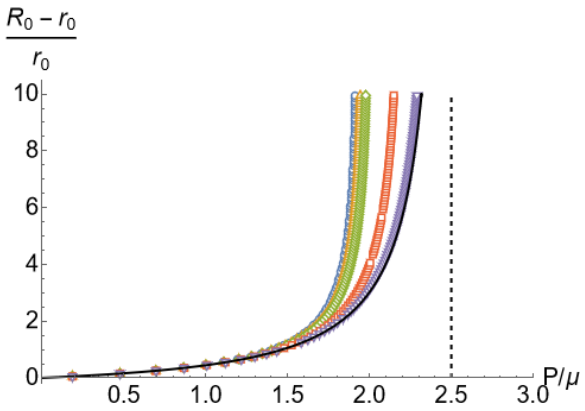

Figure 6: Radial extension ratio versus dimensionless cavity pressure P/μ for the neo-Hookean model for various values of the ratio of bulk and shear moduli: $\kappa/\mu = 0.1$ (blue, solid), $\kappa/\mu = 0.5$ (yellow, dashed), $\kappa/\mu = 1$ (green, dashed), $\kappa/\mu = 5$ (red, dotted), and $\kappa/\mu = 10$ (purple, inverted triangles). The solid black curve is the incompressible solution, while the dashed black line shows the critical pressure $P_\infty = \frac{5}{2}\mu$.

energy $F[\varphi]$ is minimized with respect to R_0. The result is shown in figure 6. Cavitation is encountered for all values of κ/μ, though the cavitation critical pressure is significantly reduced for lower values of κ/μ. Compressibility effects thus enhance cavitation. In contrast, for low pressures, the radial extension of the cavity is practically independent of the κ/μ ratio.

Figure 7 shows the effect of varing the surface tension for $\kappa/\mu = 1$. The plots are quite similar to the case of incompressible materials, apart from the fact that the critical pressure is reduced. Just as for incompressible materials, surface tension can transform cavitation into nucleation above a threshold value of

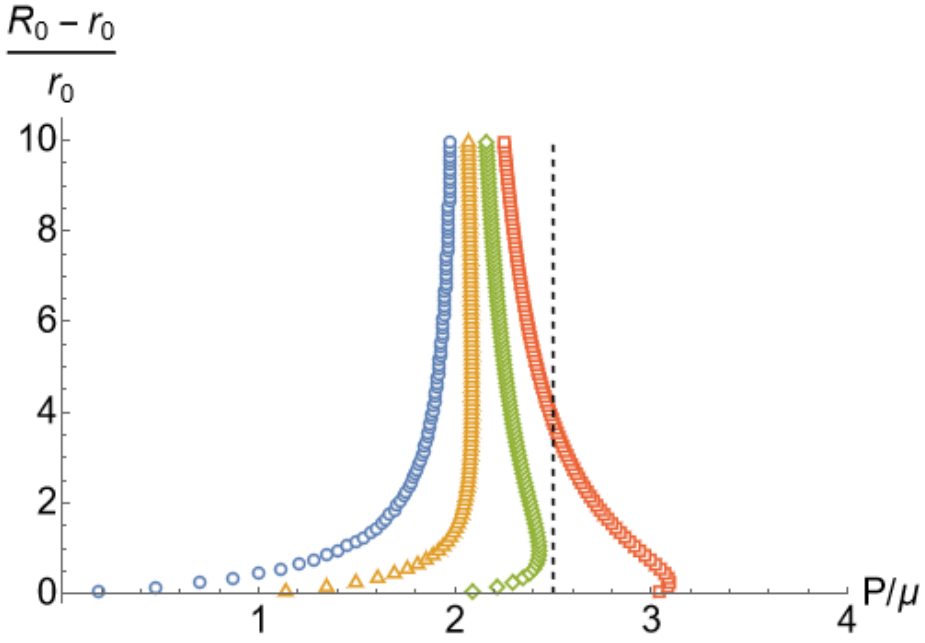

Figure 7: Radial extension ratio versus dimensionless cavity pressure P/μ for the neo-Hookean model for $\kappa/\mu = 1$ and various values of the dimensionless surface tension $\bar{\gamma} = \gamma/\mu r_0$: $\bar{\gamma} = 0$ (blue, circles), $\bar{\gamma} = 0.5$ (yellow, triangles), $\bar{\gamma} = 1$ (green, diamonds), and $\bar{\gamma} = 1.5$ (red, squares). There is no shear hardening.

the dimensionless surface tension $\bar{\gamma}$, except that this threshold value is now less than one.

Figure 8 shows what happens if one includes shear hardening for $\eta = 0.1$ and no surface tension. The plots of figure 8 show cavitation behavior in the presence of strain hardening in the case that the κ/μ ratio is less than about one. Recall that for incompressible systems, cavitation was suppressed even for a shear hardening parameter that was ten times smaller than the current value of $\eta = 0.1$. Once again, one sees that compressiblity promotes cavitation.

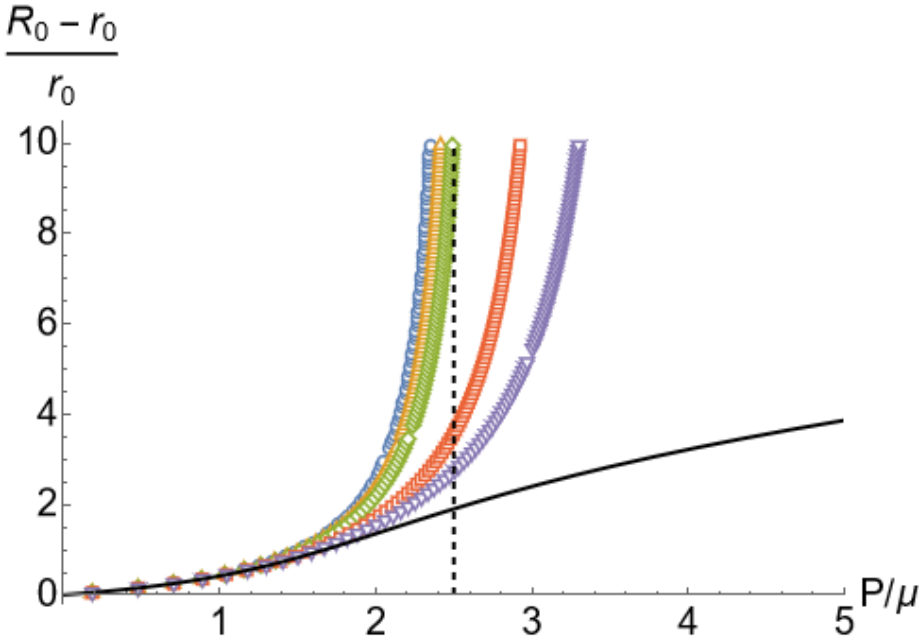

Figure 8: Radial extension ratio versus dimensionless cavity pressure P/μ for the neo-Hookean model for shear hardening parameter $\eta = 0.1$, no surface tension and various values of κ/μ: $\kappa/\mu = 0.1$ (blue, circles), $\kappa/\mu = 0.5$ (yellow, triangles), $\kappa/\mu = 1$ (green, diamonds), $\kappa/\mu = 5$ (red, squares), and $\kappa/\mu = 10$ (purple, inverted triangles). The solid black curve represents the incompressible solution, while the dashed black line shows the critical pressure $P_\infty = \frac{5}{2}\mu$.

4.5.3 Cavitation in Polymer gels with Two-Component Solvents

With the experience of incompressible and compressible neo-Hookean materials, we now can turn to the actual case of interest, namely, cavitation in polymer gels. To describe this system, we will use the Flory-Huggins mean-field theory of gels discussed in section 3.4.8.

Let the solvent be a two-component binary liquid where the majority component is a good solvent for the monomers of the gel, while the minority component is a poor solvent. In the absence of the gel, the thermodynamic work of formation of a minority phase droplet in a homogeneous supersaturated binary solution is $W = -N\Delta\mu + F_{\text{ex}}$. Here, $N = V/v_0$ is the number of minority phase molecules

in the droplet, V is the volume of the droplet, and v_0 is the molecular volume of the minority phase molecules. $\Delta\mu$ is the difference in the chemical potential of the minority phase molecules in the homogeneous mixture and those inside the drop. Finally, F_{ex} is the increase in free-energy of the surrounding environment due to the presence of the drop. In clasical nucleation theory (CNT), only the interfacial energy of the droplet is included in F_{ex}, so $F_{\text{ex}} = \gamma A$, where γ is the interfacial energy per unit area and A is the surface area of the droplet.

The radius R^* of the droplet in a stationary state in which the droplet neither grows nor shrinks is determined by the condition that the virtual work δW associated with an infinitesimal change of the droplet radius is equal to zero [8]. The positive work by the chemical potential is given by $\delta N \Delta\mu = \delta V\,(\Delta\mu/v_0)$, where $\Pi = \Delta\mu/v_0$ can be interpreted as an osmotic pressure that drives droplet swelling. The total work δW associated with an infinitesimal change δR of the radius of the droplet is then

$$\delta W = \gamma \delta A - \Pi \delta V \tag{177}$$

where $\delta A = 8\pi R \delta R$ and $\delta V = 4\pi R^2 \delta R$. The radius of the stationary droplet is then $R^* = 2\gamma/\Pi$, which is known as the critical droplet size in CNT. A stationary point with $\delta W = 0$ represents a thermodynamically stable state only if the derivative of the osmotic pressure Π with repsect to the cavity volume is positive. This derivative is negative, and thus this state is unstable - smaller droplets shrink and disappear, while larger droplets grow without limit.

Now, assume that the droplet nucleates in a solvent-filled cavity inside a gel that is originally in a state of swelling equilibrium. Let the initial radius be r_0. Once the radius of the growing droplet exceeds that of the cavity, the work of elastic deformation of the gel by the growing droplet must be included as an additional excess free-energy term in F_{ex}. This work is given by the Flory-Huggins free-

energy density in equation 52. The condition $\delta W = 0$ for a stationary state corresponds to the stationary state of the variational free-energy expression

$$F[\varphi] = \gamma\left(4\pi R_0^2\right) - P\left(\frac{4\pi}{3}R_0^3\right) + 4\pi\int_{r_0}^{\infty} dr\; r^2\,\frac{f_{\mathrm{FH}}}{\phi} \tag{178}$$

provided P is interpreted as an osmotic pressure, and γ as an interfacial free-energy per unit area. Here ϕ is the volume fraction of the monomers, and f_{FH}/ϕ is the free-energy density of the gel in the reference space - recall that, for the Flory-Huggins model, the dry, solvent-free state is used as the reference state.

4.5.4 Variational Results for the Flory-Huggins Model

The density profile in a Flory-Huggins gel surrounding a minority phase droplet under osmotic pressure is found in the same was as for neo-Hookean materials. Results for the case of no interfacial energy and no strain hardening are shown in figure 9. This density profile has a maximum near the cavity surface. For

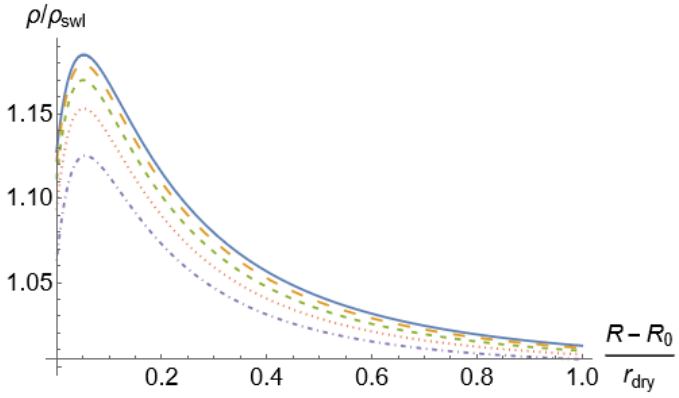

Figure 9: Relative density ρ/ρ_{swl} versus distance from cavity surface for the Flory-Huggins model, with final cavity radius twice that at swelling equilibrium, cross-link separation $N_x = 10$, and various values of the Flory χ parameter. The values of χ are $\chi = -0.4$ (solid, blue), $\chi = -0.2$ (dashed, yellow), $\chi = 0$ (dashed, green), $\chi = 0.2$ (dotted, red), and $\chi = 0.4$ (dash-dotted, purple).

Flory-Huggins gels, the snowplow effect apparently overcomes lateral stretch-

ing, just the opposite of what we found for neo-Hookean materials. The density profile is quite dependent on the Flory χ parameter. The excess density at the surface increases as the solubility of the polymers for the mixed phase decreases, i.e. for more negative values of χ, which agrees with physical intuition.

Figure 10 shows the dependence of radial extension on cavity pressure. The ra-

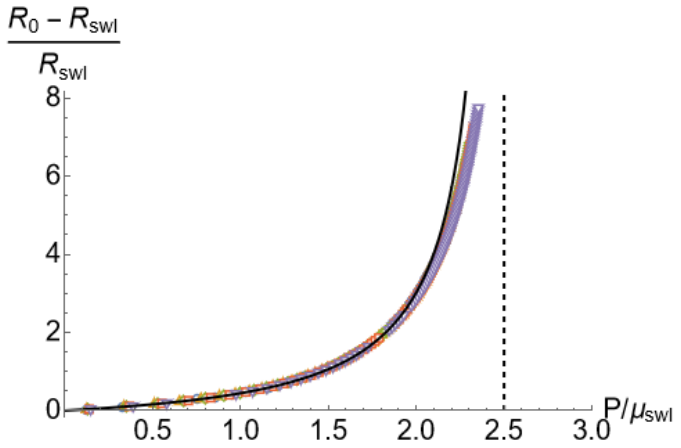

Figure 10: Radial extension ratio with respect to the equilibrium state versus dimensionless cavity pressure P/μ_{swl} for the Flory-Huggins model with μ_{swl} the shear modulus at swelling equilibrium. The cross-link separation is $N_x = 10$ and there is neither surface tension nor shear hardening. The values of the Flory χ parameter are $\chi = -0.4$ (blue, circles), $\chi = -0.2$ (yellow, triangles), $\chi = 0$ (green, diamonds), $\chi = 0.2$ (red, squares), and $\chi = 0.4$ (purple, inverted triangles). The black line shows the relation between radial extension and pressure for an incompressible material.

dial extension plots for different values of N_x and χ are surprisingly similar and close to that of incompressible materials (black line). Differences become visible only for dimensionless pressures close to the critical 5/2 ratio for incompressible materials.

A plot of the ratio of osmotic and shear moduli of the Flory-Huggins model as a function of χ is shown in figure 11. For N_x large compared to one, the ratio of osmotic and shear moduli approaches 5/3 for χ less than 1/2, independent of either χ or N_x. Since the ratio of the shear and osmotic moduli of a Flory-

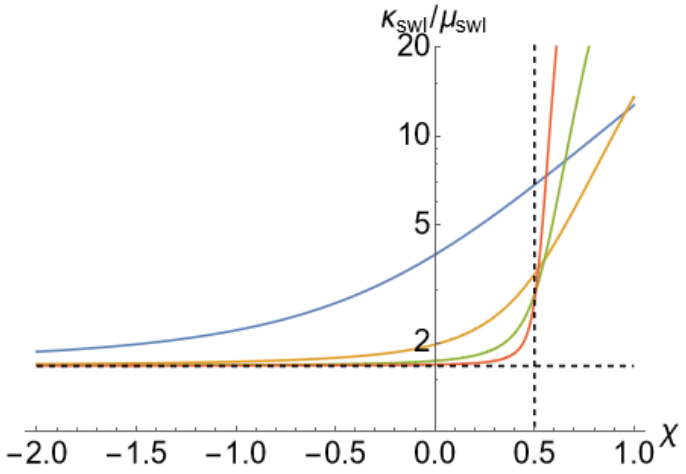

Figure 11: Dependence of the ratio of shear and bulk moduli of the FH model at swelling equilibrium on the Flory χ parameter for different values of N_x: $N_x = 1$ (blue), $N_x = 10$ (yellow), $N_x = 100$ (green), and $N_x = 1000$ (red).

Huggins gel near swelling equilibrium is of the order of one, one would have expected a significant reduction of the critical cavitation pressure as compared to that of incompressible materials, based on the earlier results for the modified neo-Hookean model, but this is not the case. Another surprise is the presistent lack of dependence of the radial extension on the Flory χ parameter and N_x outside the regime where linear elasticity holds. Recall that the density profile did not show this universality.

Figure 12 shows the effect of surface tension on the radial extension versus pressure plot, and compares it with incompressible materials. The effect of surface tension on cavitation in Flory-Huggins gels is practically the same as the effect of surface tension on cavitation for incompressible systems.

Next, we include strain hardening, replacing the first term in f_{FH} by equation 57. Figure 13 shows the effect of this term on plots of the radial extension as a function of pressure. For a strain-hardening parameter $\eta = 0.01$, there is no cavitation, just a somewhat higher rate of radial expansion for higher pressures.

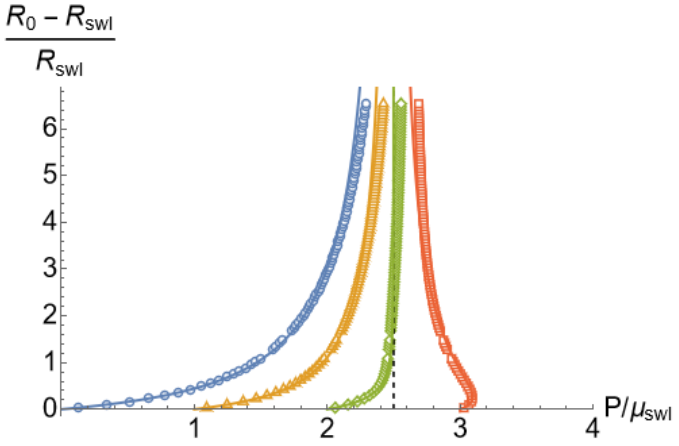

Figure 12: Radial extension ratio versus dimensionless cavity pressure $P/\mu_{\rm swl}$ for the FH model, with cross-link separation $N_x = 10$, Flory χ parameter $\chi = -0.2$, no shear hardening, and various values of dimensionless surface tension $\bar{\gamma} = \gamma/\mu_{\rm swl} r_{\rm swl}$. The values of $\bar{\gamma}$ are $\bar{\gamma} = 0$ (blue, circles), $\bar{\gamma} = 0.5$ (yellow, triangles), $\bar{\gamma} = 1$ (green, diamonds), and $\bar{\gamma} = 1.5$ (red, squares). The black dashed line shows the critical pressure for the incompressible solution, $P_\infty = \frac{5}{2}\mu_{\rm swl}$. The solid lines show the corresponding radial extension curves of an incompressible material.

Strain hardening suppresses cavitation in Flory-Huggins gels even more effectively than in incompressible systems with the same shear modulus. Next, the radial expansion plots are now significantly dependent on the Flory χ parameter for higher pressures: the suppression of cavitation becomes more pronounced as the solubility of the polymers for the mixed solvent is reduced. Similarly, if the cross-link separation N_x is increased, then cavitation is suppressed more effectively. This plot must be compared with figure 8 for modified neo-Hookean materials. There, compressiblity significantly enhanced cavitation for an η value that was ten times higher than for the present case. Strain hardening suppresses cavitation very effectively for Flory-Huggins gels.

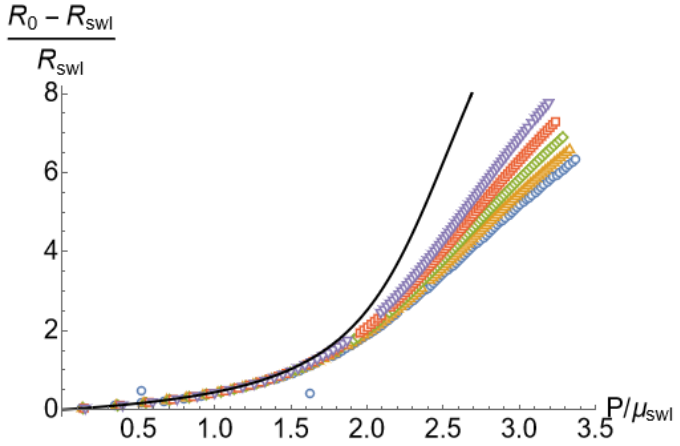

Figure 13: Radial extension ratio versus dimensionless cavity pressure P/μ_{swl} for FH gels with μ_{swl} the shear modulus at swelling equilibrium, cross-link separation $N_x = 10$, no surface tension, shear hardening parameter $\eta = 0.01$, and various values of the Flory χ parameter: χ are $\chi = -0.4$ (blue, circles), $\chi = -0.2$ (yellow, triangles), $\chi = 0$ (green, diamonds), $\chi = 0.2$ (red, squares), and $\chi = 0.4$ (purple, inverted triangles). The solid black curve shows the radial extension/pressure plot of an incompressible material for the same amount of strain hardening and the same shear modulus.

4.5.5 Finite Element Method and the Variational Ansatz

In section 4.5.2, in collaboration with Amit R. Singh from the Birla Institute of Technology and Science Department of Mechanical Engineering, we used the FEBIO STUDIO [14] software package to perform a finite element analysis for a sphere with a concentric spherical cavity made up of compressible neo-Hookean material. The simulations were force controlled, i.e., the pressure acting on the surface of the cavity was an input and displacements of the nodes of the finite element mesh were the output. We used 20-node quadratic hexahedral elements. Taking advantage of the spherical symmetry of the problem, we modeled only one-eighth of the sphere with appropriate symmetric boundary conditions. We chose the outer radius of the sphere to be 100 times the radius of the cavity. We checked for convergence by comparing the critical pressure for a mesh with 3552

elements and a mesh with 24057 elements. The resulting deformation map was shown in section 4.5.2, and compared with the map obtained by the variational method.

The density profile and radial extension versus pressure profiles obtained by the FEM are shown in figure 14. According to the top figure, there is a density

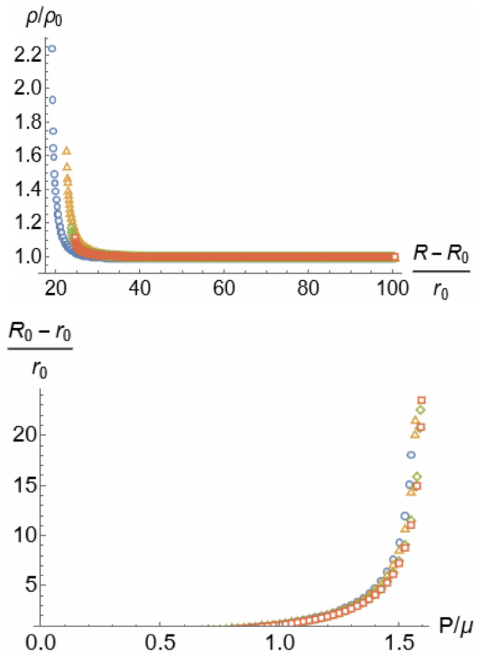

Figure 14: (Top) Radial density profiles obtained from the finite-element method (FEM) for different values of the ratio κ/μ between bulk and shear moduli. (Bottom) Cavity extension versus dimensionless cavity pressure P/μ using the FEM, for the same values of κ/μ. The values of κ/μ are 0.5 (blue circles), 1 (yellow triangles), 5 (green diamonds), and 10 (red squares).

excess instead of the density deficit that was obtained by the variational method. According to the bottom figure, there is qualitative agreement between the radial expansion plots of the FEM and the variational methods. However, the critical cavitation pressure predicted by the FEM is significantly smaller than the one predicted by the variational method, and appears to be only weakly

dependent on κ/μ. In particular, the FEM critical cavitation pressure does not approach the known critical cavitation pressure $P = \frac{5}{2}\mu$ of incompressible systems for large values of κ/μ as it should.

The density at the surface of the cavity is determined by the slope $\varphi'(r_0)$ of the deformation map through $\frac{\rho(r_0)}{\rho_0} = \frac{1}{\lambda_0^2 \varphi'(r_0)}$, where $\lambda_0 = R_0/r_0$ is the stretch ratio at the cavity surface. A density excess will occur at the cavity surface if $0 < \varphi'(r_0) < \lambda_0^{-2}$, while a density deficit occurs when $\varphi'(r_0) > \lambda_0^{-2}$. For $\lambda_0 = 6$, the variational method gives $\varphi'(r_0) \approx 0.1763$, which exceeds $1/\lambda_0^2$, corresponding to a density deficit. The FEM analysis gives for $\lambda_0 = 5.52$ a slope of $\varphi'(r_0) \approx 0.0187$, and for $\lambda_0 = 6.16$ a slope of $\varphi'(r_0) \approx 0.0119$, both of which are less than $1/\lambda_0^2$. As a result, both correspond to a surface density excess. So, even though the deformation maps of the variational and FEM methods appear to be similar in the region of smaller r, there is a substantial difference between the slopes of the deformation maps at the cavity surface. The origin of this discrepancy is not clear, but because the FEM does not reproduce for large κ/μ the exact result for incompressible systems, we believe that the variational method is more reliable in this case.

5 Dynamical Finite Strain Elasticity

5.1 Formalism for Dynamical Finite Strain Elasticity

When adapting the Lagrangian formalism to dynamics, as briefly discussed in section 3, the first main change is that now the deformation map φ is time-dependent. The other major addition is that we must now take energy dissipation into account. In a purely elastic system, energy dissipation is typically ignored, but for visco-elastic systems such as biogels it becomes very important. Let's start by discussing the rate of change of some important quantities in the

Lagrangian formalism. We have already defined the material and convective velocities in section 3, $v^i(x,t) = \frac{\partial \varphi^i}{\partial t}$ and $u^\alpha(x,t) = \left(A_t^{-1}\right)^\alpha_{\ i} v^i$ respectively. Now consider the rate of change of the deformation gradient matrix. There is a subtlety involved with taking the time derivative at fixed reference space position, resulting from the fact that the deformation gradient matrix has a deformed space index. If one were to directly take the time derivative of $\frac{\partial \varphi^i}{\partial x^\alpha}$, the commutativity of time and spatial derivatives would lead one to obtain $\frac{\partial v^i}{\partial x^\alpha}$. However, the indices on the deformation gradient matrix are tensorial, so this is not quite correct. Let $\hat{e}_\alpha(x)$ denote the reference space basis vectors, and $\hat{E}_i(\varphi(x,t))$ denote the deformed space basis vectors. Evaluating the full derivative of the "two-point" tensor, we see

$$\begin{aligned} \frac{\partial A}{\partial t} &= \frac{\partial}{\partial t}\left[\frac{\partial \varphi^i}{\partial x^\alpha}\hat{E}_i(\varphi(x,t)) \otimes \hat{e}^\alpha(x)\right] \\ &= \frac{\partial^2 \varphi^i}{\partial t \partial x^\alpha}\left(\hat{E}_i \circ \varphi\right) \otimes \hat{e}^\alpha + \frac{\partial \varphi^i}{\partial x^\alpha}\frac{\partial}{\partial t}\left(\hat{E}_i \circ \varphi\right) \otimes \hat{e}^\alpha \\ &= \frac{\partial v^i}{\partial x^\alpha}\left(\hat{E}_i \circ \varphi\right) \otimes \hat{e}^\alpha + A^i_{\ \alpha}\left(\bar{\Gamma}^k_{ij} \circ \varphi\right) v^j \left(\hat{E}_k \circ \varphi\right) \otimes \hat{e}^\alpha \end{aligned} \tag{179}$$

Define the covariant derivative of the material velocity (a vector whose index lives in a different space than its argument) as

$$\frac{Dv^i}{Dx^\alpha} = \frac{\partial v^i}{\partial x^\alpha} + A^i_{\ \alpha}\left(\bar{\Gamma}^i_{jk} \circ \varphi\right) v^j \tag{180}$$

Thus we have the time derivative of the deformation gradient matrix is equivalent to the reference space covariant derivative of the material velocity, $\frac{\partial A}{\partial t} = \nabla \otimes \vec{v}$. A similar subtlety occurs when evaluating the time derivative of the material velocity. Performing a similar argument, we find

$$\frac{\partial \vec{v}}{\partial t} = \left(\frac{\partial v^i}{\partial t} + \left(\bar{\Gamma}^i_{jk} \circ \varphi\right) v^j v^k\right) \hat{E}_i \circ \varphi \tag{181}$$

The equation of motion, originally given in the static case by equation #, will now include an inertial term. In addition, in the case of a viscous or visco-elastic system, the stress must now include a dissipative piece. For a general first Piola-Kirchhoff stress, the equation of motion is written as

$$\rho_0 \left(\frac{\partial v^i}{\partial t} + \left(\bar{\Gamma}^i_{jk} \circ \varphi \right) v^j v^k \right) = \frac{DS^{i\alpha}}{Dx^\alpha} + JB^i \tag{182}$$

For an isotropic system, we know that the viscous part of the Cauchy stress is a function of the symmetrized spatial velocity gradient, $\Sigma_{ij} = \frac{1}{2}\left(\frac{DV_i}{DX^j} + \frac{DV_j}{DX^i} \right)$. This tensor is commonly referred to as the Eulerian strain rate. The reason for this name is as follows. In the reference frame, it is fairly straightforward to show that

$$\left. \frac{DV^i}{DX^j} \right|_{\varphi_t(x)} = \frac{Dv^i}{Dx^\alpha} \left(A^{-1} \right)^\alpha_{\ j} = \left(\frac{dA}{dt} \right)^i_{\ \alpha} \left(A^{-1} \right)^\alpha_{\ i} \tag{183}$$

The pull-back of Σ is thus given by

$$\varphi_t^* \Sigma_{\alpha\beta} = A^i_{\ \alpha} \left(\Sigma_{ij} \circ \varphi_t \right) A^j_{\ \beta} = \frac{1}{2} \left(A_{i\alpha} \frac{dA^i_{\ \beta}}{dt} + \frac{dA^i_{\ \alpha}}{dt} A_{i\beta} \right) = \frac{\partial \mathcal{U}_{\alpha\beta}}{\partial t} \tag{184}$$

Clearly, the dissipative pieces of the first and second Piola-Kirchoff stress tensors are functions of the Lagrangian strain rate, $\frac{\partial \mathcal{U}}{\partial t}$.

While we have seen in section 4.4 that directly solving the equation of motion is possible for an incompressible material, if one wants to explore dissipative dynamics of compressible materials an analogue to minimizing the free-energy would be more approachable. To develop such an analogue, a brief discussion of thermodynamics will be necessary [7, 15, 16]. As with our original discussion of stress in section 3, we start in the deformed frame $\mathcal{B}_t$. Let $E(X,t)$ be the internal energy per unit volume (note this is not the free-energy density), $R(X,t)$ the incoming heat per unit volume, and $H\left(X,t,\hat{N}\right)$ be the rate of heat conduction

across a surface element with unit normal $\hat{N}$, i.e. the heat flux. We will assume that we can write the heat flux in terms of a vector field $\vec{Q}$, where $H\left(X,t,\hat{N}\right) = -\vec{Q}\left(X,t\right)\cdot\hat{N}$, similar to how we wrote the surface force in terms of a tensor field, the Cauchy stress. The first law of thermodynamics in the deformed frame can then be written in both integral and local form as

$$\frac{d}{dt}\int_{\mathcal{B}_t} dV\left(E+\frac{1}{2}\left|\vec{V}\right|^2\right) = \int_{\mathcal{B}_t} dV\left(\vec{b}\cdot\vec{V}+R\right) + \oint_{\partial\mathcal{B}_t} dS\,\hat{N}_i\left(\sigma^i_j V^j - Q^i\right) \tag{185}$$

$$\frac{DE}{Dt} + \frac{DQ^i}{DX^i} = \sigma^{ij}\Sigma_{ij} + R \tag{186}$$

In the reference frame, we have

$$\frac{\partial e}{\partial t} + \frac{Dq^\alpha}{Dx^\alpha} = s^{\alpha\beta}\frac{\partial \mathcal{U}_{\alpha\beta}}{\partial t} + r \tag{187}$$

where $e = \left(E\circ\varphi\right)/J$ is the internal energy density per unit undeformed volume, $\vec{q} = J\varphi_t^*\vec{Q}$ is the Piola transformation of the heat flux vector field, and $r = \left(R\circ\varphi\right)/J$ is the incoming heat per unit undeformed volume.

Let $N\left(X,t\right)$ denote the entropy per unit deformed volume and $\Theta\left(X,t\right)$ the temperature. The second law of thermodynamics is then expressed in the deformed frame as

$$\frac{d}{dt}\int_{\mathcal{B}_t} dV\; N \geq \int_{\mathcal{B}_t} dV\;\frac{R}{\Theta} + \oint_{\partial\mathcal{B}_t} dS\;\frac{H}{\Theta} \tag{188}$$

or, in local form,

$$\theta\frac{DN}{Dt} \geq R - \Theta\frac{D}{DX^i}\left(\frac{Q^i}{\Theta}\right) = R - \frac{DQ^i}{DX^i} + \frac{1}{\Theta}Q^i\frac{\partial\Theta}{\partial X^i} \tag{189}$$

Here $\frac{DN}{Dt} - R/\Theta + \frac{D\left(Q^i/\Theta\right)}{DX^i}$ is referred to as the entropy production rate in the literature.

Let $\eta\left(x,t\right) = \left(N\circ\varphi\right)/J$ and $\theta\left(x,t\right) = \Theta\circ\varphi$. Then in the reference frame we

have

$$\theta\frac{\partial\eta}{\partial t} \geq r - \theta\frac{D}{Dx^\alpha}\left(\frac{q^\alpha}{\theta}\right) = r - \frac{Dq^\alpha}{Dx^\alpha} + \frac{1}{\theta}q^\alpha\frac{\partial\theta}{\partial x^\alpha} \tag{190}$$

The free-energy density in the reference space is formally defined as a Legendre transformation of the internal energy, $f = e - \theta\eta$. The second law can be written in terms of f as

$$\begin{aligned}\theta\frac{\partial\eta}{\partial t} = \frac{\partial f}{\partial t} - \frac{\partial e}{\partial t} - \eta\frac{\partial\theta}{\partial t} &\geq r - \frac{Dq^\alpha}{Dx^\alpha} + \frac{1}{\theta}q^\alpha\frac{\partial\theta}{\partial x^\alpha} \\ \Rightarrow \frac{\partial f}{\partial t} - \eta\frac{\partial\theta}{\partial t} - s^{\alpha\beta}\frac{\partial\mathcal{U}_{\alpha\beta}}{\partial t} + \frac{1}{\theta}q^\alpha\frac{\partial\theta}{\partial x^\alpha} &\geq 0\end{aligned} \tag{191}$$

The second law implies that we can no longer simply minimize the free-energy to determine the state of the system, but it suggests a replacement in the form of the entropy production rate. In the case of a velocity-dependent dissipative force like friction or viscosity, this is most commonly described in terms of the Rayleigh dissipation functional $\mathcal{R}$, a measure of the rate of energy dissipation in the system. It is most naturally defined in the deformed space as

$$\mathcal{R} = \frac{1}{2}\int dV\ \zeta_{ij}V^iV^j \tag{192}$$

The motion of the system can then be found by minimizing the functional $\frac{dF}{dt} + \mathcal{R}$ with respect to variations in the velocity flow field $\vec{V}$.

In many ways the Eulerian formalism is a more natural formalism for dynamics. As discussed in section 3.5, it is built off of the formalism of fluid dynamics, with the motion of a body described by its (spatial) velocity flow field $\vec{V}\,(X,t)$. The equation of motion is written as

$$\rho\frac{DV^i}{Dt} = \frac{D\sigma^{ij}}{DX^j} + b^i \tag{193}$$

where $\frac{D}{Dt} = \frac{\partial}{\partial t} + \nabla_{\vec{V}}$ denotes the material time derivative.

5.2 Dynamics of Cavitation

5.2.1 Dynamics for Cavitation in an Elastic Incompressible Material

As in the static case, the form of the deformation map for cavitation in an incompressible material is fixed by mass conservation. The only difference is that now the cavity radius is a function of time:

$$\varphi(r,t) = \left(r^3 + R_0^3(t) - r_0^3\right)^{1/3} \tag{194}$$

Note that as a result of this the material and spatial velocities will take on simple forms:

$$v(r,t) = \frac{R_0^2(t)}{\varphi^2(r,t)}\frac{dR_0}{dt}, \quad V(R,t) = \frac{R_0^2(t)}{R^2}\frac{dR_0}{dt} \tag{195}$$

Because the spatial velocity is particularly simple, it is actually more straightforward to solve the equation of motion in the Eulerian formalism rather than the Lagrangian one. In the Eulerian formalism the Cauchy stress of an incompressible, perfectly elastic system may be written as $\sigma^{ij} = \mu\left(A^i{}_\alpha A^{j\alpha} - G^{ij}\right) - pG^{ij}$, where $p(R,t)$ is the hydrostatic pressure. The equation of motion is given by

$$\rho\frac{DV^i}{Dt} = \frac{D\sigma^{ij}}{DX^j} \Rightarrow \rho\left(\frac{\partial V}{\partial t} + V\frac{\partial V}{\partial R}\right) = \frac{\partial \sigma_R^R}{\partial R} + \frac{2}{R}\left(\sigma_R^R - \sigma_\theta^\theta\right) \tag{196}$$

Let $\Lambda(R,t) = R/\varphi_t^{-1}(R)$ be the radial stretch ratio in the Eulerian frame. Then we may write $\sigma_R^R = \mu\left(\Lambda^{-4} - 1\right) - p$ and $\sigma_\theta^\theta = \mu\left(\Lambda^2 - 1\right) - p$. Plugging both these and our expression for V into the equation of motion and simplifying, we obtain

$$\rho\left(\frac{R_0^2\ddot{R}_0}{R^2} + 2\frac{R_0\dot{R}_0^2}{R^2} - 2\frac{R_0^4\dot{R}_0^2}{R^5}\right) = -\frac{\partial p}{\partial R} + 2\mu\frac{\Lambda^3 - 1}{\Lambda^5}\frac{\partial \Lambda}{\partial R} \tag{197}$$

As in section 4.4.3, we may directly integrate this equation at fixed time, obtaining

$$\begin{aligned} P &= \rho\left(R_0\ddot{R}_0 + \frac{3}{2}\dot{R}_0^2\right) + \frac{2\gamma}{R_0} + \mu\left(\frac{5}{2} - \frac{2}{\Lambda_0} - \frac{1}{2\Lambda_0^4}\right) \\ &= \rho r_0^2\left(\Lambda_0\ddot{\Lambda}_0 + \frac{3}{2}\dot{\Lambda}_0^2\right) + \mu\left(\frac{5}{2} + \frac{2\left(\bar{\gamma}-1\right)}{\Lambda_0} - \frac{1}{2\Lambda_0^4}\right) \end{aligned} \tag{198}$$

where $\Lambda_0(t) = \Lambda\left(R_0(t), t\right) = R_0(t)/r_0$, and we have made use of the fact that $p\left(R_0(t), t\right) = P - \frac{2\gamma}{R_0(t)}$ due to the continuity of the stress tensor. This result is identical to that obtained in the static case, but now with a new inertial term. It is now a non-linear ordinary differential equation for $\Lambda_0(t)$.

Numerical solutions to equation 198 for various values of $\bar{P}$ in the absence of

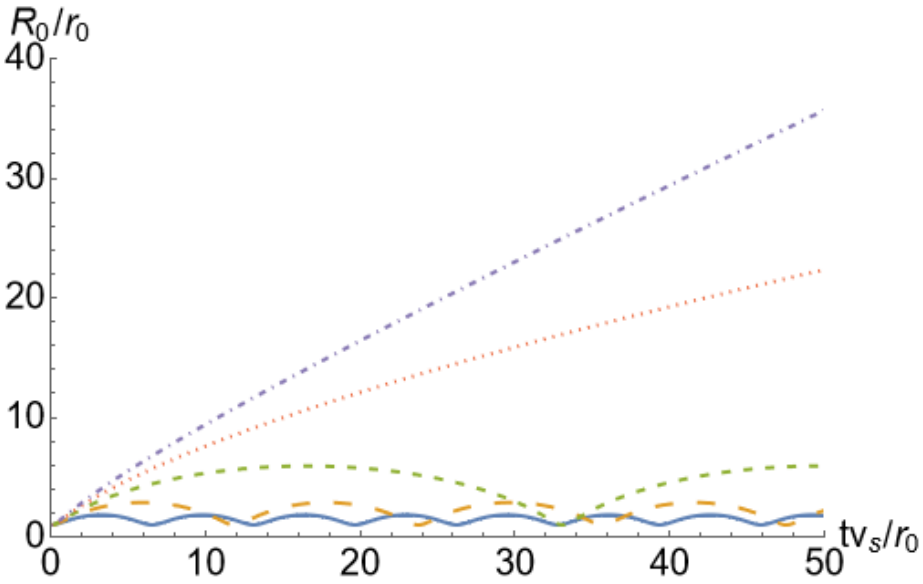

Figure 15: Radial extension ratio R_0/r_0 as a function of dimensionless time $t\frac{1}{r_0}\sqrt{\frac{\mu}{\rho}} = tv_s/r_0$ for cavitation in a purely elastic medium obtained via Mathematica's numerical differential equation solver, for various values of the dimensionless cavity pressure P/μ. The dimensionless cavity pressures are $P/\mu = 1$ (solid, blue), $P/\mu = 1.5$ (dashed, yellow), $P/\mu = 2$ (dashed, green), $P/\mu = 2.5$ (dotted, red), and $P/\mu = 3$ (dash-dotted, purple).

surface tension are shown in figure 15. Below the cavitation critical pressure, the cavity oscillates anharmonically about its equilibrium value, as one would expect in a system with no energy dissipation. Above the critical pressure, cavitation occurs, with $\Lambda_0(t) \sim t$ at long times. It should be noted that the value of the critical pressure, $\frac{5}{2}\mu$, is unchanged by the introduction of the inertial term.

5.2.2 Cavitation in a Maxwell Material

This approach for finding the equation of motion for cavitation in an incompressible material can be easily adapted for any kind of incompressible material, not just perfectly elastic ones. When applied to a viscous fluid, the resulting equation is known as the Rayleigh-Plesset equation,

$$P = \rho r_0^2 \left(\Lambda_0 \ddot{\Lambda}_0 + \frac{3}{2}\dot{\Lambda}_0^2 \right) + \frac{2\gamma}{r_0 \Lambda_0} + 4\eta \frac{\dot{\Lambda}_0}{\Lambda_0} \tag{199}$$

As in the purely elastic case, the Rayleigh-Plesset equation predicts cavitation, with $\Lambda_0 \sim t$ at long times. The main difference is that now there is no cavitation critical pressure. Instead, cavitation will occur for all pressures greater than the Laplace capillary pressure, while below the Laplace pressure the cavity collapses. Note that this implies that cavitation is not really a result of elasticity, but rather a result of the non-linear nature of large deformations.

For a visco-elastic system, the relationship between the Cauchy stress and the strain is more complex. One of the simpler non-linear models of visco-elasticity is the upper-convected Maxwell model, a generalization of the linear Maxwell model, whose constituative equation is given by

$$\sigma^{ij} + \tau \frac{\mathcal{D}\sigma^{ij}}{\mathcal{D}t} = 2\eta \Sigma^{ij} \tag{200}$$

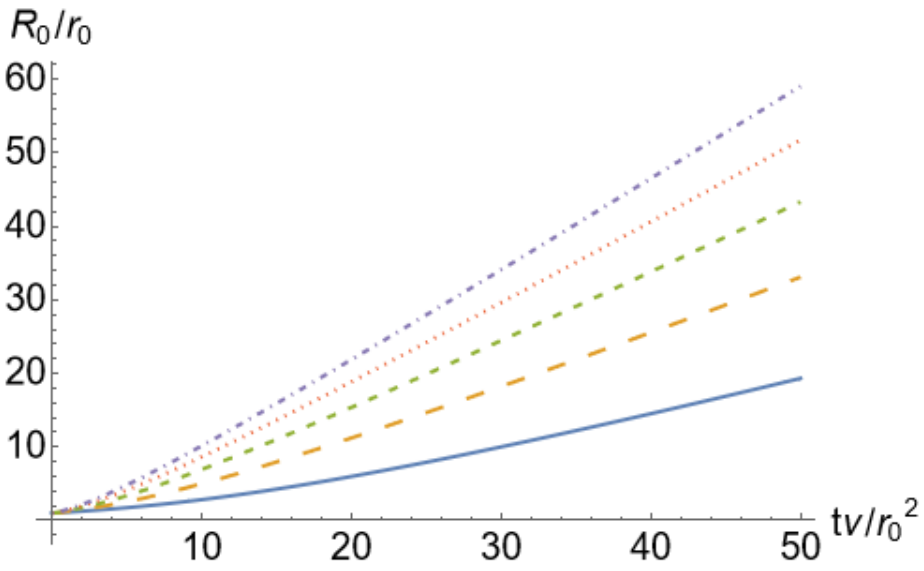

Figure 16: Radial extension ratio R_0/r_0 as a function of dimensionless time $t\eta/\rho r_0^2 = t\nu/r_0^2$ for cavitation in a viscous fluid obtained via Mathematica's numerical differential equation solver, for various values of the dimensionless cavity pressure $P^* = P\rho r_0^2/\eta^2$. The dimensionless cavity pressures are $P^* = 0.5$ (solid, blue), $P^* = 1$ (dashed, yellow), $P^* = 1.5$ (dashed, green), $P^* = 2$ (dotted, red), and $P^* = 2.5$ (dash-dotted, purple).

where $\tau = \eta/\mu$ is a relaxation time, while η represents the viscosity. To get some intuition regarding the solution of these equations, let's first consider method of solving the problem exclusively in the Eulerian picture, making use of a limiting case. Suppose that the stress relaxation time is small. We can then approximate the Cauchy stress to first order in τ as

$$\begin{aligned} \sigma^{ij} &= -pG^{ij} + 2\eta\Sigma^{ij} - \tau\frac{\mathcal{D}\sigma'^{ij}}{\mathcal{D}t} \approx -pG^{ij} + 2\eta\left(\Sigma^{ij} - \tau\frac{\mathcal{D}\Sigma^{ij}}{\mathcal{D}t}\right) \\ &\approx -pG^{ij} + 2\eta\left[\Sigma^{ij} - \tau\left(\frac{\partial\Sigma^{ij}}{\partial t} + V^k\frac{D\Sigma^{ij}}{DX^k} - \frac{DV^i}{DX^k}\Sigma^{kj} - \Sigma^{ik}\frac{DV^j}{DX^k}\right)\right] \end{aligned} \tag{201}$$

Due to the spherical symmetry of the system, the velocity gradient is diagonal, and thus $\Sigma^i_j = \frac{DV^i}{DX^j} = \frac{DV_j}{DX_i}$. Hence

$$\sigma^i_j = -p\delta^i_j + 2\eta\left[\Sigma^i_j - \tau\left(\frac{\partial\Sigma^i_j}{\partial t} + V^k\frac{D\Sigma^i_j}{DX^k} - 2\left(\Sigma^2\right)^i_j\right)\right] \tag{202}$$

In spherical coordinates,

$$\sigma^R_R = -p - 4\eta\frac{R_0^2}{R^3}\dot{R}_0 + 4\eta\tau\frac{R_0^2}{R^3}\ddot{R}_0 + 8\eta\tau\frac{R_0}{R^3}\dot{R}_0^2 + 4\eta\tau\frac{R_0^4}{R^6}\dot{R}_0^2 \tag{203}$$

$$\sigma^\theta_\theta = -p + 2\eta\frac{R_0^2}{R^3}\dot{R}_0 - 2\eta\tau\frac{R_0^2}{R^3}\ddot{R}_0 - 4\eta\tau\frac{R_0}{R^3}\dot{R}_0^2 + 10\eta\tau\frac{R_0^4}{R^6}\dot{R}_0^2 \tag{204}$$

The divergence of the Cauchy stress is thus given by

$$\frac{\partial\sigma^R_R}{\partial R} + \frac{2}{R}\left(\sigma^R_R - \sigma^\theta_\theta\right) = -\frac{\partial p}{\partial R} - 36\eta\tau\frac{R_0^4\dot{R}_0^2}{R^7} \tag{205}$$

Plugging this into the equation of motion, we have

$$\begin{aligned} \rho\left(\frac{\partial V^i}{\partial t} + V^j\Sigma^i_j\right) &= \frac{D\sigma^{ij}}{DX^j} \\ \Rightarrow \rho\left(\frac{R_0^2\ddot{R}_0}{R^2} + 2\frac{R_0\dot{R}_0^2}{R^2} - 2\frac{R_0^4\dot{R}_0^2}{R^5}\right) &= -\frac{\partial p}{\partial R} - 36\eta\tau\frac{R_0^4\dot{R}_0^2}{R^7} \end{aligned} \tag{206}$$

Integrating over R at fixed time, we obtain

$$\rho\left(R_0\ddot{R}_0 + \frac{3}{2}\dot{R}_0^2\right) = p\left(R_0\right) - 6\eta\tau\frac{\dot{R}_0^2}{R_0^2} \tag{207}$$

Here, using the continuity of the stress tensor,

$$p\left(R_0\right) = P - \frac{2\gamma}{R_0} - 4\eta\tau\frac{\dot{R}_0}{R_0} + 4\eta\tau\frac{\ddot{R}_0}{R_0} + 12\eta\tau\frac{\dot{R}_0^2}{R_0^2} \tag{208}$$

Therefore,

$$\begin{aligned} \rho R_0\ddot{R}_0 + \frac{3}{2}\rho\dot{R}_0^2 &= P - \frac{2\gamma}{R_0} - 4\eta\frac{\dot{R}_0}{R_0} + 4\eta\tau\frac{\ddot{R}_0}{R_0} + 6\eta\tau\frac{\dot{R}_0^2}{R_0^2} \\ \Rightarrow P &= \rho\left(R_0\ddot{R}_0 + \frac{3}{2}\dot{R}_0^2\right) + \frac{2\gamma}{R_0} + 4\eta\frac{\dot{R}_0}{R_0} - 4\frac{\eta\tau}{R_0^2}\left(R_0\ddot{R}_0 + \frac{3}{2}\dot{R}_0^2\right) \end{aligned} \tag{209}$$

The first three terms recover the Rayleigh-Plesset equation. The order τ correction term has a similar dependence on R_0 as the inertial term. The effect of adding a weak elasticity to the system is thus to essentially add a time-dependent correction to the density. Let $l^2 = \eta\tau/\rho = \mu\tau^2/\rho = (\tau v_s)^2$, where $v_s = \sqrt{\mu/\rho}$ is the speed of sound. We then have

$$P = \rho\left(1 - \frac{4l^2}{R_0^2}\right)\left(R_0\ddot{R}_0 + \frac{3}{2}\dot{R}_0^2\right) + 4\eta\frac{\dot{R}_0}{R_0} + \frac{2\gamma}{R_0} \tag{210}$$

At long times, when $R_0 \gg l$, the correction to the inertial term will go to zero as t^{-2}, and the growth of the cavity will be well approximated by the Rayleigh-Plesset equation. At shorter time-scales, the effect of elasticity is to cause the medium to appear less dense than it actually is. It also should be noted that when l exceeds $r_0/2$ the inertial term in equation 210 will change sign. This suggests the presence of a shock wave instability, which is reasonable to expect when $\dot{R}_0$ approaches v_s.

While this method of approximating the solution provides some insight into how the density is renormalized as a result of elasticity, it should be noted that, even if we were to continue the perturbative expansion to arbitrarily high powers of τ, it cannot be an exact solution. We know from linear theory that in a Maxwell material the elastic response decays exponentially with time-scale τ. However, equation 210 shows that the correction terms introduced by the perturbative expansion will decay as power laws. Clearly, a purely Eulerian approach to solving this problem is insufficient.

To derive a full equation of motion for a Maxwell material, we can perform a similar iterative calculation, but now within the Lagrangian picture. If we pull the constituitive equation back to the reference frame, noting that $J = 1$ due to incompressibility, we may write it as

$$s^{\alpha\beta} + \tau \frac{\partial s^{\alpha\beta}}{\partial t} = -\eta \frac{\partial}{\partial t} \left(\left(A^{-1}\right)^{\alpha}_{\ i} \left(A^{-1}\right)^{\beta i} \right) \tag{211}$$

where $\left(A^{-1}\right)^{\alpha}_{\ i} \left(A^{-1}\right)^{\beta i} = \left(\varphi_t^* G^{-1}\right)^{\alpha\beta}$ is the pullback of the deformed frame inverse metric. If we now integrate over time and add in the hydrostatic pressure, we obtain

$$s^{\alpha\beta} = -\pi \left(A^{-1}\right)^{\alpha}_{\ i} \left(A^{-1}\right)^{\beta i} - \mu \left(\left(A^{-1}\right)^{\alpha}_{\ i} \left(A^{-1}\right)^{\beta i} - g^{\alpha\beta} \right) - \frac{1}{\tau} \int_0^t dt' \ s'^{\alpha\beta} \tag{212}$$

where $\mu = \eta/\tau$ is the shear modulus, $\pi(r,t) = p(\varphi(r,t),t)$, and $s'^{\alpha\beta} = s^{\alpha\beta} - \pi \left(A^{-1}\right)^{\alpha}_{\ i} \left(A^{-1}\right)^{\beta i}$ is the visco-elastic contribution to the second Piola-Kirchhoff stress.

If we now iterate similarly to before, we find

$$\begin{aligned} s^{\alpha\beta} = &-\pi \left(A^{-1}\right)^{\alpha}_{\ i} \left(A^{-1}\right)^{\beta i} - \mu \left(\left(A^{-1}\right)^{\alpha}_{\ i} \left(A^{-1}\right)^{\beta i} - g^{\alpha\beta} \right) \\ &-\mu \sum_{n=1}^{\infty} \left(\prod_{k=1}^{n} \left(-\frac{1}{\tau} \right) \int_0^{t_{n-1}} dt_n \right) \left(\left(A^{-1}\right)^{\alpha}_{\ i} \left(A^{-1}\right)^{\beta i} - g^{\alpha\beta} \right) \end{aligned} \tag{213}$$

where $t_0 \equiv t$. Define the linear functional

$$\mathcal{L}_t [f(s)] = f(t) - \frac{1}{\tau} \int_0^t ds \ f(s) + \frac{1}{\tau^2} \int_0^t dt' \int_0^{t'} ds \ f(s) - \dots \tag{214}$$

Note that

$$\frac{d}{dt} \mathcal{L}_t [f(s)] = f'(t) - \frac{1}{\tau} f(t) + \frac{1}{\tau^2} \int_0^t ds \ f(s) - \dots = f'(t) - \frac{1}{\tau} \mathcal{L}_t [f(s)] \tag{215}$$

and therefore

$$\begin{aligned}\mathcal{L}_t\left[f\left(s\right)\right] &= f\left(0\right)e^{-t/\tau} + \int_0^t dt'\; e^{-\left(t-t'\right)/\tau} f'\left(t'\right) \\ &= f\left(t\right) - \frac{1}{\tau}\int_0^t dt'\; e^{-\left(t-t'\right)/\tau} f\left(t'\right)\end{aligned} \tag{216}$$

We can then write

$$s^{\alpha\beta} = -\pi\left(A^{-1}\right)_{\;i}^{\alpha}\left(A^{-1}\right)^{\beta i} - \mu\mathcal{L}_t\left[\left(A^{-1}\right)_{\;i}^{\alpha}\left(A^{-1}\right)^{\beta i} - g^{\alpha\beta}\right] \tag{217}$$

The components of the second Piola-Kirchhoff stress tensor are thus given by

$$s_r^r\left(r,t\right) = -\pi\left(r,t\right)\lambda^4\left(r,t\right) - \mu\mathcal{L}_t\left[\lambda^4\left(r,s\right) - 1\right] \tag{218}$$

and

$$s_\theta^\theta\left(r,t\right) = -\pi\left(r,t\right)\lambda^{-2}\left(r,t\right) - \mu\mathcal{L}_t\left[\lambda^{-2}\left(r,s\right) - 1\right] \tag{219}$$

where $\lambda\left(r,t\right) = \varphi\left(r,t\right)/r$. Pushing this back to the deformed frame, we see that the components of the Cauchy stress are given by

$$\begin{aligned}\sigma_R^R\left(R,t\right) &= \Lambda^{-4}\left(R,t\right)s_r^r\left(\varphi_t^{-1}\left(R\right),t\right) \\ &= -p\left(R,t\right) - \mu\mathcal{L}_t\left[\left(1 - \frac{R_0^3\left(t\right) - R_0^3\left(s\right)}{R^3}\right)^{4/3} - \Lambda^{-4}\left(R,t\right)\right]\end{aligned} \tag{220}$$

and

$$\begin{aligned}\sigma_\theta^\theta\left(R,t\right) &= \Lambda^{2}\left(R,t\right)s_\theta^\theta\left(\varphi_t^{-1}\left(R\right),t\right) \\ &= -p\left(R,t\right) - \mu\mathcal{L}_t\left[\left(1 - \frac{R_0^3\left(t\right) - R_0^3\left(s\right)}{R^3}\right)^{-2/3} - \Lambda^{2}\left(R,t\right)\right]\end{aligned} \tag{221}$$

where $\Lambda(R,t) = \lambda\left(\varphi_t^{-1}(R),t\right) = R/\varphi_t^{-1}(R)$. Plugging the components into the equation of motion and simplifying, we obtain

$$\begin{aligned}\rho\left(\frac{R_0^2\ddot{R}_0}{R^2}+2\frac{R_0\dot{R}_0^2}{R^2}-2\frac{R_0^4\dot{R}_0^2}{R^5}\right) &= -\frac{\partial p}{\partial R}\\ -2\mu\mathcal{L}_t\left\{\frac{1}{R}\left(\frac{R_0^3(t)-R_0^3(s)}{R^3}\right)^2\left(1-\frac{R_0^3(t)-R_0^3(s)}{R^3}\right)^{-2/3}\right.&\\ \left.+\frac{\Lambda^3(R,t)-1}{\Lambda^5(R,t)}\frac{\partial\Lambda}{\partial R}(R,t)\right\}&\end{aligned} \tag{222}$$

Integrating over R at fixed time, we find

$$\begin{aligned}P &= \rho r_0^2\left(\Lambda_0(t)\ddot{\Lambda}_0(t)+\frac{3}{2}\dot{\Lambda}_0^2(t)\right)+\frac{2\gamma}{r_0\Lambda_0(t)}\\ &\quad+\mu\mathcal{L}_t\left[2\frac{\Lambda_0(s)-1}{\Lambda_0(t)}+\frac{1}{2}\frac{\Lambda_0^4(s)-1}{\Lambda_0^4(t)}\right]\\ &= \rho r_0^2\left(\Lambda_0(t)\ddot{\Lambda}_0(t)+\frac{3}{2}\dot{\Lambda}_0^2(t)\right)+\frac{2\gamma}{r_0\Lambda_0(t)}+\mu\left[\left(\frac{5}{2}-\frac{2}{\Lambda_0(t)}\right.\right.\\ &\left.\left.-\frac{1}{2\Lambda_0^4(t)}\right)-\frac{1}{\tau}\int_0^t dt'\,e^{-(t-t')/\tau}\left(2\frac{\Lambda_0(t')-1}{\Lambda_0(t)}+\frac{1}{2}\frac{\Lambda_0^4(t')-1}{\Lambda_0^4(t)}\right)\right]\end{aligned} \tag{223}$$

In the limit $\tau\to\infty$, the integral term becomes negligible and we recover the case for pure elasticity found in equation 198.

At short times, we then expect the solution to equation 223 to resemble the solution found for the pure elastic case - oscillatory if $P<\frac{5}{2}\mu$, and monotonically increasing for $P>\frac{5}{2}\mu$. Assuming $t\ll\tau$, we may approximate the integral term using the trapezoidal rule,

$$\begin{aligned}\int_0^t dt'\,e^{-(t-t')/\tau}\left(2\frac{\Lambda_0(t')-1}{\Lambda_0(t)}+\frac{1}{2}\frac{\Lambda_0^4(t')-1}{\Lambda_0^4(t)}\right)&\\ \approx\frac{1}{2}t\left(\frac{5}{2}-\frac{2}{\Lambda_0(t)}-\frac{1}{2\Lambda_0^4(t)}\right)&\end{aligned} \tag{224}$$

Hence, for $t \ll \tau$,

$$P \approx \rho r_0^2 \left(\Lambda_0 \ddot{\Lambda}_0 + \frac{3}{2} \dot{\Lambda}_0^2 \right) + \frac{2\gamma}{r_0 \Lambda_0} + \mu \left(1 - \frac{t}{\tau} \right) \left(\frac{5}{2} - \frac{2}{\Lambda_0} - \frac{1}{2\Lambda_0^4} \right) \tag{225}$$

Numerical solutions to equation 225 are shown in figure 17. The oscillatory behavior is fairly weak at small values of l, but become more visible as l increases.

At long times, the system will forget the elastic response, and the cavity radius should eventually grow linearly in time regardless of the value of the cavity pressure, as in the Rayleigh-Plesset equation. Note that, if $t \gg \tau$, the integral term in equation 223 will be dominated by the region where $t - t' \ll \tau$. As such, it is reasonable to expand $\Lambda_0 (t')$ about t. We may then approximate the integral term in equation 223 as

$$\begin{aligned} & \int_0^t dt' \, e^{-(t-t')/\tau} \left(2 \frac{\Lambda_0 (t') - 1}{\Lambda_0 (t)} + \frac{1}{2} \frac{\Lambda_0^4 (t') - 1}{\Lambda_0^4 (t)} \right) \\ \approx & \int_0^t dt' \, e^{-(t-t')/\tau} \left[\left(\frac{5}{2} - \frac{2}{\Lambda_0 (t)} - \frac{1}{2\Lambda_0^4 (t)} \right) - 4 \frac{\dot{\Lambda}_0 (t)}{\Lambda_0 (t)} (t - t') \right. \\ & \left. + \frac{2}{\Lambda_0^2 (t)} \left(\Lambda_0 (t) \ddot{\Lambda}_0 (t) + \frac{3}{2} \dot{\Lambda}_0^2 (t) \right) (t - t')^2 + \ldots \right] \end{aligned} \tag{226}$$

Noting that $\int_0^t dt' \, e^{-(t-t')/\tau} (t - t')^n = \tau^{n+1} (n! - \Gamma (n+1, t/\tau))$
$= n! \tau^{n+1} \left[1 - e^{-t/\tau} \sum_{k=0}^n \frac{(t/\tau)^k}{k!} \right]$, define $G_n (t) = 1 - \Gamma (n+1, t/\tau) / n!$. We may then write

$$\begin{aligned} & \int_0^t dt' \, e^{-(t-t')/\tau} \left(2 \frac{\Lambda_0 (t') - 1}{\Lambda_0 (t)} + \frac{1}{2} \frac{\Lambda_0^4 (t') - 1}{\Lambda_0^4 (t)} \right) \\ & \approx \tau \left(\frac{5}{2} - \frac{2}{\Lambda_0} - \frac{1}{2\Lambda_0^4} \right) G_0 (t) - 4\tau^2 \frac{\dot{\Lambda}_0}{\Lambda_0} G_1 (t) \\ & + \frac{4\tau^3}{\Lambda_0^2} \left(\Lambda_0 \ddot{\Lambda}_0 + \frac{3}{2} \dot{\Lambda}_0^2 \right) G_2 (t) + \ldots \end{aligned} \tag{227}$$

where $G_0 (t) = 1 - e^{-t/\tau}$, $G_1 (t) = 1 - e^{-t/\tau} \left(1 + \frac{t}{\tau} \right)$,
$G_2 (t) = 1 - e^{-t/\tau} \left(1 + \frac{t}{\tau} + \frac{1}{2} \left(\frac{t}{\tau} \right)^2 \right)$, etc.. Equation 223 may then be approxi-

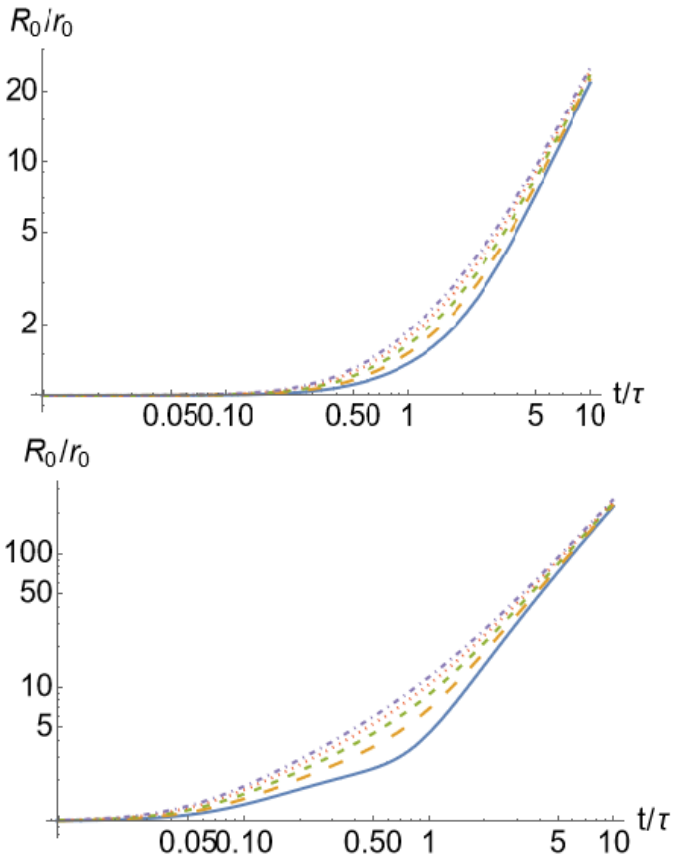

Figure 17: Radial extension ratio R_0/r_0 as a function of dimensionless time t/τ for cavitation in a Maxwell material at short times, obtained via Mathematica's numerical differential equation solver, at various values of dimensionless cavity pressure $P^* = P/\mu$. In the top image, the length-scale l has a value of r_0, while in the bottom image it has a value of $10r_0$. The dimensionless cavity pressures are $P^* = 1$ (solid, blue), $P^* = 1.5$ (dashed, yellow), $P^* = 2$ (dashed, green), $P^* = 2.5$ (dotted, red), and $P^* = 3$ (dash-dotted, purple). The data is plotted on a log-log scale to make the oscillatory behavior below the critical pressure more visible.

mated at long times (or, equivalently, at small τ) as

$$P \approx \frac{2\gamma}{r_0\Lambda_0} + \mu e^{-t/\tau}\left(\frac{5}{2} - \frac{2}{\Lambda_0} - \frac{1}{2\Lambda_0^4}\right) + 4\eta G_1(t)\frac{\dot{\Lambda}_0}{\Lambda_0} + \rho\left(r_0^2 - \frac{4l^2}{\Lambda_0^2}G_2(t)\right)\left(\Lambda_0\ddot{\Lambda}_0 + \frac{3}{2}\dot{\Lambda}_0^2\right) + \ldots \tag{228}$$

As $t \to \infty$, equation 228 approaches the Rayleigh-Plesset equation, as expected. The elastic response decays exponentially, as it should for a Maxwell material. In addition, the viscosity is renormalized by $G_1(t)$. Finally, the density is again renormalized, although with a more complicated correction term. Clearly, to obtain the full solution the method of utilizing both the Eulerian and Lagrangian formulations is required.

Numerical solutions to equation 228 with two different values for the length-scale $l = \tau\sqrt{\mu/\rho}$ are shown in figure 18, although it should be noted that our approximations will become less accurate at times less than or on the scale of τ. Because we are limited to small values of l to avoid the shock wave instability, the oscillatory behavior at shorter times is too small to be visible in these approximations.

6 Conclusion

Our goal in this dissertation was to explore the use of non-linear elasticity in describing the physics of biogels and biogel-like materials, a regime that falls in between the more well explored areas of incompressible solids and viscous fluids. In particular, we chose to focus on cavitation as an example phenomenon due to its relevance to the physics of biogels, as well as the simplifications provided by the spherical symmetry inherent to the problem. First exploring the static case, we made use of a variational approximation to explore the effects of compressibility, strain-hardening, and droplet surface/interfacial tension on cavitation in both neo-Hookean materials similar to those previously explored in the engineering literature, and Flory-Huggins gels. The results for these two types of materials were then compared.

The effect of surface tension on cavitation is described by the dimensionless

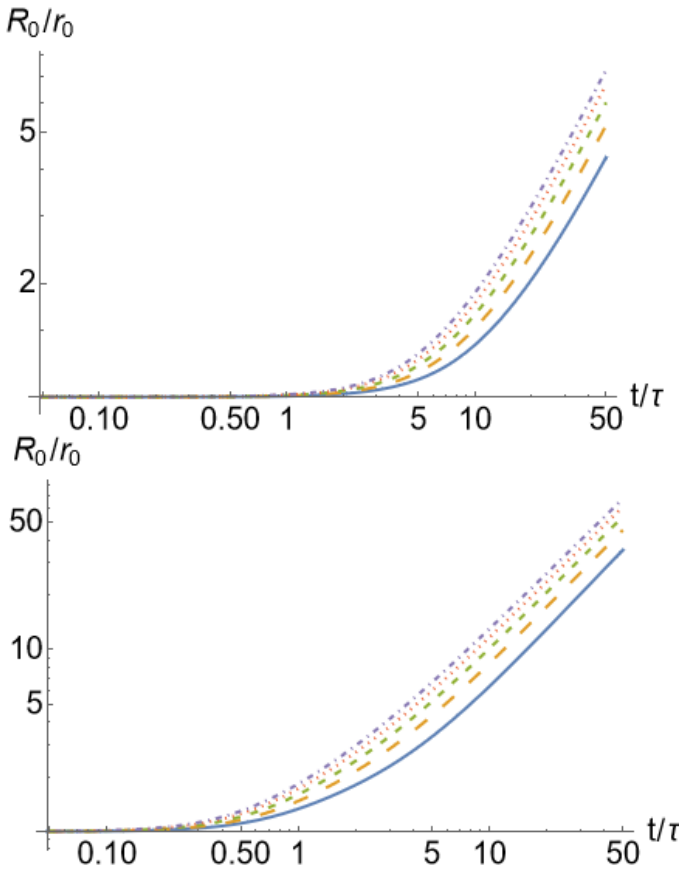

Figure 18: Radial extension ratio R_0/r_0 as a function of dimensionless time t/τ for cavitation in a Maxwell material obtained via Mathematica's numerical differential equation solver, at various values of dimensionless cavity pressure $P^* = P/\mu$. In the top image, the length-scale l has a value of $0.1r_0$, while in the bottom image it has a value of r_0. The dimensionless cavity pressures are $P^* = 1$ (solid, blue), $P^* = 1.5$ (dashed, yellow), $P^* = 2$ (dashed, green), $P^* = 2.5$ (dotted, red), and $P^* = 3$ (dash-dotted, purple)

parameter $\bar{\gamma} = \frac{\gamma}{\mu r_0}$. If $\bar{\gamma}$ is less than a number close to one then the effects of surface tension on cavitation are secondary, but if $\bar{\gamma}$ is greater than this threshold number then cavitation is replaced by activated droplet nucleation-and-growth. Biomolecular condensates in aqueous environments have interfacial energies in the range of 10^{-4} mN/m to 10^{0} mN/m [26]. If the cavity radius r_0 for the dry

gel is estimated to be of the order of the size of a monomer of a synthetic flexible polymer (of the order of one nm) and μ is taken to be of the order of the G' modulus of hydrogels (about 10^3 Pa), then $\bar{\gamma}$ falls in the range of 0.1 to 10^3. This estimate suggests that both the case of cavitation and nucleation-and-growth are possible.

The second important result found for the static case is that compressibility significantly reduces the critical cavitation pressure of neo-Hookean materials provided the compressional modulus is comparable to (or less than) the shear modulus. For Flory-Huggins gels on the other hand, the critical cavitation pressure is practically the same as that of incompressible materials. Because the shear and compressional moduli of a Flory-Huggins gel are comparable at swelling equilibrium, this was surprising. In fact, the elastic properties of Flory-Huggins gels were also in other respects more similar to incompressible materials than compressible ones with similar elastic moduli. We encountered this for the case of surface tension, strain hardening, and density profile. The observation that Flory-Huggins gels behave in some respects as incompressible materials was actually made before in an experimental study of the responsse of hydrogels to externally applied osmotic pressure [2]. The proposed explanation there was that this effect is due to the pre-stress in the state of swelling equilibrium.

While compressibility seemed to have a very minimal effect on cavitation in Flory-Huggins gels, we instead saw that it is very sensitive to strain hardening. We found that cavitation is suppressed for strain hardening parameters η as small as 0.01. Shear hardening in biogels strongly depends on cross-linking density. While synthetic polymer gels composed of highly flexible polymers with low cross-linking densities show no observable strain hardening [19], sythetic biomimetic gels do, with effective η values in the range of one to ten [5, 19]. For collagen gel, the η value increase from about 10^1 to about 10^3 under increasing

cross-linking density [24]. All of these η values are well above 0.01, which would mean that none of these systems ought to show cavitation according to our results.

In chapter five we explored the dynamics of cavitation. Seeing as we previously found that cavitation in compressible Flory-Huggins gels appeared qualitatively similar to that in incompressible materials, we focused exclusively on incompressible materials. Our main result is that, while purely elastic solids can be described entirely within either a Lagrangian or Eulerian frame of reference, visco-elastic materials such as the Maxwell materials we explored cannot be fully described without making use of both reference frames. In particular, we saw that to properly derive the exponentially decaying elastic response, the equation of motion had to first be pulled back to the reference frame. What makes this possible to do is that the deformation map φ is known for an incompressible material, being forced to take on a specific form by mass conservation. Unfortunately, this means that performing a similar calculation for a compressible material, where we do not know the form of φ ahead of time, is not feasible in general. A variational ansatz could potentially be used to approximate the form of the deformation map, as we did in the static case, although the presence of dissipative terms in the free energy would make determining the correct values of any variational parameters more complicated.

In the case of the incompressible Maxwell material, we found that the effects of finite-strain elasticity was to renormalize the viscosity and density in a time-dependent way, in addition to the exponentially decaying elastic response. The renormalized density, in particular, can become negative when the stress relaxation time becomes very large, which suggests the presence of a shock-wave like instability. While the presence of this instability could be derived when staying exclusively in the Eulerian frame, as in equation 210, properly deriving

time dependence of both the density and the viscosity renormalization, like the elastic response, requires the use of both the Eulerian and Lagrangian frames of reference. The final equation, equation 228, acts as something of a union of both approaches.

As long as the deformation map φ is known, similar calculations may be performed for other models of visco-elastic materials. When it comes to the Flory-Huggins gels we explored in chapter four, however, the deformation map is sadly not fixed by incompressibility. This is because of the fact that Flory-Huggins gels are two-component systems - while the full system of polymer and solvent together is incompressible, the polymer network and solvent individually are not. The elastic response will be determined by the deformation map of the polymer network alone, and as such translating between a Lagrangian and Eulerian frame of reference is no longer feasible. While we could, in principle, derive a set of differential equations for the deformation maps of both the polymer network and solvent, these equations would be incredibly complex and infeasible to solve.

References

[1] W H Besant. *A Treatise on Hydrostatics and Hydrodynamics*. Deighton, Bell, 1859.

[2] Abir Bhattacharyya, Chris O'Bryan, Yongliang Ni, Cameron D Morley, Curtis R Taylor, and Thomas E Angelini. Hydrogel compression and polymer osmotic pressure. *Biotribology*, 22:100125, 2020.

[3] Masao Doi. *Introduction to polymer physics*. Oxford university press, 1996.

[4] Masao Doi. Gel dynamics. *Journal of the Physical Society of Japan*, 78(5):052001, 2009.

[5] Kendra A Erk, Kevin J Henderson, and Kenneth R Shull. Strain stiffening in synthetic and biopolymer networks. *Biomacromolecules*, 11(5):1358–1363, 2010.

[6] AN Gent and C Wang. Fracture mechanics and cavitation in rubber-like solids. *Journal of Materials Science*, 26(12):3392–3395, 1991.

[7] Albert Edward Green and Wolfgang Zerna. *Theoretical Elasticity*. Dover, New York, 1992.

[8] Dimo Kashchiev. On the relation between nucleation work, nucleus size, and nucleation rate. *The Journal of Chemical Physics*, 76(10):5098–5102, 1982.

[9] Philip Kollmannsberger and Ben Fabry. Linear and nonlinear rheology of living cells. *Annual Review of Research Material*, 41:75–97, 2011.

[10] L D Landau and E M Lifshitz. *Theory of Elasticity 3rd edition*. Oxford, 1986.

[11] L D Landau and E M Lifshitz. *Fluid Mechanics Second Edition*. Pergamon Press, Oxford, 1987.

[12] John M Lee. *Introduction to Smooth Manifolds: Second Edition*. Springer, New York, 2013.

[13] Justin Little, Alex J Levine, Amit R Singh, and Robijn Bruinsma. Finite-strain elasticity theory and liquid-liquid phase separation in compressible gels. *Phys. Rev. E*, 107:024418, 2023.

[14] Steve A Maas, Benjamin J Ellis, Gerard A Ateshian, and Jeffrey A Weiss. Febio: finite elements for biomechanics. *Journal of biomechanical engineering*, 134(1), 2012.

[15] Jerrold E. Marsden and Thomas J. R. Hughes. *Mathematical Foundations of Elasticity*. Dover, New York, 1994.

[16] R. W. Ogden. *Non-Linear Elastic Deformations*. Dover, New York, 1997.

[17] Robyn H Pritchard and Eugene M Terentjev. Mechanics of biological networks: From the cell cytoskeleton to connective tissue. *Soft Matter*, 10:1864–1884, 2014.

[18] Lord Rayleigh. On the pressure developed in a liquid during the collapse of a spherical cavity. *The London, Edinburgh, and Dublin Philosophical Magazine and Journal of Science*, 34:94–98, 1917.

[19] M Fernández-Castaño Romera. *Biomimetic strain-stiffening hydrogels*. Technische Universiteit Eindhoven, 2018.

[20] Michael Rubinstein, Ralph H Colby, et al. *Polymer physics*, volume 23. Oxford university press New York, 2003.

[21] Yair Shokef and Samuel A. Safran. Scaling laws for the response of nonlinear elastic media with implications for cell mechanics. *Physical Review Letters*, 108:178103, 2012.

[22] Cornelis Storm, Jennifer J Pastore, Fred C MacKintosh, Tom C Lubensky, and Paul A Janmey. Nonlinear elasticity in biological gels. *Nature*, 435(7039):191–194, 2005.

[23] Robert W Style, Tianqi Sai, Nicoló Fanelli, Mahdiye Ijavi, Katrina Smith-Mannschott, Qin Xu, Lawrence A Wilen, and Eric R Dufresne. Liquid-liquid phase separation in an elastic network. *Physical Review X*, 8(1):011028, 2018.

[24] David Vader, Alexandre Kabla, David Weitz, and Lakshminarayana Mahadevan. Strain-induced alignment in collagen gels. *PloS one*, 4(6):e5902, 2009.

[25] Peter W Voorhees. The theory of ostwald ripening. *Journal of Statistical Physics*, 38(1):231–252, 1985.

[26] Huan Wang, Fleurie M Kelley, Dragomir Milovanovic, Benjamin S Schuster, and Zheng Shi. Surface tension and viscosity of protein condensates quantified by micropipette aspiration. *Biophysical Reports*, 1(1):100011, 2021.

[27] Xuefeng Wei, Jiajia Zhou, Yanting Wang, and Fanlong Meng. Modeling elastically mediated liquid-liquid phase separation. *Physical Review Letters*, 125(26):268001, 2020.

[28] Yaojun Zhang, Daniel SW Lee, Yigal Meir, Clifford P Brangwynne, and Ned S Wingreen. Mechanical frustration of phase separation in the cell nucleus by chromatin. *Physical review letters*, 126(25):258102, 2021.